

Activity Report 2005

**Association
EURATOM / IPP.CR**

INSTITUTE OF PLASMA PHYSICS
ACADEMY OF SCIENCES OF THE CZECH REPUBLIC

TABLE OF CONTENTS

PREFACE.....	4
I. RESEARCH UNIT.....	5
1 ASSOCIATION EURATOM/IPP.CR	5
2 MANPOWER AND BUDGET	7
3 INTERNATIONAL COLLABORATION.....	8
4 MAIN FACILITIES.....	9
II. PHYSICS	13
OVERVIEW OF ACTIVITIES - PHYSICS	13
LIST OF PUBLICATIONS (PHYSICS)	17
1 EDGE PLASMA AND MAGNETIC CONFINEMENT PHYSICS	22
<i>Relaxation phenomena induced by edge biasing experiments in the CASTOR tokamak</i>	22
<i>Hydrogen retention in metallic membranes in a tokamak environment</i>	24
<i>Temporally and spatially resolved measurements of VUV lines intensity profile</i> <i>in the tokamak CASTOR</i>	25
<i>Carbon transport in TCV</i>	27
<i>Modeling of magnetic equilibria and current drive expected in the IPP Prague</i> <i>re-installation of the Culham COMPASS-D tokamak</i>	28
<i>Plasma sprayed tungsten-based coatings and their usage in the edge plasma region</i> <i>of tokamaks</i>	31
2 DIAGNOSTICS DEVELOPMENT	33
<i>Measurements of magnetic fields in TORE Supra and CASTOR by means of Hall sensors</i>	33
<i>The ball-pen probe for direct measurements of the electron temperature and the first</i> <i>results of the PIC simulations</i>	34
<i>VUV imaging Seya-Namioka spectrometer & 2D fast detection system</i>	36
<i>Ion temperature measurements in the tokamak scrape-off layer</i>	37
<i>Fast bolometry on the CASTOR tokamak</i>	39
<i>Development of an advanced probe for edge tokamak plasmas</i>	41
<i>Improvement of the radiometer on CASTOR - design of the antenna for oblique view</i> <i>of the plasma</i>	42
3 WAVE INTERACTIONS IN PLASMAS	44
<i>Modeling of tokamak edge plasma flows and interpretation of probe diagnostics</i> <i>in the presence of suprathermal electrons by the quasineutral particle-in-cell</i> <i>(QPIC) method</i>	44
<i>Positive biasing of plasma in front of LH antennas</i>	48
<i>Numerical simulation of EC emission in MAST</i>	49
<i>Fast particle energy measurements in the scrape-off layer during lower hybrid current drive</i> <i>experiments on Tore Supra, and the analysis and interpretation of the measurements</i>	51
<i>Electron acceleration near ICRF antennas</i>	53
4 ATOMIC PHYSICS AND DATA FOR EDGE PLASMA AND PLASMA-WALL INTERACTIONS. 56	56

	<i>Energy transfer and chemical reactions in collisions of ions with surfaces</i>	56
5	JET COLLABORATION	59
III.	TECHNOLOGY	61
1	TECHNOLOGY TASKS	61
	OVERVIEW OF TECHNOLOGY TASKS	61
	<i>Development and testing of components for the liquid metal loop (cold traps, high temperature flanges and circulation pump)</i>	63
	<i>Static and dynamic toughness testing at the transition temperature: Neutron irradiation of plates and weldments up to 2.5 dpa at 200-250°C and post irradiation examination</i>	64
	<i>In-pile PbLi corrosion testing of TBM's weldments (stiffeners and bottom plate relevant)</i>	65
	<i>Activation experiment on tantalum in the NPI p-D2O neutron field</i>	66
	<i>Analysis of welding distortions obtained in manufacturing of VV segment</i>	67
2	UNDERLYING TECHNOLOGY	69
	<i>Measurement of activation cross sections at neutron energies below 35 MeV: activation experiment on tantalum in the NPI p-7Li neutron field</i>	69
	<i>Validation of new methodology of recovery strain hardening. Simulation of SS during multipass welding</i>	70
	<i>Development of methods of fracture toughness and notch toughness measurement with irradiated sub-size specimens</i>	71
	<i>Development of methods for post-irradiation examination of in-pile compatibility of EUROFER with Pb-17%Li</i>	71
IV.	KEEP-IN-TOUCH ACTIVITY ON INERTIAL CONFINEMENT FUSION	73
1	<i>Investigation of ablation pressure dynamics in structured laser targets</i>	73
2	<i>Laser imprint smoothing by low-density foam layers</i>	76
V.	TRAINING, EDUCATION, OUTREACH AND PUBLIC INFORMATION	
	ACTIVITES	79
1	<i>Training and Education</i>	79
2	<i>Outreach and Public Information</i>	81

PREFACE

This report summarizes the main activities and achieved results of the Association EURATOM/IPP.CR in the year 2005. The Association participates in the joint European effort in mastering controlled fusion by carrying out relevant plasma physics and technology R&D, including participation in JET and other European devices and activities related to the international fusion experiment ITER.

The Association was founded on December 22, 1999 through a contract between the European Atomic Energy Community (EURATOM) represented by the European Commission and the Institute of Plasma Physics, Academy of Sciences of the Czech Republic (IPP). Several other institutions have been included in the Research Unit to contribute to the work programme in physics and technology research:

- Faculty of Mathematics and Physics, Charles University in Prague
- Institute of Physical Chemistry, Academy of Sciences of the Czech Republic
- Faculty of Nuclear Science and Physical Engineering, Czech Technical University
- Nuclear Physics Institute, Academy of Sciences of the Czech Republic
- Nuclear Research Institute, Rez, Plc
- Institute of Applied Mechanics, Brno, Ltd

The overall manpower involved in the Association's fusion research at the end of 2005 was 97, of which 75 were professionals (i.e. those with a University degree). The total effort expended is about 49 person years of which roughly 60% is devoted to physics tasks and the remaining 40% to underlying technology and technology tasks. The overall 2005 budget was about 2.2 M€.

Our activities in physics were based on the approved Work Programme 2005 both in experiment and theory. The fusion-relevant plasma physics is experimentally studied on the small tokamak CASTOR. The research is focused on the study of phenomena at the plasma edge, such as biasing and the measurement of the structure of edge turbulence. A part of our activities was devoted to studies of wave-plasma interaction. Some selected atomic processes relevant to fusion plasmas, such as the interaction of molecular ions with first wall elements, were studied in test-bed experiments. The research was performed in close collaboration with other Associations (CEA, HAS, the Belgium State, ENEA (RFX), ŐAW, UKAEA, TEKES, FZK, CIEMAT, IST and IPPLM).

In the technology area, the R&D was substantially enhanced and focused on the fields Vessel/In Vessel, Tritium Breeding and Materials and Physics Integration. In total 15 Technology Tasks, mostly exploiting the cyclotron, the fission reactor and computational capabilities have been solved.

Finally, the COMPASS-D tokamak was offered by the Association EURATOM/UKAEA to be re-installed in the Institute of Plasma Physics, Prague. Our possibilities and the required expenditures were carefully assessed. The national support for this project was secured by a decision of the Government of the Czech Republic at the end of 2005. Following this decision, we started to prepare an application for preferential support.

Jan Stöckel
Head of Research Unit
Association EURATOM/IPP.CR

I RESEARCH UNIT

1 Association EURATOM/IPP.CR

Composition of the Research Unit

**IPP Institute of Plasma Physics,
Academy of Sciences of the CR**
Address: Za Slovankou 3,
182 00 Praha 8, Czech Republic
Tel: +420 286 890 450
Fax: +420 286 586 389
Contact Person: Jan Stöckel
e-mail: stockel@ipp.cas.cz

**FMP Faculty of Mathematics and Physics,
Charles University**
Address: V Holešovičkách 2,
182 00 Praha 8, Czech Republic
Tel: +420 221 912 305
Fax: +420 221 912 332
Contact person: Milan Tichý
tichy@mbox.troja.mff.cuni.cz

**JHIPC J Heyrovský Institute of Physical
Chemistry, Academy of Sciences of
the CR**
Address: Dolejškova 3,
182 23 Praha 8, Czech Republic
Tel: +420 266 053 514
Fax: +420 286 582 307
Contact person: Zdeněk Herman
zdenek.herman@jh-inst.cas.cz

**FNSPE Faculty of Nuclear Science and
Physical Engineering,
Czech Technical University**
Address: Břehová 7,
115 19 Praha 1, Czech Republic
Tel: +420 224 358 296
Fax: +420 222 320 862
Contact person: Vojta Svoboda
svoboda@br.fjfi.cvut.cz

**NPI Institute of Nuclear Physics,
Academy of Sciences of the CR**
Address: 250 68 Řež, Czech Republic
Tel: +420 266 172 105 (3506)
Fax: +420 220 941 130
Contact person: Pavel Bém
e-mail: bem@ujf.cas.cz

NRI Nuclear Research Institute pls., Řež
Address: 250 68 Řež, Czech Republic
Tel: +420 266 172 453
Fax: +420 266 172 045
Contact person: Karel Šplíchal
e-mail: spl@ujv.cz

**IAM Institute of Applied Mechanics Brno,
Ltd.**
Address: Veveří 85,
611 00 Brno, CR
Phone: +420 541 321 291
Fax: +420 541 211 189
Contact person: Lubomír Junek
e-mail: junekl@uam.cz

Steering Committee

EURATOM

Johannes P.M. Spoor, Head Unit J7, DG RTD
David Campbell, Unit J6, DG RTD
Barry Green, Unit J6, DG RTD

Head of Research Unit

Jan Stöckel

IPP.CR

Ivan Wilhelm (Charles University)
Petr Křenek (Ministry of Education, Youth and Sports)
Pavel Chráska (Institute of Plasma Physics)

Secretary of the SC

Pavol Pavlo

International Board of Advisors of the Association EURATOM-IPP.CR

Dr. Michael Endler	Max-Planck-Institut für Plasmaphysik, Greifswald, Germany
Dr. Carlos Hidalgo	CIEMAT, Madrid, Spain
Dr. Jochen Linke	Forschungszentrum Jülich GmbH, Jülich, Germany
Dr. Yves Peysson	CEA, Cadarache, France
Prof. Michael Tendler	Royal Inst. of Technology, Alfvén Laboratory, Stockholm, Sweden
Dr. Martin Valovič	UKAEA, Culham laboratory, United Kingdom
Prof. Guido Van Oost	Ghent University, Gent, Belgium
Dr. Henri Weisen	EPFL, Lausanne, Switzerland
Prof. Hannspeter Winter	Technische Universität Wien, Austria

The Board was established to help with the formulation of scientific program, and assess the scientific achievements of the Association.

Representatives of the Association in European Committees

Consultative Committee for the EURATOM Specific Programme on Nuclear Energy Research - Fusion

Pavel Chráska	Institute of Plasma Physics, Academy of Sciences of the Czech Republic
Milan Tichý	Faculty of Mathematics and Physics, Charles University, Prague

Scientific and Technical Advisory Committee

Jan Stöckel	Institute of Plasma Physics, Academy of Sciences of the Czech Republic
Karel Šplíchal	Nuclear Research Institute pl.s., Řež

Administration and Finance Advisory Committee

Pavol Pavlo	Institute of Plasma Physics, Academy of Sciences of the Czech Republic
-------------	--

EFDA Steering Committee

Jan Dobeš	Institute of Nuclear Physics, Academy of Sciences of the Czech Republic
Jan Kysela	Nuclear Research Institute pl.s., Řež

Committee for Fusion Industry

Jan Musil	Škoda Power, Plzeň
-----------	--------------------

2 Manpower and Budget

Manpower Analysis of the Association EURATOM/IPP.CR 2005

Institution	STAFF, PY			STAFF, Person					
	Physics	Technology	TOTAL	Female	Male	Prof.	Non-Prof.	TOTAL	Total, %
IPP	23.93	3.48	27.41	6	40	34	12	46	47.4
FMP	2.40	0	2.40	0	7	7	0	7	7.2
IAM	0	1.80	1.80	0	2	1	1	2	2.1
JHIPC	1.80	0	1.80	1	4	5	0	5	5.2
FNSPE	0.80	0.50	1.30	0	4	4	0	4	4.1
NRI	0	6.15	6.15	3	15	15	3	18	18.6
NPI	0	8.45	8.45	1	14	9	6	15	15.4
TOTAL	28,93	20,38	49,305	11	86	75	22	97	
Total, %	58.7	41.3							100.0

Expenditures 2005

	Euro
Physics	784 923
Underlying Technologies	189 919
Inertial Fusion Energy	18 366
Sub-total	993 208
Technology tasks Art 5.1a	884 824
Technology tasks Art 5.1b	296 673
EFDA Article 6.3 Contracts	1 412
EFDA Article 9 - secondment to Garching	32 172
EFDA Article 9 - secondment to Culham	14 089
Sub-total	1 229 170
Mobility Actions	51 411
TOTAL	2 273 789

3 International Collaboration

Collaborative Projects 2005

PROJECT NO.1: Fluctuation measurements and edge plasma biasing

Measurement of the edge fluctuations by Langmuir probe arrays in ohmic regime and in discharges with the edge plasma biasing, searching for zonal flows. Measurement of Reynolds stress in the edge of a tokamak, without or with biasing - comparison of CASTOR and TEXTOR.

Collaborating Associations:

- CEA Cadarache
- Etat Belge (RMS + Ghent University)
- ENEA - Consorzio RFX, Padova
- CIEMAT
- IST
- HAS
- OAW – Innsbruck University

PROJECT NO. 2: Development of advanced probes

Development of advanced probes for edge plasma diagnostics, such as the tunnel probe for electron and ion temperature measurements, Gundestrup probe for flow measurements and emissive/ ball-pen probes for direct measurements of plasma potential, probes for the Reynolds stress etc. Development of numerical simulation tools to model the interaction of the probes with the scrape-off layer.

Collaborating Associations:

- CEA Cadarache
- Etat Belge (RMS + Ghent University)
- ENEA - Consorzio RFX, Padova
- OAW – Innsbruck University
- CIEMAT
- IST

PROJECT NO. 3: Edge plasma measurements on Tore Supra

Measurements of the edge plasma parameters (electron temperature, density, ion temperature and ion flows) in large - scale devices (Tore Supra, JET) and interpretation of *experimental data*.

Collaborating Associations:

- CEA Cadarache
- JET

PROJECT NO. 4: Edge plasma modelling

Modelling of the particle transport (bulk ions + impurities) at the plasma edge and comparison with experiment.

Collaborating Associations:

- ÖAW (Innsbruck Uni)
- VR – Alfvén Laboratory

PROJECT NO. 5: Multilateral cooperation on impurity transport

The aim of this project is to improve our knowledge of impurity behaviour in tokamaks (specially TCV and JET) and strengthen the physics basis to allow extrapolations to reactor conditions.

Collaborating Associations:

- Confederation Suisse
- HAS
- ENEA – Consorzio RFX

PROJECT NO. 6: EBW on MAST and CASTOR

Modelling of the conversion of Electron Bernstein Waves and comparison of the results with measurements of microwave radiation by means of radiometers.

Collaborating Associations:

- UKAEA

PROJECT NO. 7: Generation of fast particles in front of LH grills and ICRH antennae

Modeling of the generation of fast particles in front of Lower Hybrid (LH) grills and ICRH antennae and comparison of results with experiments.

Collaborating Associations:

- CEA Cadarache
- TEKES
- OAW (Innsbruck Uni)
- JET
- IPP Garching

PROJECT No. 8: Ion-surface Interactions

Studies of interaction of molecular ions with fusion-relevant surfaces

Collaborating Associations:

- OAW (Innsbruck Uni)

PROJECT NO. 9: Nuclear data for IFMIF

Measurement of activation cross sections for EUROFER constituents at neutron energies below 35 MeV.

Collaborating Associations:

- FZ Karlsruhe
- ENEA Frascati

4 Main Facilities

The CASTOR Tokamak

The CASTOR tokamak is a small device built in the year 1958 in the Kurchatov Institute in Moscow, which has been in operation in the IPP Prague since 1977. The vacuum vessel and plasma control systems were substantially reconstructed in the year 1985. The basic characteristics of the device are:

Major radius	40 cm
Minor radius	8,5 cm
Toroidal magnetic field	0,5-1,5 T
Plasma current	5-20 kA
Pulse length	<50 ms
Working gas	Hydrogen

The vacuum vessel (minor radius 100 mm) is made of stainless steel. The plasma cross section is defined by the poloidal limiter made of Molybdenum. Auxiliary microwave power ($f=1.25\text{GHz}$, $P=40\text{kW}$) can be injected into the ohmic plasma via a multijunction grill for non-inductive current drive. A graphite electrode is routinely used to polarize the edge plasma.

A great advantage of CASTOR is its flexibility. Good quality plasma discharges can be achieved within 1-2 days after opening the vessel to atmospheric pressure which makes it ideal for testing new diagnostics. Up to 70 reproducible discharges can be achieved during one experimental day. Typical plasma parameters are:

Central electron temperature	100-300 eV
Central ion temperature	50-100 eV
Line average density	$0.5-3 \cdot 10^{19} \text{ m}^{-3}$
Energy confinement time	<1 ms

Diagnostics:

- Magnetic diagnostics
- Microwave interferometer at 70GHz
- Photomultipliers with interference filters for measurement of hydrogen and light impurities lines
- VUV spectrometer Seya-Namioka with a high spatial resolution
- XUV spectrometer with multi-layer mirror as disperse element
- Bolometer array for measurements of radiation losses
- Langmuir probe arrays for edge plasma monitoring both in radial and poloidal directions
- Advanced probes for measurements of ion and electron temperatures, plasma potential, and flows in the edge plasma
- Array of coils for measurement of magnetic fluctuations
- Radiometer of electromagnetic radiation at 17-27 GHz and 27-40 GHz
- Microwave reflectometer at 29, 33, and 35 GHz
- Charge exchange analyzer for measurement of ion temperature

Measured signals are digitalized by several A/D converters. Basic data (24 channels) are digitalized with the sampling frequency 40 kHz. For fluctuation data, the digitizers with a higher sampling frequency (80 channels, 1 MHz) are used. Data are stored in a database and processed *a posteriori* either by IDL or Matlab based software.

NRI Fission reactor LVR-15

LVR-15 is a light water moderated and cooled tank nuclear reactor with forced cooling, operated by the Nuclear Research Institute in Rez . The maximum power of the reactor is 10 MW. The reactor core is situated in the reactor vessel (outer diameter 2300 mm, total height of the vessel 6235 mm), which is made of stainless steel, the internal part of the reactor are made of an aluminium alloy. The reactor has a forced circulation of the coolant. The generated heat is transported via three cooling circuits to the river.

The irradiation capacity

Main irradiation channels	Thermal neutron flux density (cm⁻².s⁻¹)
Irradiation channels 60 mm in fuel	1.10 ¹⁴
Irradiation channels 60 mm, core periphery	7.10 ¹³
Irradiation channels 60/40 mm in reflector	3-5.10 ¹³
Horizontal channels 100/60 mm	1.10 ⁸
Graphite thermal column	1.10 ¹¹
High pressure water loop	5.10 ¹³
Doped silicon facility	1.10 ¹³

The irradiation facilities are complemented with well-equipped hot cells, which allow the irradiated specimens handling.

Experimental facilities: Light water loops

RVS-3: The loop is designed for material and radioactivity transport investigation under PWR/VVER conditions. It enables the performance of irradiation experiments over a wide range of operational parameters limited by the following maximum parameters:

Pressure	16,5 MPa
Temperature	345°C
Water flow rate	10 000 kg/hour
Neutron flux	10 ¹⁸ n/m ² .s ⁻¹
Electrical capacity heat	100 kW

BWR-1: The loop is designed for the investigation of structural materials behaviour and radioactivity transport under BWR conditions

Pressure	10 MPa
Temperature	300°C
Water flow rate	2 000 kg/hour
Neutron flux	10 ¹⁸ n/m ² .s ⁻¹

BWR-2: The loop is designed for material research simulating conditions of BWR reactors

Pressure	12 MPa
Temperature	300°C
Water flow rate	1 000 kg/hour
Force applied to the specimen	152 kN
Duration of the specimen loading cycle	30 hours
Working fluid	ultra-pure water

The NPI cyclotron-based Fast Neutron Facility (NPI FNF)

The project of the International Fusion Material Irradiation Facility (IFMIF) aims to provide neutron irradiation tests of fusion materials at fusion-reactor relevant fluency. For testing the neutronic calculations of the IFMIF test cell, the NPI cyclotron-based Fast Neutron Facility (FNF) provides neutron beams with the IFMIF-like spectrum – the only such source operated within the EU s.

Accelerator

The variable-energy cyclotron U-120M (K=40) of the Nuclear Physics Institute Rez is a versatile machine operating in both positive and negative regimes and accelerating light particles with the mass-to-charge ratio $A/Z = 1-2.8$. Accelerated beams and energy ranges are shown in the Table 1.

Table 1. *Beam parameters of the cyclotron U-120M*

Accelerated ions	H(+)	D(+)	³ He(++)	⁴ He(++)	H(-)	D(-)
Energy range (MeV)	10 - 24	10 - 17	17 - 53	20 - 40	10 - 37	10 - 18
Internal beam current (μA)	100	80	40	40	40 -15	25 -10
External beam current (μA)	3	3	3	3	40 -15	25 -10

The beam-line system with ion-optic equipment and target stations consists of three lines in the experimental hall (positive-ion mode, extraction by the deflection system) and one line in the cyclotron hall (negative-ion mode, extraction by the stripping-foil method). Two of them are dedicated to fast-neutronic experiments within the IFMIF project.

Neutron-spectrometry facility NG1

The cross-section data of neutron emitting reactions induced by charged-particle beams on investigated nuclides are experimentally investigated at the NG1 target station. The angular distributions of emitted fast neutrons (in the energy range from 0.7 to 35 MeV) are measured by the scintillator pulse-height unfolding technique based on the n-gamma discrimination hardware and many-parameter data-acquisition on PC. A different target technique (including solid, liquid and gas samples) can be utilized on the NG1 target station. To conduct the benchmark tests of neutron-transport calculations provided for fusion relevant materials the neutron source reactions $D_2O(^3He, xn)$ and $D_2O(p, xn)$ were investigated and for the first time employed as the best simulation of the IFMIF spectrum.

High-power neutron beam facility NG2

To reach a high-fluence neutron field for the activation-cross-section benchmark tests relevant to IFMIF neutronic calculations, a novel fast-neutron source was developed taking advantage in high beam current of a negative-ion mode of cyclotron operation. With this aim, the proton-induced reaction on a heavy-water flow target was investigated for the first time and utilized for the NG2 target station. Further, the standard Be-targets for protons and deuterons of the NG2 beam line are routinely operated as well. The white-spectrum neutron fields with an energy range up to 35 MeV and a flux density up to 3×10^{11} n/cm²/s are available for irradiation purposes.

Overview of Activities - PHYSICS

The main areas of the research undertaken in the Association EURATOM/IPP.CR in 2005 were as follows:

1. Edge Plasma, Plasma-Wall Interaction and Magnetic Confinement Physics
2. Diagnostics Development
3. Wave Interactions in Plasmas
4. Atomic Physics and Data for Edge Plasma and Plasma Wall Interactions

Here, the most important results, activities and achievements are briefly summarized; details are given in sections II.1 – II.5 following the list of publications.

1.

A clear and reproducible transition to a regime with improved particle confinement is routinely observed, if the biasing electrode is inserted deep enough into the plasma ($r/a \approx 0.5$) of the CASTOR tokamak and biased up to +250V. Steepening of the radial profiles of the plasma density and potential demonstrate the formation of a transport barrier just inside the last closed flux surface. Fast relaxations of the edge profiles, with a frequency of about 10 kHz are observed when the value of the average radial electric field within the barrier reaches values of about 20 kV/m and the density gradient increases up to a factor 3 with respect to the ohmic phase [16, 41].

Investigation of Hydrogen retention in metallic membranes in a tokamak environment: Group V metals are capable of hydrogen particle absorption. Experiments with Nb and V have been performed in the CASTOR tokamak to investigate the role of nonmetallic coatings upon plasma-facing materials, and to develop a method of the registration and diagnostic of the flux of suprathreshold hydrogen. The possibility of a reliable registration of suprathreshold hydrogen was demonstrated in spite of the short plasma pulse duration and a relatively high background H_2 pressure. Composition of the hydrogen flux (molecules, atoms, ions) impinging on the tokamak walls was analyzed, including the ion energy distribution [36].

Temporal and spatial evolution of the light impurities emission was investigated on the CASTOR tokamak by the VUV imaging spectrometer coupled with fast, 1 kHz, detection imaging system in the plasma periphery. Temporal measurements of the radial profile behaviour of the chord-integrated line intensity were mostly performed in the spectral range of 90-130 nm. In a fixed tilting position of the spectrometer, the imaging of $Ly\alpha$ H I (121.6 nm) and O VI (103.2 nm, 103.7 nm) emission was created and analysed. In some "polarized discharges", a flat maximum of the $Ly\alpha$ and O VI emission power has been observed near the biasing electrode. This maximum moves in the radial direction from the electrode to the column centre with a velocity about 10 m/s. Since the line emission power is influenced by the "local" electron density, the observed density perturbation is probably caused by neutrals escaping the electrode during the biasing [40].

Carbon impurity transport studies in the TCV tokamak: The 4-channel ultrasoft X-ray (USX) monochromator on TCV was modified for radial emission profile measurements in specially designed, radially swept discharges. The results show that the line integrated radial emission profiles provide a significant constraint for determining the diffusion coefficient in the outer part $r_{\text{pol}} > 0.6$ of the discharge. A series of discharges in different conditions shows that there is no simple proportionality between the Carbon ion diffusion coefficient and the effective heat diffusivity. The currently used instrument was only intended as a feasibility demonstration and is not adapted for routine measurements of ionisation balance.

Modelling of magnetic equilibria and current drive expected in the COMPASS-D tokamak: In the course of 2005 we started preparing for the installation of the COMPASS-D tokamak (major radius=0.56 m, minor radius=0.2 m, $B_t = 1.2$ T, $I_p = 0.2$ MA) at IPP Prague, by activating locally the ACCOME equilibrium and current drive modelling code. The first task was to set up free-boundary magnetic equilibria sustained by the COMPASS-D plasma current and poloidal field coils, and then assess the plasma performance with the planned lower hybrid (LH) and neutral beam injection (NBI) systems (the LH system provides $P_{\text{LH}} = 0.4$ MW at refractive index $n_{\parallel} = 2.1$ and $f_{\text{LH}} = 1.3$ GHz, and the NBI system has two 40 keV deuterium beams, for unbalanced injection in co- or counter-directions with a total power of 0.6 MW, as well as in balanced injection). Our principal results are thus the expected equilibria and the LH and NB power deposition profiles and driven currents.

The behaviour of plasma-sprayed tungsten-based coatings was studied in the tokamak CASTOR plasma (30 ms discharge, 30 kW ohmic heating). Biasing of certain samples was applied to increase electron and ion interaction with the sample surface. The Imaging VUV Seya-Namioka Spectrometer monitored radial profiles of the impurity line intensities with 1 ms temporal resolution (HI 102.6 nm and 121.6 nm, CIII 97.7 nm and 117.3 nm, NIII 99.0 nm and 107.9 nm, OVI 103.2+103.7 nm). The solid target surface becomes a source of hydrogen and low-Z atoms due to the recombination of the plasma ions and the re-erosion of deposited impurity layers on the coating surface. A tungsten inflow seen at the W I line at 400.9 nm was significant only during arcing. The tested tungsten coatings are suitable for covering different edge plasma diagnostics because of their low surface erosion and negligible influence on the discharge parameters [14, 18, 40, 43].

2.

A new magnetic probe diagnostics based on Hall sensors was put in operation on CASTOR as an intermediate step prior to in-vessel installation of such a system on Tore Supra. The magnetic field vector was measured well within the plasma confinement region of CASTOR. Errors of the measurement caused by imperfect alignment of the probe head were analyzed and corrected. A significant remaining magnetic field up to 5 mT due to eddy currents persists in the tokamak chamber up to 300 ms after the termination of the discharge. The radial profile of the magnetic field factor was measured on a shot to shot basis up to $r = 57$ mm. The measured profile of q is consistent with theoretical expectations assuming the downward shift of the plasma column by 8 mm and a rather flat current density profile with a peaking factor of 0.6 [31].

Ball-pen probe was optimized for direct measurements of the plasma potential on the CASTOR tokamak. An effect of secondary electron emission and photoemission from the collector on the probe performance was not observed. Direct measurements of the electron temperature have been performed by using a combination of the ball-pen and Langmuir probe. Numerical PIC simulations provide the I-V characteristics of the ball-pen probe for different collector positions. The probe behaviour is in good agreement with theoretical assumptions [9].

Segmented tunnel probe: The ion temperature is a particularly important but rarely measured plasma boundary characteristic. We present a new electric probe, the segmented tunnel probe (STP), which measures the ion temperature, electron temperature, and the parallel ion current density simultaneously and with a high temporal resolution. The probe was built and successfully tested in the CASTOR tokamak. The STP was operated in a Mach-probe arrangement in a DC mode, providing bi-directional measurements, and radial profiles of the ion temperature in the CASTOR tokamak have been obtained [50].

Two arrays of fast AXUV-based bolometers were installed on the CASTOR tokamak in mutually perpendicular directions. A temporal resolution of 1 ms and a spatial resolution of 1 cm were reached. Asymmetrical Abel inversion is used for a 1-D reconstruction of the radiation profile at each time step and the 2-D tomography based on the Cormack method is under implementation at present. Usage of fast bolometers is very suitable for analyses of the edge plasma biasing experiments, in which very fast oscillations (10-50 kHz) were observed. These oscillations affect the radiation width and the intensity in the opposite ways so that the total radiated power remains constant. Radiation from the edge plasma region is influenced by turbulent events. Subtracting the mean value from a bolometric signal, changes of radiation caused by turbulence can be visualized. Cross-correlation and multifractal analyses were used to get information on their presence, lifetime and poloidal rotation frequency [16, 18, 29, 30, 41, 43].

The first version of an original three-dimensional code for simulation of the processes in high-temperature plasma in the presence of magnetic field was successfully tested [65-68]. The code is intended mainly to improve the interpretation of probe measurements.

An antenna for oblique reception was constructed in support of experimental studies of the ECE - EBW conversion. However, the radiometry experiments on CASTOR have not been successful so far since the antenna turned out to be not selective enough to suppress the background radiation which overlaps the ECE. The antenna receives the radiation from a too wide space angle, probably due to the reflections on the tokamak chamber close to the antenna mouth. Therefore, the design of the antenna will have to be reconsidered.

3.

Modeling of tokamak edge plasma flows and interpretation of probe diagnostics in the presence of suprathermal electrons by the quasineutral particle-in-cell (QPIC) method resulted in four separate themes as follows:

- Calibration of QPIC using known kinetic results, and extension of Mach probe theory for a double Maxwellian;
- Interpretation of Langmuir probe diagnostics in the presence of LH-generated supra-thermal electrons [33], and the study of fast electrons near ion cyclotron antennas [38];
- Measurements, supported by computation, of scrape-off layer flows in the Tore Supra tokamak [81];
- Development of a novel integration technique for the particle equations of motion in QPIC [63].

Measurements in front of the CASTOR LH grill, using a double, movable, emissive probe, confirmed formation of radially narrow layer with a negative drop of the cold probe floating potential, while the floating potential of the heated probe (i.e. plasma potential) near to the grill is increasing [1,2]. This fact can be taken as experimental evidence of the edge plasma electrons' acceleration just in this layer, with a successive escape of these electrons along the magnetic field lines. Certain changes of the toroidal electric field just in this interaction region have been also observed. Assessment and design of two double RF probes for the new Tore Supra launcher C4 have been done. The flange with four RF glass sealed 50 Ohm feed-

throughs for transmitting the RF probes signal from Tore Supra has been already manufactured and tested in IPP [11], [44].

Electron Bernstein Waves: During the last few years, we developed a code for simulation of the EBW emission from spherical tokamaks, specially, from MAST and NSTX. On MAST, we found a good agreement between the simulation of the EBW emission and the detected signals for L-modes and ELMy H-modes. On the other hand, the emission from ELM free H-modes in MAST suggests that the magnetic field in the transport barrier as determined by EFIT is too low [55, 42]. The code has been further improved [57], and upgraded to full 3D geometry to allow the study of EBW propagation in stellarators.

Fast particle energy measurements by RFA in Tore Supra: A retarding field analyzer (RFA) was used during lower hybrid (LH) current drive experiments in the Tore Supra tokamak, to measure the flux of supra-thermal particles emanating from the near-field region in front of the LH grill mouth. For the first time, qualitative data about the accelerated electron distribution function were obtained. The radial location of the most energetic electrons in the beam is about 1 cm shifted radially into the plasma. The RFA measurements indicate that the fast electron beam is generated at a distance of 1 or 2 cm in front of the LH grill.

Electron acceleration near ICRF antennas: A novel process of electron acceleration near the ICRF antenna, the physics of which is similar to the well-known electron acceleration process in front of LH grills, was identified and explored. It was demonstrated that thermal electrons can be accelerated to energies of several keV, when moving along magnetostatic field lines near an ICRF (Ion Cyclotron Resonance Frequency) antenna. The electron can gain energy in passing the near antenna rf field inhomogeneity, because of the temporal phase changes of the field, which do not average out on the electron quiver motion time scale. The fast electrons can then produce hot spots directly, or indirectly by enhancing the sheath potential and in turn the ion acceleration in the sheath.

4.

Collisions of slow (10-50 eV) hydrocarbon ions $C_3H_n^+$ ($n=2-8$) and dication/cation ions $C_7H_m^{2+/+}$ ($m=8,7,6$) with room-temperature and heated (600°C) carbon surfaces were studied by the scattering method. The ion survival probability for ions incident on the surface under 30° was about 1-10% for usually closed-shell ions ($C_3H_7^+$, $C_3H_5^+$, $C_3H_3^+$; $C_7H_7^+$), about 0.5-2% for radical cations ($C_3H_8^+$, $C_3H_6^+$), and much smaller for non-hydrocarbon ions (Ar^+ 0.002 %, CO_2^+ 0.0015%). For dications ($C_7H_m^{2+}$), the survival probability was about twice as high as for the respective cations. Product ions originated from simple fragmentation of the projectile ions or from chemical reactions of H-atom transfer between radical cations and surface hydrocarbons on room-temperature surfaces. The ions were formed in inelastic collisions with 45 % (room-temperature surfaces) or 66 % (heated surfaces) of incident energy in translational energy [71-76].

LIST OF PUBLICATIONS 2005 – PHYSICS

- [1] **Devynck P., Bonhomme G., Martines E., Stöckel J., Van Oost G., Voitsekhovitch I., Adámek J., Azeroual A., Doveil F., Duran I., Gravier E., Gunn J., Hron M.:** Spatially resolved characterization of electrostatic fluctuations in the scrape-off layer of the CASTOR tokamak. *Plasma Phys. Control. Fusion* **47** (2005) 269.
- [2] **Stöckel J., Devynck P., Gunn J., Martines E., Bonhomme G., Voitsekhovitch I., Van Oost G., Hron M., Duran I., Stejskal P., Adámek J., Weinzettl V., Žáček F.:** Formation of convective cells during scrape-off layer biasing in the CASTOR tokamak. *Plasma Phys. Control. Fusion* **47** (2005) 635.
- [3] **Pánek R., Gunn J.P., Bucalossi J., Duran I., Geraud A., Hron M., Loarer T., Pégourié B., Stöckel J., Tsitrone E.:** The response of the Tore Supra edge plasma to different gas fueling techniques. *Journal of Nuclear Materials* **337-339** (2005) 530.
- [4] **Sánchez E., Hidalgo C., Gonçalves B., Silva C., Pedrosa M.A., Hron M., Erents K.:** On the energy transfer between flows and turbulence in the plasma boundary of fusion devices. *Journal of Nuclear Materials* **337-339** (2005) 296.
- [5] **Pitts R.A., Andrew P., Bonnin X., Chankin A.V., Corre Y., Corrigan G., Coster D., Duran I., Eich T., Erents S.K., Fundamenski W., Huber A., Jachmich S., Kirnev G., Lehnen M., Lomas P.J., Loarte A., Matthews G.F., Rapp J., Silva C., Stamp M.F., Strachan J.D., Tsitrone E. and contributors to the EFDA-JET Workprogramme:** Edge and divertor physics with reversed toroidal field in JET. *Journal of Nuclear Materials* **337-339** (2005) 146.
- [6] **Sedláček Z.:** A study of the non-linear Landau damping in the Fourier transformed velocity space. *Transport Theory and Statistical Phys.* **34** (2005) 63.
- [7] **Nanobashvili S., Žáček F., Zajac J.:** Microwave correlation reflectometry for tokamak CASTOR. *Czech. J. Phys.* **55** (2005) 701.
- [8] **Pánek R., Krlín L., Tendler M., Tskhakaya D., Kuhn S., Svoboda V., Klíma R., Pavlo P., Stöckel J., Petržílka V.:** Anomalous ion diffusion and radial electric field generation in turbulent edge plasma potential weakly correlated in time and space. *Physics Scripta* **72** (2005) 327-332.
- [9] **Adámek J., Duran I., Hron M., Pánek R., Stöckel J., Balan P., Schrittwieser R., Ionota C., Martines E., Tichý M., Van Oost G.:** Comparative measurements of the plasma potential with the ball-pen and emissive probes on the CASTOR tokamak. *Czech. J. Phys.* **55** [3] (2005) 235.
- [10] **Gryaznevich M.P., Del Bosco E., Malaquias A., Mank G., Van Oost G., Yexi He, Hegazy H., Hron M., Hirose A., Kuteev B., Ludwig G.O., Nascimento I.C., Silva C. and Vorobyev G.M.:** Joint research using small tokamaks. *Nucl. Fusion* **45** (2005) S245.
- [11] **Žáček F., Petržílka V., Goniche M.:** Positive biasing of plasma in front of LH antennae. *Plasma Phys. Control. Fusion* **47** (2005) L17.
- [12] **Rantamäki K.M., Petržílka V., Andrew P., Coffey I., Ekedahl A., Erents K., Fuchs V., Goniche M., Granucci G., Joffrin E., Karttunen S.J., Lomas P., Mailloux J., Mantsinen M., Mayoral M.-L., Mc Donald D.C., Noterdaeme J.-M., Parail V., Tucillo A.A., Žáček F. and Contributors to the EFDA-JET Programme:** Bright Spots Generated by Lower Hybrid Waves on JET. *Plasma Phys. Control. Fusion* **47** (2005) 1101.
- [13] **Polosatkin S., Burdakov A., Piffil V., Postupaev V., Weinzettl V.:** Investigation of impurity dynamics at GOL-3 facility. *Transaction of Fusion Science and Technology* **47** [1T] (2005) 267.
- [14] **Matějčíček J., Koza Y., Weinzettl V.:** Plasma sprayed tungsten-based coatings and their performance under fusion relevant conditions. *Fusion Engineering and Design* **75-79** (2005) 395.
- [15] **Taylor G., Efthimion P.C., LeBlanc B.P., et al.:** Efficient coupling of thermal electron Bernstein waves to the ordinary electromagnetic mode on the National Spherical Torus Experiment. *Physics of Plasmas* **12** [5] (2005) Art. No. 052511.

- [16] Spolaore M., Martines E., Brotánková J., Stöckel J., Adámek J., Dufková E., Ďuran I., Hron M., Weinzettl V., Peleman P., Van Oost G., Devynck P., Figueiredo H., Kirnev G.: Relaxation phenomena induced by edge plasma biasing experiments in the CASTOR tokamak. *Czech. J. Phys.* **55** (2005) 1597.
- [17] Zajac J., Dufková E., Weinzettl V., Budaev V.P., Nanobashvili S.: Multifractal analysis of plasma turbulence in biasing experiments on CASTOR tokamak. *Czech. J. Phys.* **55** (2005) 1615.
- [18] Weinzettl V., Piffl V., Matějčiček J., Dufková E., Zajac J., Dejarnac R., Peřina V.: The effect of the use of different electrode materials for edge plasma biasing on plasma density and floating potential modifications. *Czech. J. Phys.* **55** (2005) 1607.
- [19] Counsell G.F., Akers R.J., Appel L.C., Applegate D., Axon K.B., Baranov Y., Brickley C., Bunting C., Buttery R.J., Carolan P.G., Challis C., Ciric D., Conway N.J., Cox M., Cunningham G., Darke A., Dnestrovskij A., Dowling J., Dudson B., Dunstan M.R., Delchambre E., Field A.R., Foster A., Gee S., Gryaznevich M.P., Helander P., Hender T.C., Hole M., Howell D.H., Joiner N., Keeling D., Kirk A., Lehane I.P., Liso S., Lloyd B., Lott F., Maddison G.P., Manhood S.J., Martin R., McArdle G.J., McClements K.G., Meyer H., Morris A.W., Nelson M., O'Brien M.R., Patel A., Pinfold T., Preinhaelter J., Price M.N., Roach C.M., Rozhansky V., Saarelma S., Saveliev A., Scannell R., Sharapov S., Shevchenko V., Shibaev S., Stammers K., Storrs J., Sykes A., Tabasso A., Tallents S., Taylor D., Tournianski M.R., Turner A., Turri G., Valovic M., Volpe F., Voss G., Walsh M.J., Watkins J.R., Wilson H.R., Wisse M., MAST Team, NBI Team, ECRH Team: Overview of MAST results. *Nuclear Fusion* **45** [10] (2005) S157.
- [20] Gunn J.P., Pánek R., Stöckel J., Van Oost G., Van Rompuy T.: Simultaneous measurements of fluctuations of ion current, electron temperature, and floating potential with a tunnel probe. *Czechoslovak Journal of Physics* **55** [3] (2005) 255.
- [21] Mlynar J., Adams J.M., Bertalot L., Conroy S.: First results of Minimum Fisher Regularisation as unfolding method for JET NE213 liquid scintillator neutron spectrometry. *Fusion Engineering and Design* **74** [1-4] (2005) 781.
- [22] Fuchs V.: Asymptotic treatment of the three-wave nonlinear parametric interaction. *Journal of Plasma Physics* **71** (2005) Part 2, 151.
- [23] Ekedahl A., Granucci G., Mailloux J., Baranov Y., Erents S.K., Joffrin E., Litaudon X., Loarte A., Lomas P.J., McDonald D.C., Petržílka V., Rantamäki K., Rimini F.G., Silva C., Stamp M., Tuccillo A.A. and JET EFDA Contributors: Long distance coupling of lower hybrid waves in JET plasmas with edge and core transport barriers. *Nucl. Fusion* **45** (2005) 351.
- [24] Tuccillo A.A., Barbato E., Bae Y.S., Bécoulet A., Bernabei S., Bibet P., Calabrò G., Cardinali A., Castaldo C., Cesario R., Cho M.H., Cirant S., Crisanti F., Ekedahl A., Eriksson L-G., Farina D., Giruzzi G., Goniche M., Granucci G., Ide S., Imbeaux F., Karttunen S., Litaudon X., Mailloux J., Mazon D., Mirizzi F., Moreau D., Nowak S., Namkung W., Panaccione L., Pericoli-Ridolfini V., Peysson Y., Petržílka V., Podda S., Rantamäki K., Santini F., Saveliev A., Schneider M., Sozzi C., Suzuki T.: Progress in LHCD: a tool for advanced regimes on ITER. *Plasma Phys. Control. Fusion* **47** (2005) B363 (invited talk at 32 EPS Tarragona).
- [25] Preinhaelter J., Urban J., Vahala L., Vahala G., Taylor G.: Time Development of Electron Cyclotron Emission in NSTX. *2005 International Sherwood Fusion Theory Conference*, 11-13 Apr, 2005, Stateline, Nevada, USA, P1-40.
- [26] Adámek J., Stöckel J., Schrittwieser R., Ionita C., Tichý M., Van Oost G.: Direct Measurements of the Electron Temperature by a Ball-pen/Langmuir probe. *32nd EPS Conference on Plasma Physics and Controlled Fusion*, Tarragona, 27 June - 1 July 2005, ECA Vol.29C, P5.081.
- [27] Bencze A., Berta M., Zoletnik S., Stöckel J., Adámek J., Hron M.: Detection of radially localized and poloidally symmetric structures in the poloidal flow of tokamak plasmas. *Ibid.*, P-5.022
- [28] Brotánková J., Stöckel J., Martines E., Van Oost G., Svoboda V., Görler T., Hansen T.: Fluctuation measurements with 2D matrix of Langmuir probes on the CASTOR tokamak. *Ibid.*, P-5.018.

- [29] **Budaev V.P., Dufková E., Nanobashvili S., Weinzettl V., Zajac J.:** Multifractal analysis of tokamak plasma turbulence in biasing experiments. *Ibid.*, P-5.019
- [30] **Dufková E., Weinzettl V., Sarychev D., Kočan M.:** Fast bolometry on the CASTOR tokamak. *Ibid.*, P-2.074.
- [31] **Đuran I., Hron M., Stöckel J., Sentkerestiová J., Kovařík K., Trošková Z., Viererbl L., Bolshakova I., Holyaka R., Erashok V., Moreau P.J., Saint-Laurent F., Gunn J.P.:** Magnetic field measurements using the galvanomagnetic devices on Tore Supra and CASTOR tokamaks. *Ibid.*, P-2.086.
- [32] **Dux R., Bobkov V., Kallenbach A., Krieger K., Neu R., Pütterich T., Petržílka V., Rohde V., Stober J., and ASDEX Upgrade Team:** Tungsten Erosion at Auxiliary Limiters in ASDEX Upgrade. *Ibid.*
- [33] **Fuchs V., Gunn J.P., Dejarnac R.:** Langmuir probe characteristics in the presence of supra-thermal electrons generated by a lower hybrid grill. *Ibid.*, P-4.005.
- [34] **Gonçalves B., Hidalgo C., Silva C., Pedrosa M.A., Hron M.:** Turbulence experiments in reversed and standard-B field configurations in the JET tokamak. *Ibid.*, P-4.038.
- [35] **Kočan M., Pánek R., Gunn J.P., Stöckel J., Skalný J.D.:** A new probe for ion temperature measurements in the tokamak scrape-off layer. *Ibid.*, P-2.082.
- [36] **Notkin M., Hron M., Stöckel J.:** Absorption experiments on the CASTOR tokamak. *Ibid.*, P-1.084.
- [37] **Pánek R., Krlín L., Stöckel J., Tskhakaya D. jr., Kuhn S., Pavlo P., Tendler M.:** Anomalous impurity diffusion in an experimentally measured turbulent potential. *Ibid.*, P-5.020
- [38] **Petržílka V., Fuchs V., Krlín L., Colas L., Goniche M., Heurax S., Bobkov V., Braun F., Dux R., Neu R., Noterdaeme J.M.:** Electron Acceleration Near ICRF Antennas. *Ibid.*, P-2.095.
- [39] **Petržílka V., Gunn J., Goniche M., Devynck P., Ekedahl A., Gauthier E., Pascal J.-Y., Saint-Laurent F., Žáček F.:** Fast Particle Energy Measurements in the Scrape-off Layer During Lower Hybrid Current Drive Experiments on Tore Supra. *Ibid.*, P-2.096.
- [40] **Piffl V., Weinzettl V., Burdakov A., Polosatkin S.:** Temporally and spatially resolved measurements of VUV lines intensity in the CASTOR tokamak. *Ibid.*, P-2.075.
- [41] **Spolaore M., Brotánková J., Peleman P., Devynck P., Figueiredo H., Kirnev G., Martines E., Stöckel J., Van Oost G., Adámek J., Dufková E., Đuran I., Hron M., Weinzettl V.:** Relaxation phenomena during edge plasma biasing in the CASTOR tokamak. *Ibid.*, P-4.031.
- [42] **Urban J., Preinhaelter J., Shevchenko V., Taylor G., Valovic M., Pavlo P., Vahala L., Vahala G.:** Methodology of electron Bernstein wave emission simulations. *Ibid.*, P-1.121.
- [43] **Weinzettl V., Piffl V., Matějčiek J., Dufková E., Zajac J., Peřina V.:** Biasing experiments with solid and porous electrodes. *Ibid.*, P-4.006.
- [44] **Žáček F., Petržílka V., Goniche M.:** Radial and toroidal electric field measurements in front of the CASTOR tokamak LH launcher. *Ibid.*, P-4.004.
- [45] **Adámek J., Brotánková J., Dejarnac R., Gunn J., Hron M., Ionita C., Pánek R., Schrittwieser R., Stöckel J., Tichý M., Van Oost G.:** Simultaneous measurements of the electron temperature with a ball-pen and tunnel probe. *8th Workshop on the Electric Fields, Structures, and Relaxation in Edge Plasmas*, Tarragona, Spain, July 3-4, 2005.
- [46] **Bencze A., Berta M., Zoletnik S., Stöckel J., Adámek J., Hron M.:** Detection of radially localized and poloidally symmetric structures in the poloidal flow of tokamak plasmas. *Ibid.*
- [47] **Dejarnac R., Gunn J.P., Stöckel J.:** Electron and ion side asymmetries measured by the Tunnel probe at the edge of the CASTOR tokamak. *Ibid.*
- [48] **Devynck P., Stöckel J., Brotánková J., Spolaore M., Martines E., Kirnev G., Peleman P., Van Oost G.:** The radial structure of turbulence and its dynamics in CASTOR. *Ibid.*
- [49] **Weinzettl V., Piffl V., Matějčiek J., Dufková E., Zajac J.:** Density profile modification and fast events induced by radial electric field of edge and core plasma biasing. *Ibid.*

- [50] **Kočan M., Skalný J., Pánek R., Stöckel J., Gunn J., Kuhn S.:** Particle-in-Cell Simulations of the Segmented Tunnel Probe for Ion-Temperature Measurements in the Tokamak Scrape-off Layer. *In: Proc. Int. Conference Nuclear Energy for New Europe*, Bled, Slovenia, September 5-8, 2005.
- [51] **Schrittwieser R., Ioniță C., Balan P.C., Varandas C.A.F., Figueiredo H.F.C., Silva C., Stöckel J., Adámek J., Hron M., Tichý M., Hidalgo C., Pedrosa M.A., Calderón E., Martines E., Van Oost G., Rasmussen J.J., Naulin V.:** Edge Plasma Fluctuations Measurements In Fusion Experiments. *Ibid.*
- [52] **Matějčíček J., Weinzettl V., Dufková E., Piffl V., Peřina V.:** Plasma sprayed tungsten-based coatings and their usage in edge plasma region of tokamaks. *EUROMAT 2005, FEMS, Prague, Czech Republic, September 5-8, 2005, paper # C32-482 (oral).*
- [53] **Urban J., Preinhaelter J., Taylor G., Vahala L., Vahala G.:** Simulation of ECE frequency spectra for NSTX and comparison with new radiometer results. *47th Annual Meeting of the Division of Plasma Physics*, October 24-28, 2005. Denver, Colorado.
- [54] **Taylor G., Diem S., Efthimion P.C., Ellis R.A., Fredd E., Hosea J., Wilson J.R., Bigelow T.S., Carter M.D., Caughman J.B., Jaeger F., Rasmussen D.A., Wilgen J.B., Harvey R.W., Smirnov A.P., Ershov N.M., Urban J., Preinhaelter J., Bers A., Decker J., Ram A.K.:** Electron Bernstein Wave Physics in NSTX. *Ibid.*
- [55] **Preinhaelter J., Taylor G., Shevchenko V., Urban J., Valovic M., Pavlo P., Vahala L., Vahala G.:** EBW simulation for MAST and NSTX experiments. *16th RFPP Topical Conference proceedings*, Park City, Utah USA (2005). AIP Conference Proceedings 787, (2005), pp. 349-352.
- [56] **Taylor G., Bers A., Bigelow T.S., Carter M.D., Caughman J.B., Decker J., Diem S., Efthimion P.C., Ershov N.M., Fredd E., Harvey R.W., Hosea J., Jaeger F., Preinhaelter J., Ram A.K., Rasmussen D.A., Smirnov A.P., Wilgen J.B., Wilson J.R.:** Electron Bernstein Wave Research on the National Spherical Torus Experiment. *Ibid.*, pp. 337-340.
- [57] **Urban J., Preinhaelter J.:** Adaptive finite elements for a set of 2nd order ODE's. *19th ICNSP&APPTC proceedings*, Nara, Japan (2005).
- [58] **Weinzettl V.:** disertační práce *Prostorové a časové chování lehkých nečistot ve vysokoteplotním plazmatu tokamaku CASTOR*. 25.4.2005, katedra fyzikální elektroniky Fakulta jaderná a fyzikálně inženýrská ČVUT (*PhD Thesis, in Czech*).
- [59] **Cahyna P.:** *Stochastičnost dynamiky částic v systému magnetických ostrovů tokamaku*. Diplomová práce, MFF UK Praha, 2005. (*Master Thesis, in Czech*)
- [60] **Řípa M., Weinzettl V., Mlynář J., Žáček F.:** Řízená termojaderná syntéza pro každého. 2. vydání. ČEZ, Praha 2005. (*Thermonuclear Fusion for Everybody, in Czech, 2nd Edition*).
- [61] **Bolshakova I., Brudnyi V., Ďuran I., Holyaka R., Kolin N., Leroy C., Luschikov V., Shoorygin F., Stöckel J., Viererbl L.:** Magnetic Field Sensors under Harsh Radiation Conditions of Neutron Irradiation. *Submitted to Sensors and Actuators A and B journal*
- [62] **Cahyna P., Krlín L.:** Full Hamiltonian description of the interaction of particles with magnetic islands in tokamak, *accepted in Czech. J. Phys.*
- [63] **Fuchs V. and Gunn J.P.:** On the integration of equations of motion for particle in cell codes. *Journal of Computational Physics*, *in press*, available online 21 Nov 2005.
- [64] **Urban J., Preinhaelter J.:** Adaptive finite elements for a set of 2nd order ODE's, *accepted in Journal of Plasma Physics and Controlled Fusion*
- [65] **Šimek J., Hrach R., Bařina O., Hrachová V.:** Multi-dimensional codes for particle modeling in Tokamak edge plasma. *9th European Vacuum Congress EVC-9*, Paris 5.-7.4.2005, France
- [66] **Šimek J., Hrach R.:** Multi-dimensional particle codes in modeling in low-temperature and high-temperature plasmas in the presence of magnetic field. *32 EPS Conf. on Plasma Physics*, Tarragona 27.6.-1.7.2005, Spain.
- [67] **Šimek J., Hrach R., Bařina O., Hrachová V.:** Multi-dimensional codes for particle modeling in Tokamak edge plasma. *Vacuum (in print)*.

- [68] **Šimek J., Hrach R.:** Multi-dimensional particle codes in modeling in low-temperature and high-temperature plasmas in the presence of magnetic field. *32nd EPS Conf. on Plasma Physics*, Tarragona 2005, Spain, Editors van Milligen B.Ph. and Hidalgo C., ECA Vol. 29C (2005), P-4.003.
- [69] **Holík M., Bilyk O., Marek A., Picková I., Kudrna P., Tichý M.:** Measurements with Langmuir and Emissive Probe in Magnetically Supported DC Discharge in Cylindrical Symmetry. *Proc. 15th Symp. Appl. Plasma Processes and & EU-Japan Joint Symposium on Plasma Processing*, Podbanske, Slovakia, January 15 – 20, 2005, ISBN 80-223-2018-8, pp. 175-176.
- [70] **Marek A., Holík M., Bilyk O., Picková I., Apetrei R.P., Schrittwieser R., Ionita-Schrittwieser C., Kudrna P., Tichý M.:** Magnetized Plasma in Cylindrical Coordinates – Experiment and Model. *17th Intern. Symposium on Plasma Chemistry*, Toronto, Canada, August 7-12, 2005, Abstracts and full-papers CD, abstract p.197-8, CD - ISPC-635.pdf.
- [71] **Herman Z., Märk T.D.:** Collisions of hydrocarbon ions of energies 10-50 eV with carbon surfaces: Ion survival, dissociation, chemical reactions, scattering. In: “*Data for molecular processes in edge plasmas*”, I.A.E.A. TechDoc., I.A.E.A. Vienna (*in print*).
- [72] **Herman Z.:** Studies of hydrocarbon ion collisions with carbon surfaces at IPP.CR. *EFDA Newsletter*, Vol 2005/3, p.7 (June 5, 2005).
- [73] **Jašík J., Žabka J., Feketeová L., Ipolyi I., Märk T.D., Herman Z.:** Collisions of slow polyatomic ions with surfaces: Dissociation and Chemical Reactions of $C_2H_2^+$, $C_2H_3^+$, $C_2H_4^+$, $C_2H_5^+$ and their deuterated variants $C_2D_2^+$ and $C_2D_4^+$ on room-temperature and heated carbon surfaces. *J. Phys. Chem. A* **109** (2005), p.10208-10215.
- [74] **Jašík J., Roithová J., Žabka J., Pysanenko A., Feketeová L., Ipolyi I., Märk T.D., Herman Z.:** Surface-induced dissociation of dications and cations: Collisions of dications $C_7H_8^{2+}$, $C_7H_7^{2+}$ and $C_7H_6^{2+}$ and a comparison with the respective cations $C_7H_8^+$ and $C_7H_7^+$. *Int. J. Mass Spectrom.* **249-250** (2005), p.162-170.
- [75] **Herman Z., Španěl P., Polášek M., Roithová J.:** Ion chemistry in the gaseous phase and in collisions with surfaces. *Czech J. Phys.* **55** (2005) p. 591.
- [76] **Feketeová L., Tepnual T., Grill V., Scheier P., Roithová J., Herman Z., Märk T.D.:** Surface-induced dissociation and reactions of cations and dications $C_7H_8^{+/2+}$, $C_7H_7^{+/2+}$, and $C_7H_6^{2+}$: Dependence of mass spectra of product ions on incident energy of the projectiles. *J. Phys. Chem. A* (*in print*).
- [77] **Mlynar J., Kamendje R., Borba D., Antidormi R., Orlando M.T., Carpenter C. and Casci F.:** Public Information in European Fusion Energy Research: Methods and Challenges. In: *ICENES 2005-Proceedings of the 12th International Conference on Emerging Nuclear Energy Systems*, Brussels, 21-26 August 2005, ISBN-907-69711-02 (2005); JET Preprint EFDA–JET–PR(05)27.
- [78] **Murari A., Bertalot L., Bonheure G., Conroy S., Ericsson G., Kiptily V., Lawson K., Popovichev S., Tardocchi M., Afanasyiev V., Angelone M., Fasoli A., Källne J., Mironov M., Mlynar J., Testa D., Zastrow K.D., and JET EFDA contributors:** "Burning Plasma" Diagnostics for the Physics of JET and ITER. *Plasma Phys. Control. Fusion* **47** (2005) B249-B262
- [79] **Bonheure G., Mlynar J., et al.:** 2-D spatial distribution of D-D and D-T neutron emission in JET ELMy H-mode plasmas with Tritium puff, *Proc. 32nd EPS Plasma Physics Conference*, 27 June-1 July, Tarragona, Spain.
- [80] **Bonheure G., ... Mlynar J., et al.:** Neutron Profiles and Fuel Ratio nT/nD Measurements in JET ELMy H-mode Plasmas with Tritium Puff. EFDA-JET-PR(05)06, *submitted to Nuclear Fusion*.
- [81] **Gunn J.P., Boucher C., Ďuran I., Fuchs V. et al.:** Plasma flows in the scrape-off layer of the Tore Supra tokamak. *The International Conf. PLASMA-2005 on Research and Application of Plasmas*, Opole-Turawa, Poland, 6-9 Sept., 2005, AIP Conference Proceedings **812**.

1 Edge Plasma and Magnetic Confinement Physics

Relaxation phenomena induced by edge biasing experiments in the CASTOR tokamak

J. Brotánková, J. Stöckel, J. Adámek, E. Dufková, I. Ďuran, M. Hron, V. Weinzettl

In collaboration with:

M. Spolaore, E. Martines, Consorzio RFX, Associazione EURATOM-ENEA, Padova, Italy

P. Peleman, G. Van Oost, Department of Applied Physics, Ghent University, Ghent, Belgium

P. Devynck, Association EURATOM-CEA, France

H. Figueiredo, Association EURATOM/IST, Lisbon, Portugal

G. Kirnev, Nuclear Fusion Institute, Kurchatov Institute, Moscow, Russia

Abstract

A clear and reproducible transition to a regime with improved particle confinement is routinely observed, if the biasing electrode is inserted deep enough into the plasma ($r/a \sim 0.5$) of the CASTOR tokamak and biased up to +250V. The steepening of the radial profiles of the plasma density and potential demonstrate the formation of a transport barrier just inside the last closed flux surface. Fast relaxations of the edge profiles, with a frequency of about 10 kHz are observed when the value of the average radial electric field within the barrier reaches values of about 20 kV/m and the density gradient increases up to a factor 3 with respect to the ohmic phase.

Arrangement

The biasing effects on the edge plasma parameters have been monitored by an insertable rake probe, placed on the top of the torus to measure the radial profiles of the floating potential, V_f , and the ion saturation current, I_s , with spatial resolution 2.5 mm and temporal resolution 1 μ s. The Gundestrup probe is used to measure the parallel and perpendicular Mach numbers.

Results

Typically, the line-averaged plasma density increases and H_α emission is reduced during the biasing phase of the discharge up to about a half of its value in the ohmic phase preceding the bias. The ratio $n/H\alpha$, which can be considered as an indicator of the global particle confinement time, increases by a factor of 3. A noticeable modification of the radial electric field, E_r , (from -5kV/m to +10 kV/m) and consequently of the $E \times B$ velocity radial profiles is observed and a noticeable increase of the $E \times B$ velocity shear is deduced from about $+0.5 \times 10^6$ s^{-1} to 1.0×10^6 s^{-1} . The average density gradient at biasing is more than twice that measured during the ohmic phase.

The temporally resolved measurements at the edge allowed the investigation of fast features, which are observed when the biasing electrode is immersed deep into the core plasma and biased to the voltage above +200 V. In particular, the onset of a quite regular oscillating behavior with a characteristic frequency of about 10 kHz is observed on electrostatic quantities measured at the edge, as evident from Fig. 1. The oscillations on V_f are well correlated with a bursty behavior on I_s and on the H_α signal. The onset of these oscillations suddenly appears when switching on the bias. This fact can be easily deduced from the 2-D picture (Fig. 2), which represents the time behavior of the radial profiles of V_f .

These observations are interpreted as periodic collapses of the transport barrier [1]. Two interesting features are identified:

- The collapse of the transport barrier is associated with a burst of density, which propagates radially toward the wall with a velocity of about 0.4 km/s. This is documented in Fig. 3 by conditional analysis.
- The poloidal flow velocity follows the temporal evolution of the radial electric field, as expected. It is interesting to note that the parallel flow velocity relaxes as well, however its value is in anti-phase to the poloidal velocity. This is demonstrated in Fig. 4.

More detailed study of relaxation phenomena at biasing is underway.

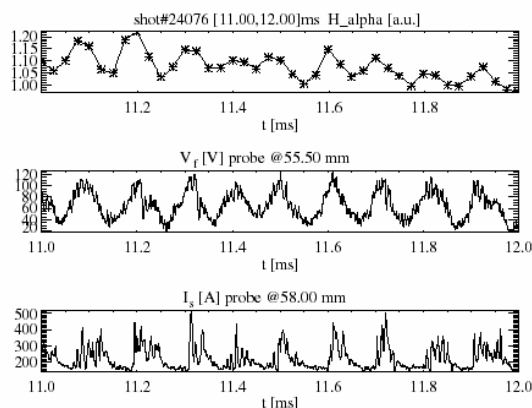


Fig. 1 Typical periodic oscillations observed on H_α (top), V_f (middle) and I_s (bottom) signals measured simultaneously.

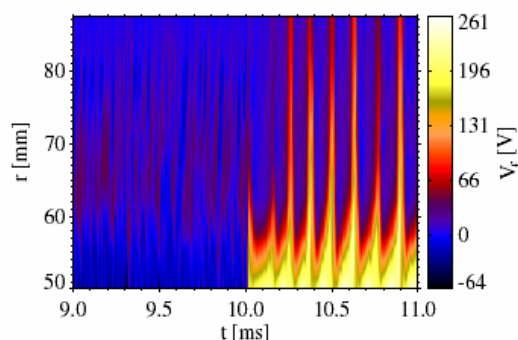


Fig. 2 Time behavior of V_f radial profile, biasing starts at 10 ms; shot#24000 [9.00, 11.00] ms.

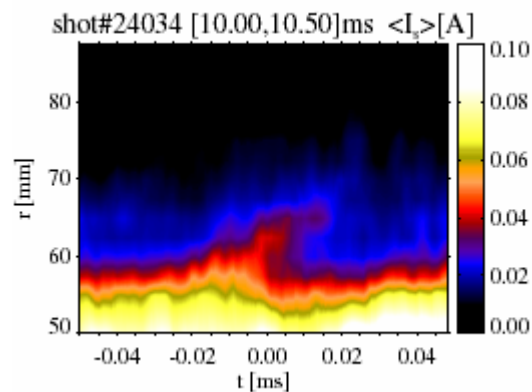


Fig. 3. Time behaviour of average radial profile of I_s obtained as the conditional average on relaxation events with 0.1ms time window width.

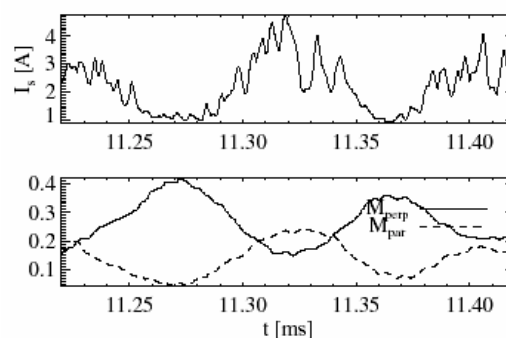


Fig. 4. Time traces of I_s (top) parallel and perpendicular Mach numbers (bottom) as deduced from Gundestrup measurements; shot #2407.

References

- [1] M. Spolaore, E. Martines, J. Brotanková, J. Stockel, J. Adamek, E. Dufková, I. Duran, M. Hron, V. Weinzettl, P. Peleman, G. Van Oost, P. Devynck, H. Figueredo, G. Kirnev, Czech. J. Phys., 55 (2005), No. 12, 1597-1606.

Hydrogen retention in metallic membranes in a tokamak environment

M. Hron, J. Stöckel

In collaboration with:

M.E. Notkin, A.I. Livshits, Bonch Bruyevich State University, Saint Petersburg, Russia

Introduction

The interactions of neutral and charged hydrogen particles with plasma facing materials is of prime importance in the present-day fusion devices, as they define D/T fuel recycling and inventory [1,2]. For that reason, measurement of hydrogen flux from plasma, its energetic distribution, and its molecular and charge composition is of a great interest.

Experiment

The measurements of hydrogen absorption from plasma were performed by an absorption probe (AP) made of a thin metallic foil. First, the probe was moved into the CASTOR, an operational hydrogen pressure was established, and a plasma shot was executed. After the exposure, the probe was moved back into a separate vacuum chamber. The amount of absorbed hydrogen was measured at H₂ thermal desorption from the probe by its heating to 1300 K, a typical example of thermodesorption curve is presented in fig. 1, curve 1. Second, the above procedure was fully repeated, but without the plasma. The number of suprathreshold hydrogen particles absorbed from the plasma is then proportional to the difference of the areas under the curves 1 and 2 (see fig. 1).

Results

The number of suprathreshold particles absorbed during the tokamak discharge, N_H , was measured as a function of AP temperature (fig. 2, curve 3). The amount of absorbed suprathreshold particles is in the range of $(1 - 3) \times 10^{16}$ H atoms and it is approximately proportional to the pulse length. The absorption coefficient α is calculated for Nb and V foils. We found that the absorption probability α for Nb and V is almost identical and it depends weakly on the probe temperature ($\alpha = 0.1-0.2$).

References

- [1] T. Tanabe et al., J. Nucl. Mater. 313-316 (2003) 478.
 [2] Y. Kubota et al., J. Nucl. Mater. 313-316 (2003) 239.

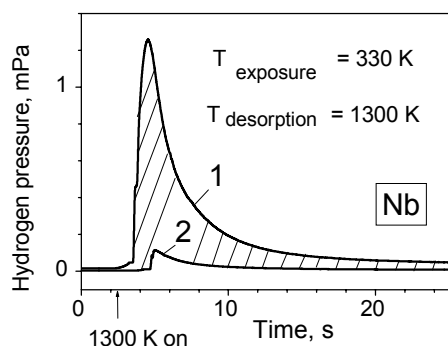


Fig. 1. Hydrogen thermodesorption from the probe. 1 – suprathreshold particles (hatched area), 2 – hydrogen molecules.

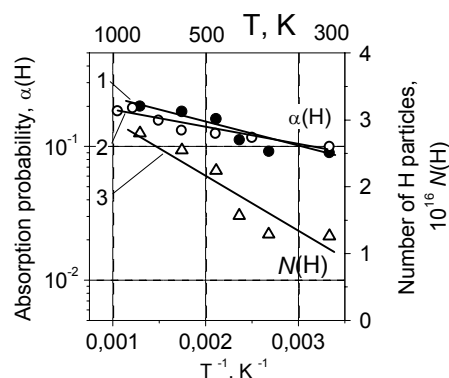


Fig. 2. Temperature dependence of hydrogen atom absorption probability (1 – vanadium, 2 – niobium) and of hydrogen accumulation during plasma discharge

Temporally and spatially resolved measurements of VUV lines intensity profile in the tokamak CASTOR

V.Piffl, V.Weinzettl

In collaboration with:

A.Burdakov, S.Polosatkin, Budker Institute of Nuclear Physics, Novosibirsk, Russia

The VUV spectroscopy study was performed in the spectral range from 90 to 130 nm during the so-called “polarized discharge”. A biasing tungsten or carbon electrode is movable in the radial direction of the plasma column and is positioned in the VUV spectrometer field of view. The biasing pulse duration is 5 – 10 ms long and can be triggered from 0 to 15 ms after the beginning of the discharge. Depending on the electrode radial position and applied biasing potential, an influence on the plasma confinement is expected. In a fixed tilting position of the spectrometer, the imaging of Ly α H I (121.6 nm) and O VI (103.2 nm, 103.7 nm) was created, Fig 1.

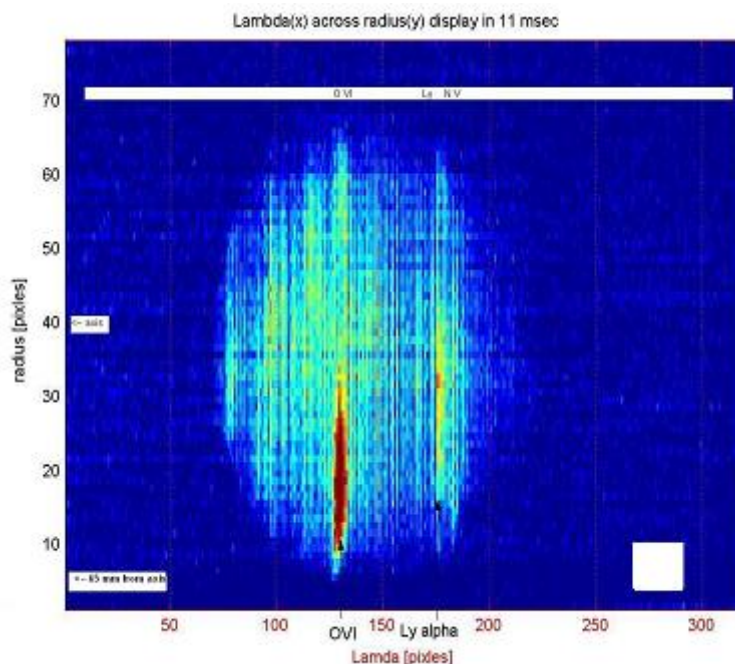


Fig. 1 The imaging of Ly α H I (121.6 nm) and O VI (103.2 nm, 103.7 nm) was created in 11 ms after discharge start in a fixed tilting position of the spectrometer

During the plasma build up, the electron density as well as the temperature grows. The content of highly ionised stages of light impurities, especially at the plasma edge, is matched to the local ionisation equilibrium influenced by transport process.

An interesting feature of the radial intensity profile behaviour during the plasma “polarized discharge” (the biasing potential, +200 V, was applied in a period from 10 to 15 ms, and the electrode was located 65 mm from the chamber axis) was observed, Fig.2. The flat maximum of the Ly α and O VI emission power moves in radial direction from the electrode to the column centre with a velocity near to 10 m/s. The line emission power is influenced by “local” electron density, and the observed density perturbation is probably caused by neutrals escaping from the electrode during the biasing.

Summary

The real possibility to analyse the spatial (radial) image of the line emission spectrum created by a VUV Imaging Spectrometer & 2D Fast Detection System in tokamak discharges has been demonstrated. The experimental data on time and spatial behaviour of line emission power which have been obtained are used for quantifying the transport behaviour and the dynamics of ionization processes of light impurities in plasma periphery. Comparing our experimental results with the STRAHL code calculations the impurity densities derived from

line radiation power measurements are $(0.5 - 1.5) \times 10^{16} \text{ m}^{-3}$ for oxygen and $(0.2 - 0.3) \times 10^{16} \text{ m}^{-3}$ for carbon.

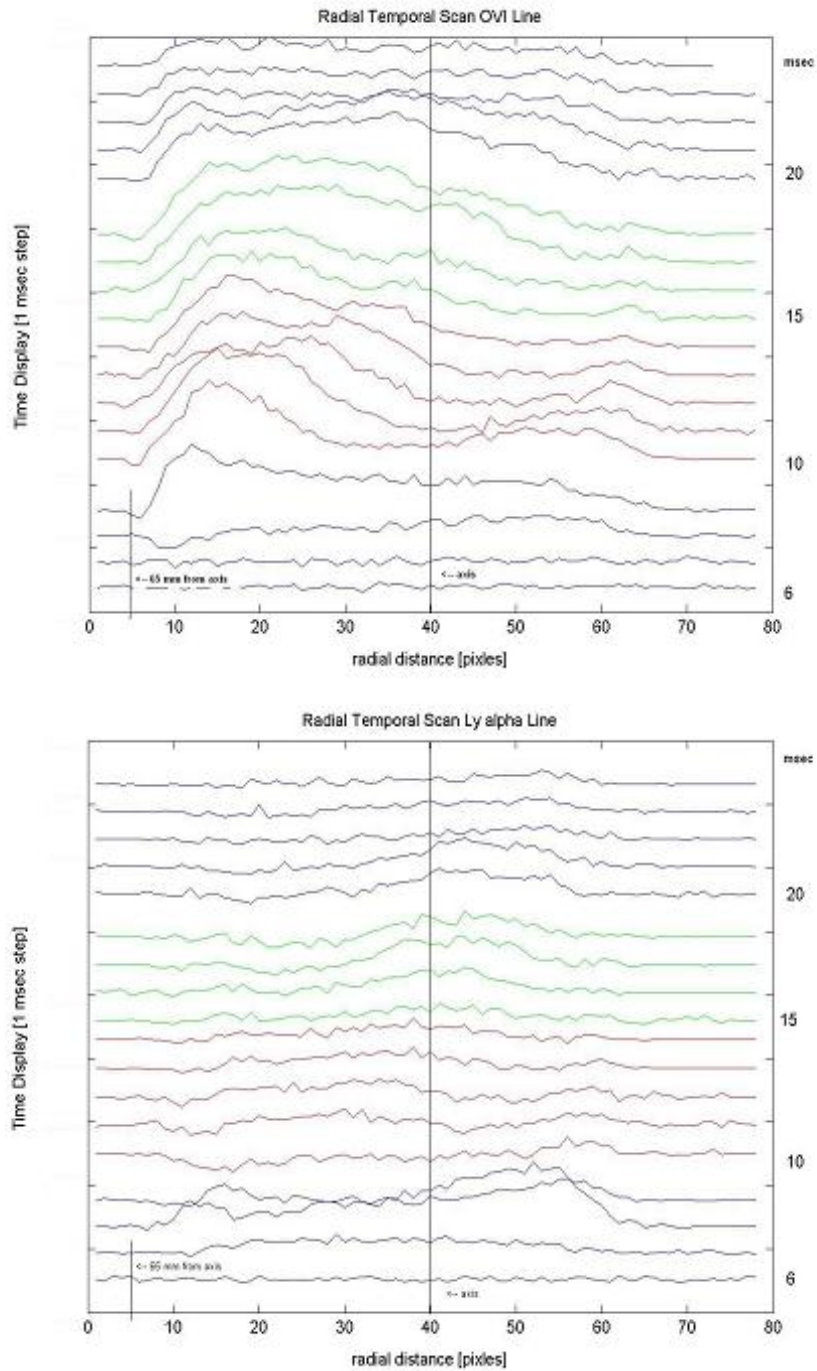


Fig. 2 In some “polarized discharges”, the flat maximum of the Ly α and OVI line emission power is observed near the biasing electrode, which moves in a radial direction from the electrode to the column centre.

Carbon transport in TCV

V. Piff

In collaboration with:

A. Zabolotsky, M. Bernard, H. Weisen, A. Bortolon, B.P. Duval, A. Karpushov, CRPP, EURATOM – Confederation Suisse, EPFL, CH-1015 Lausanne, Switzerland

The method we use for Carbon impurity transport study is based on relative measurements of the active signal of CX emission in near-by channels during the neutral beam pulse injection. Since part of the channels in the detection system was reinstalled, the relative calibration of the 16 channels in the visible range was done in a swept plasma discharge regime. If the plasma is swept in the front of the spectrometer entrance window the same plasma cross-section appears subsequently at neighbouring channel chords. For subtracting the background the slow position changing of Last Closed Surface (LCS) was used consequently. The correction factors for different channels were implemented in the signal evaluation program.

The vertically viewing detection set was mostly used for observation of active and passive signals of the CV and CIV lines. There is a non-trivial problem to separate the contribution of CV ($n=7 \rightarrow 6$), 4944 Å line from the Boron line, which appears in the close vicinity. Luckily, the shots were performed a sufficiently long time after the boronization so the contribution of the Boron line was negligible.

The other problem is a correct interpretation of the passive signal. “Passive” emission is detected during the breaks of a chopped neutral beam injection. In contrast with the active signal, which conforms to the local emission power of the ions, the passive signal measurement reflects the chord integrated plasma emission power. We know well that the observed line emission is influenced by the presence of neutral particles especially at the plasma edge. So the development of the method of impurity transport study based on the utilization of the chord-integrated emission power (passive signal) needs additional effort and understanding of the elementary processes. A database of about ten discharges has been established which contains the emission profiles of the CV line. However, the CIV line emission was covered by intensive background in our last experimental campaign.

Recently, remarkable progress was achieved in particle transport (convection) studies in the TCV tokamak. Electron density profiles are observed to be peaked. The presence of additional core heating by ECRH results in a flattening of the electron density profiles, the profiles become broader in comparison with the Ohmic target plasma.

In stationary Ohmic and ECR heated L-mode discharges, the profiles of carbon density are always peaked. In low current (edge safety factor $q_{95} > 4$) discharges they are noticeably more peaked than the electron density profiles. Since these discharges are dominated by anomalous transport, the convective effects, although reminiscent of those predicted by neoclassical theory, must be interpreted as being of anomalous origin. In discharges with higher safety factor, sawtooth activity and large inversion radii appear to be responsible for equalizing the peaking factors for carbon and electron density profiles, cf. Fig. 3.

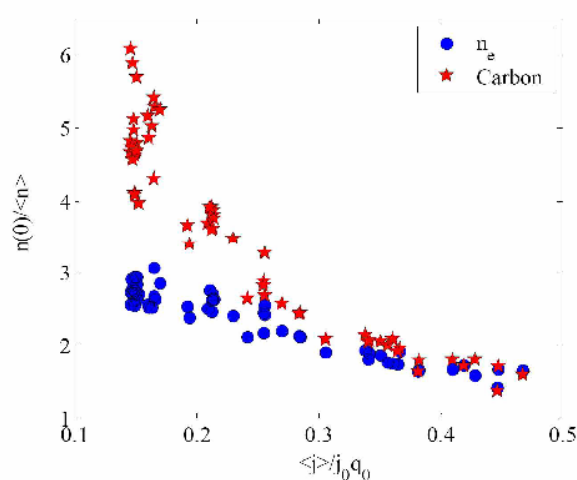


Fig. 3 Peaking of electron and carbon densities versus $\langle j \rangle / (j_0 q_0) \sim 1/q_{95}$

Modeling of magnetic equilibria and current drive expected in the IPP Prague re-installation of the Culham COMPASS-D tokamak

V. Fuchs, O. Bilyková, R. Pánek, J. Preinhaelter, J. Urban, J. Stöckel, F. Žáček

In collaboration with:

M. Valovič, I. Voitsekhovitch, EURATOM / UKAEA Fusion Association, Culham Science Centre, Abingdon, OXON, OX14 3DB, UK

In the course of 2005 we started preparing for the installation of the COMPASS-D tokamak (major radius=0.56m, minor radius=0.2m, $B_t=1.2$ T, $I_p=0.2$ MA) at IPP Prague, by activating locally the ACCOME equilibrium and current drive modelling code [1,2]. The first task was to set up free-boundary magnetic equilibria sustained by the COMPASS-D plasma current and poloidal field coils, and then assess the plasma performance with the planned lower hybrid (LH) and neutral beam injection (NBI) systems (the LH system provides $P_{LH}=0.4$ MW at refractive index $n_{||}=2.1$ and $f_{LH}=1.3$ GHz., and the NBI system has two 40 keV deuterium beams with a total power of 0.6 MW; the beams can be arranged for co-injection or counter-injection). Our principal results are thus the expected equilibria, the LH and NB power deposition profiles and the driven currents.

Our results can be summarized in three subjects as follows:

- 1) Adaptation of the ACCOME code to the IPP Prague computer environment and production of the magnetic equilibria.
- 2) Set-up of neutral beam injection input and calculation of NB power deposition and current drive.
- 3) Analysis of lower hybrid slow wave penetration, ray propagation, and absorption at the specific COMPASS-D conditions given above.

1) The ACCOME code, previously set up to run on CRAY and DEC alpha platforms had to be adapted to x86 architecture and Linux platforms available at IPP Prague. The modified code is now executable on Redhat and Gentoo Linux (32 bit PC architecture) and Scientific Linux (SUN 64 bit architecture). The code executes very rapidly and is therefore suitable for exploratory studies. ACCOME is a time-slice code, i.e. it computes equilibria and currents for given plasma density and temperature profiles. Thus, for example, ten iterations between the Shafranov equation equilibrium and the current drive modules (ohmic, bootstrap, LH and NB), typically necessary to reach a self-consistent state, takes about 15 mins of CPU time. COMPASS-D is coming to Prague from Culham together with its poloidal field coil system. Our first task was to reproduce the two standard COMPASS-D equilibrium configurations: SND (single null divertor) and SNT (single null divertor with higher triangularity) by activating specific coil groups and making sure that the coil currents do not exceed the power supply specifications. Figures 1 and 2 show results produced by the SELENE Shafranov equation solver of ACCOME [3].

2) The neutral beam injection module has a very fast Fokker-Planck solver for the high-energy ion population, which together with electron trapping determines the beam-driven current. The deposited energy and driven current depend sensitively on plasma density, and via the plasma current on orbit losses. The ACCOME NB module, however, does not follow individual orbits so that it cannot calculate orbit losses. For that purpose we plan acquiring the Monte-Carlo FAFNER or NUBEAM codes. The orbit losses are presently estimated from

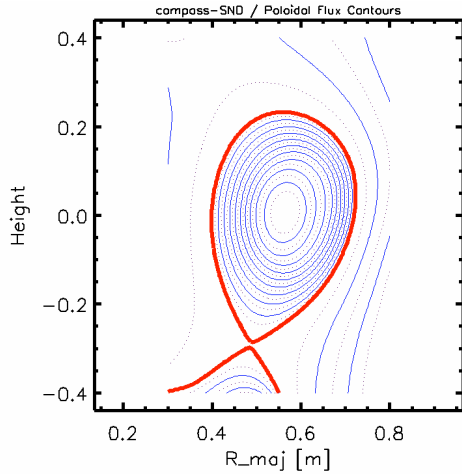


Fig. 1 *SND equilibrium*

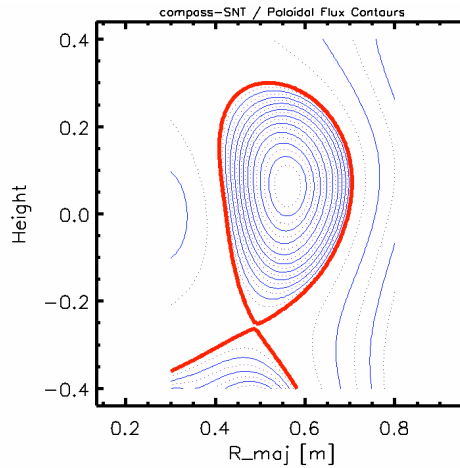


Fig. 2 *SNT equilibrium*

FAFNER (collaboration with IPP Garching) at about 20% for NB co-injection (i.e. in the direction of the toroidal plasma current) and 50% for NB counter-injection [4]. We have considered two basic configurations of the planned NBI modules: co-injection and balanced injection (i.e. with one of the beams counter-injected). In Figs. 3 and 4, we show power

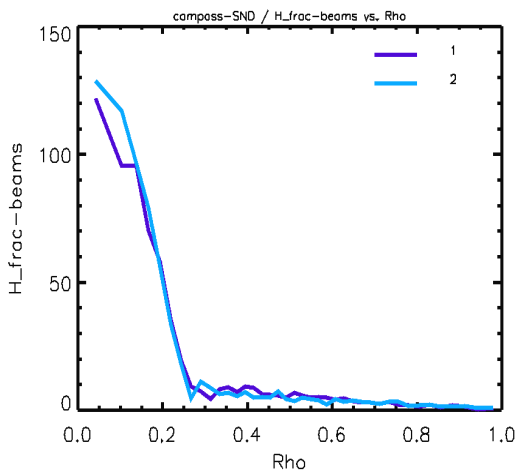


Fig. 3a *Power deposition profiles of two on-centre co-injected beams.*

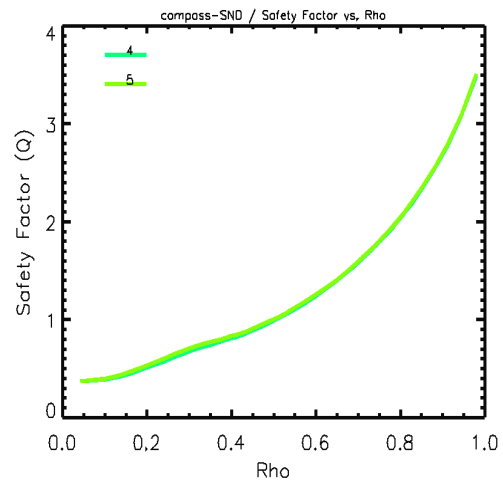


Fig. 3b *Safety factor profile corresponding to the conditions of Fig. 3a.*

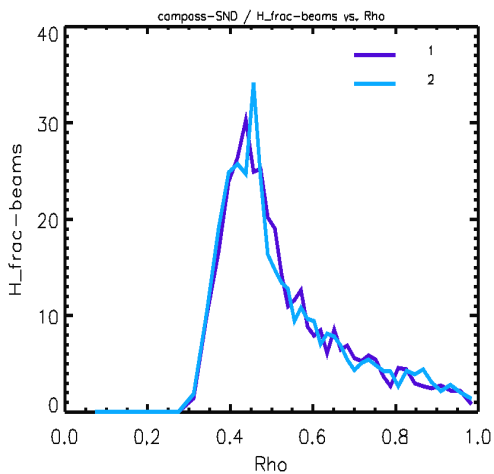


Fig. 4a *Power deposition profiles of two off-centre co-injected beams.*

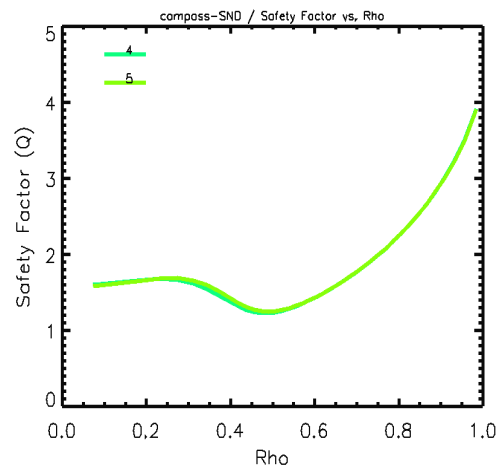
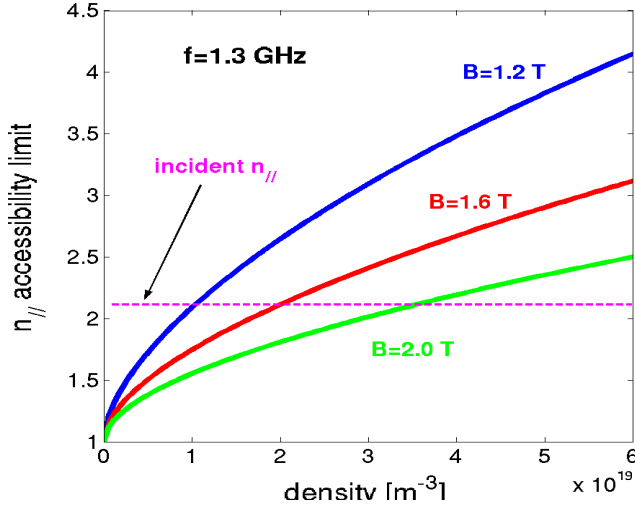


Fig. 4b *Safety factor profile with a reversed shear region corresponding to Fig. 4a.*

deposition and q-profiles from on-centre and off-centre co-injected beams, respectively. We note the reversed shear for off-centre deposition. The driven current is about 40 kA per beam.

3) Lower hybrid heating and current drive on COMPASS-D at $I_p=0.2$ MA, $B_t=1.2$ T, and at LH power source frequency 1.3 GHz appears marginal. The reasons are, first, that only about 200 kW of LH power is coupled to the plasma. Next, LH slow wave accessibility is poor at the conditions given above (see Fig. 5), and finally, NBI deposits about 30% of its



$$n_{\parallel} \geq n_{\parallel \text{acc}} = \frac{\omega_{pe}}{\omega_{ce}} + \sqrt{K_{\perp}}$$

$$K_{\perp} = 1 + \left(\frac{\omega_{pe}}{\omega_{ce}} \right)^2 - \frac{\bar{\omega}_{pi}^2}{\omega^2}$$

Fig 5 Lower hybrid slow wave accessible n_{\parallel} as a function of electron density for a few values of the toroidal magnetic field.

power on the electrons and therefore constitutes the principal electron heating mechanism. Figs. 6 and 7 illustrate the bad accessibility at the COMPASS-D conditions given above, and the improvement at a higher magnetic field $B_T=2.1$ T [3]. We point out that accessibility also improves with increasing LH frequency, which is of course irrelevant in the present context, unless the old inherited LH system is replaced by one more compatible with the COMPASS-D scientific program of H-mode operation at a relatively high density (the Greenwald limit for COMPASS-D is about $2 \times 10^{20} \text{ m}^{-3}$).

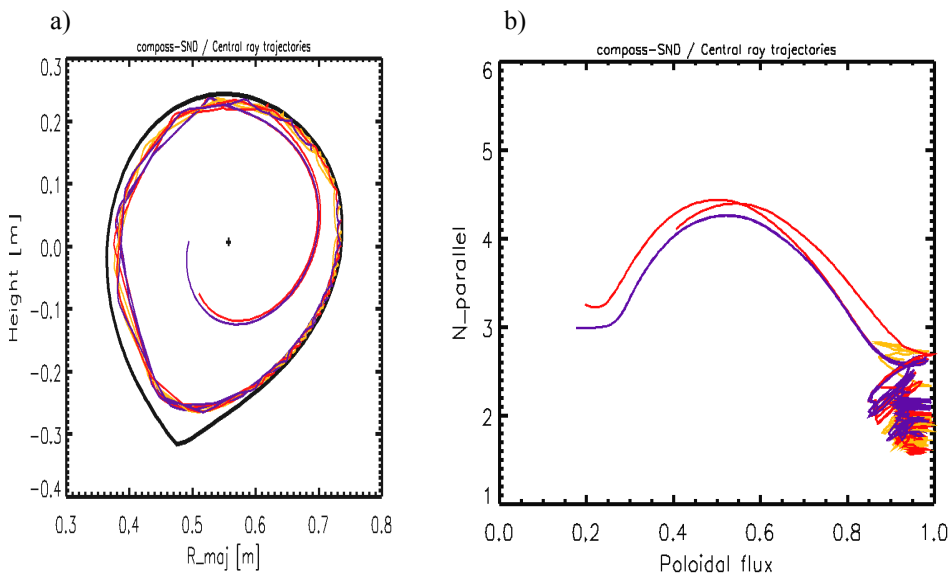


Fig. 6 a) LH rays paths in the poloidal plane and b) n_{\parallel} as a function of normalized poloidal flux (or radius), for $I_p=0.2$ MA, $B_T = 1.2$ T. The rays are injected at the outboard midplane at $n_{\parallel} = 2.1$.

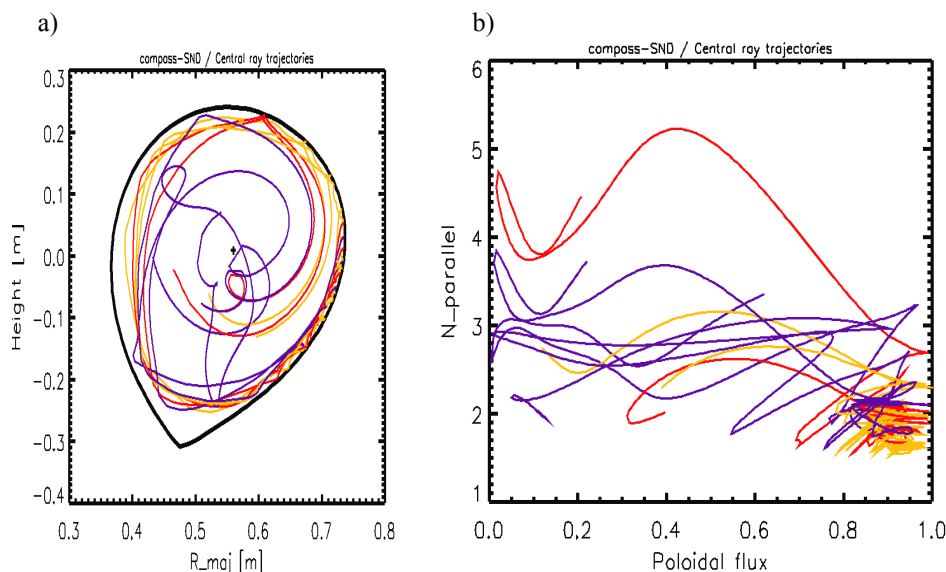


Fig. 7 a) LH rays paths in the poloidal plane and b) n_{\parallel} as a function of normalized poloidal flux (or radius), for $I_p=0.35$ MA, $B_T = 2.1$ T. The rays are injected at the outboard midplane at $n_{\parallel} = 2.1$.

References

- [1] K. Tani, M. Azumi, and R. S. Devoto, J. Comput. Phys.
- [2] R. S. Devoto, et al., in Control. Fusion and Plasma Phys., **13B**, Part IV (1989) 1292.
- [3] O. Bilykova et al., submitted to Czech J. Phys.
- [4] J. Urban et al., submitted to Czech J. Phys

Plasma sprayed tungsten-based coatings and their usage in the edge plasma region of tokamaks

V. Weinzettl, J. Matějček, V. Piffel, E. Dufková, J. Zajac, R. Dejarnac

In collaboration with:

V. Peřina, Nuclear Physics Institute, Řež u Prahy, Czech Republic

A. Burdakov, S. Polosatkin, Budker Institute, Novosibirsk, Russia

Y. Koza, EURATOM Association FZJ, Forschungszentrum Juelich, Germany

The behavior of plasma-sprayed tungsten-based coatings, prepared at IPP Prague, in the tokamak edge plasma was tested at the CASTOR device. Semi-cylindrical and mushroom-shaped specimens were inserted (Fig. 1) into the plasma at various radii and exposed to tokamak discharges (30 ms pulse length, 30 kW ohmic heating). Moreover, positive and negative voltages were applied on certain samples to increase electron and ion interaction with the sample surface. The Imaging VUV Seya-Namioka Spectrometer was installed to monitor radial profiles of the impurity line intensities with 1 ms temporal resolution (HI 102.6 nm and 121.6 nm, CIII 97.7 nm and 117.3 nm, NIII 99.0 nm and 107.9 nm, OVI 103.2+103.7 nm), Figs. 3, 4. The solid target surface becomes a source of hydrogen and low-Z atoms due to the recombination of the plasma ions and the re-erosion of deposited impurity layers on the coating surface. The spectroscopic observations are confirmed by ex-situ compositional measurements of the sprayed surfaces by RBS and ERDA methods, where hydrogen and carbon deposition, and an oxygen content decrease were observed. A tungsten inflow monitored by a photo multiplier equipped with an interference filter for the W I line at 400.9 nm was non-negligible only during arcing (Fig. 2), indicating a very low erosion of the tungsten itself. Generally, pure tungsten coatings are suitable for covering different edge

plasma diagnostics because of their low surface erosion and negligible influence on the discharge parameters [1]-[4].

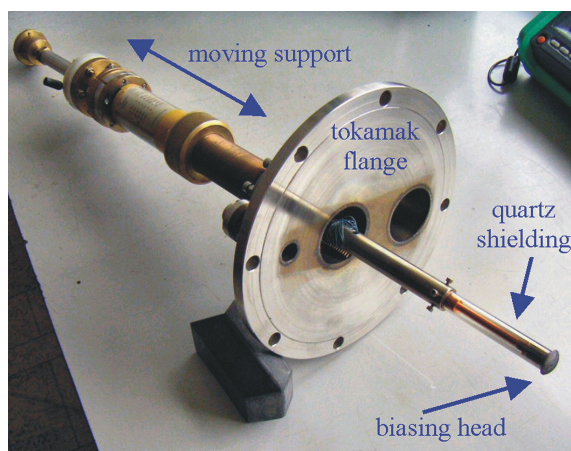


Fig. 1 The movable holder for the insertion and biasing of plasma-sprayed tungsten specimens into a tokamak chamber.

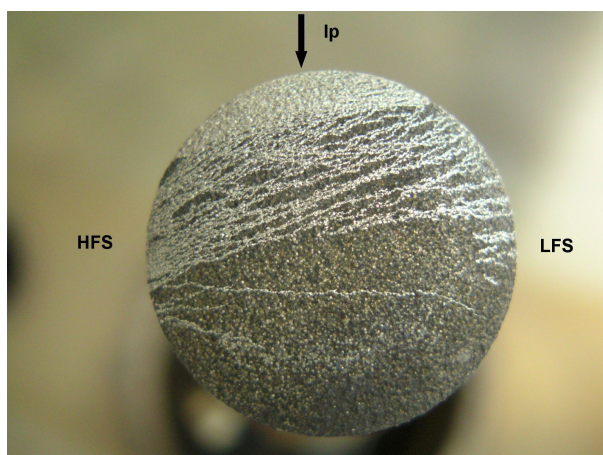


Fig. 2 The surface of the biased plasma-sprayed tungsten-based coating (natural light photo), showing the bright traces where a thin oxide layer was removed from the surface by arcing.

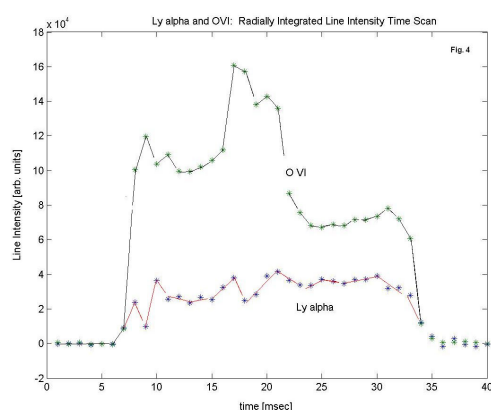


Fig. 3 The time evolution of the $L\alpha$ H I (121.6 nm) and O VI (103.2 nm+ 103.7 nm) lines in a shot with a specimen biasing.

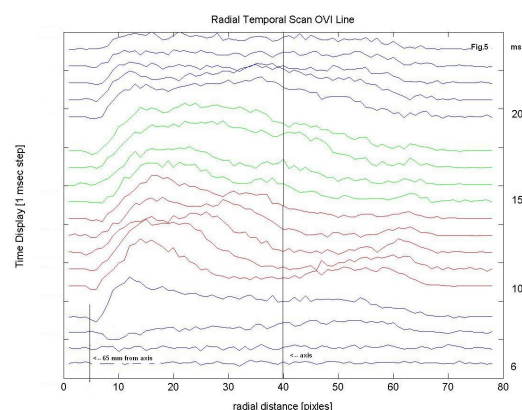


Fig. 4 The spatio-temporal behavior of the O VI (103.2 nm+ 103.7 nm) lines in a shot with a specimen biasing. The position of the specimen is indicated by a vertical line in the left-bottom corner of the figure.

References

- [1] V.Weinzettl, V.Piffll, J.Matějčiček, E.Dufková, J.Zajac, R.Dejarnac, V.Peřina: Biasing experiments with solid and porous electrodes, 32nd EPS Conference on Plasma Phys. Tarragona, 27 June - 1 July 2005, ECA Vol.29C, P-4.006 (2005).
- [2] V.Weinzettl, V.Piffll, J.Matějčiček, E.Dufková, J.Zajac, R.Dejarnac: The effect of the use of different electrode materials for edge plasma biasing on plasma density and floating potential modifications, Czech J. Phys., Vol. 55 (2005), No.12, 6106C.
- [3] V.Piffll, V.Weinzettl, A.Burdakov, S.Polosatkin: Temporally and spatially resolved measurements of VUV lines intensity profile in the tokamak CASTOR, 32nd EPS Conference on Plasma Phys. Tarragona, 27 June - 1 July 2005, ECA Vol.29C, P-2.075 (2005).
- [4] J.Matějčiček, Y.Koza, V.Weinzettl: Plasma sprayed tungsten-based coatings and their performance under fusion relevant conditions, Fusion Eng.&Design, 75-79 (2005) 395.

2 Diagnostics Development

Measurements of magnetic fields in TORE Supra and CASTOR by means of Hall sensors

I. Ďuran, K. Kovářík, J. Stöckel

In collaboration with:

I. Bolshakova, R. Holyaka, V. Erashok, Magnetic Sensor Laboratory, LPNU, Lviv, Ukraine
P. Moreau, F. Saint-Laurent, Ass. EURATOM/CEA Cadarache, Saint Paul Lez Durance, France

Use of various configurations of flux loops for measurement of magnetic field in fusion devices is inherently limited by the pulsed operation of these machines. A principally new diagnostic method must be developed to complement the magnetic measurements in the true steady state regime of operation of a fusion reactor. One of the options is the use of diagnostics based on Hall sensors. This technique is well established for many applications in experimental physics as well as industry, although it is rarely implemented in the fusion plasma physics. Therefore, besides the tests of radiation hardness of the ITER candidate Hall sensors, the growing experience with their use in the environment of present day tokamaks is highly desirable. Although, principally aimed for steady state applications, Hall sensors offer some advantages over magnetic coils also for present pulsed fusion devices. The advantages are mainly their smaller size and direct relation of the measured signal to the magnetic field. The frequency response is typically limited to few tens of kilohertz.

The performance of a 3D Hall probe was successfully tested on Tore Supra tokamak ex-vessel taking advantage of its long pulse capabilities [1, 2]. The new probe is being developed for use in the Tore Supra in-vessel environment by MSL, Ukraine in collaboration with CEA and IPP.CR. Besides radiation, the Tore Supra offers in many aspects a similar environment as the Hall sensors would experience on ITER e.g. required high vacuum compatibility, survival limit of the probe head at least 200°C, operation temperature 120°C, and long pulse lengths.

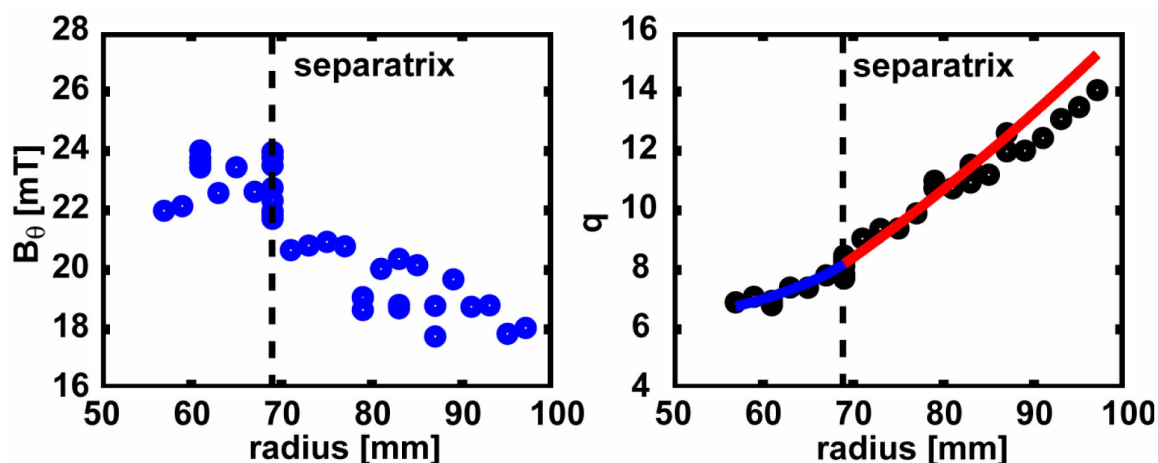


Fig. 1. Left panel: radial profile of B_θ . Right panel: radial profile of safety factor q . Solid line shows the theoretically expected q profile inside the confinement region (blue)

As an intermediate step, the installation and tests of a 3D Hall probe-based magnetometric system on the CASTOR tokamak in-vessel has been done. The magnetic probe head was constructed to measure the magnetic field vector at a quasi-single-point of space inside the confinement region of the CASTOR tokamak. It consists of 3 perpendicular Hall sensors mounted within a hard aluminum casing. The structure of the probe head is covered by MACOR ceramic cap to protect it from direct contact with the plasma. The electronic box that controls and drives the probe head is placed at a distance of approximately 3 meters from the probe head. The measured data, amplified, conditioned, and digitized by electronics, are transferred via a RS232 interface to a PC where they are stored and further analyzed. The size of the probe head is $20 \times 20 \times 25 \text{ mm}^3$. The bandwidth of the system is up to 200 kHz and the precision below 0.1%. The probe head was installed on a radially moveable manipulator to allow measurement of profiles on a shot to shot basis. The measured profiles of toroidal and poloidal magnetic fields were used to deduce the profile of the safety factor q well inside the confinement region up to $r=57 \text{ mm}$ (see Fig.1). The measured profile of q is consistent with theoretical expectations assuming a downward shift of the plasma column by 8 mm and a rather flat current density profile with a peaking factor of 0.6.

References

- [1] I. Bolshakova et al., Present-day experience in the use of galvanomagnetic radiation hard transducers in fusion devices, to be published at the 13th International Congress on Plasma Physics, Kiev, 2006.
- [2] I. Ďuran et al., Magnetic field measurements using the galvanomagnetic devices on Tore Supra and CASTOR tokamaks, P-2.086, 32nd EPS Conference on Plasma Physics, Tarragona, 2005, ECA Vol. 29C.

The ball-pen probe for direct measurements of the electron temperature and the first results of the PIC simulations

J. Adámek, J. Stöckel, R. Pánek

In collaboration with:

R. Schrittwieser, C. Ionita, EURATOM-ÖAW, Innsbruck, Austria

G. Van Oost, Ghent University, Belgium

The measurements of the electron temperature

The usual and best known method to determine T_e is to register the current-voltage characteristic of a Langmuir probe and to evaluate the exponential increase of the electron current in the retarding field region. A disadvantage of this method is its low temporal resolution which naturally is limited by the frequency with which the characteristic can be scanned. This is usually not more than about 1 kHz.

In principle also the difference between the floating potential V_{fl} and the plasma potential Φ_{pl} contains information of the electron temperature. From simple probe theory we obtain the relation:

$$T_e = \frac{\Phi_{pl} - V_{fl}}{\alpha} \quad (1)$$

with $\alpha = \ln \left| I_{sat}^- / I_{sat}^+ \right|$ being the logarithm of the ratio between the electron and ion saturation currents to a Langmuir probe, respectively. In a hydrogen plasma α is around 3 [1]. If we use

the so-called ball-pen probe [1,2] and a Langmuir probe to determine Φ_{pl} and V_{fl} simultaneously, Eq. (1) could be used to determine T_e very quickly, with the good temporal resolution.

The probe head which consists of the ball-pen and Langmuir probe is shown in Fig. 1. The collector is retracted typically 1 mm within the ceramic shielding tube. Figure 2 shows the electron temperature determined from Eq. (1) with $\alpha=2.89$ (black triangles) and from the

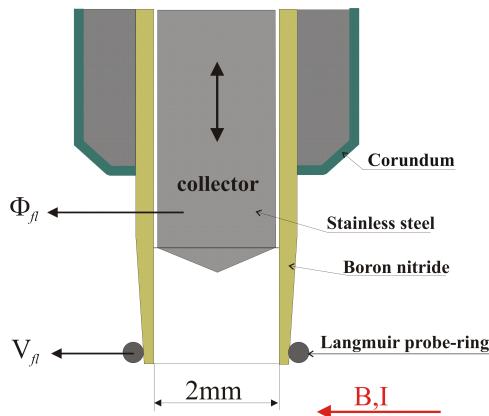


Fig. 1 The probe head for T_e measurements consists of the ball-pen and Langmuir probe.

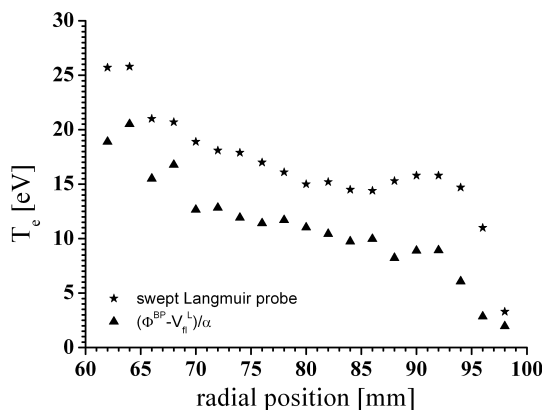


Fig. 2 The radial profiles of the electron temperature determined from the swept Langmuir probe (asterisk) and from difference of the plasma and floating potential (triangle).

I-V characteristics of the Langmuir probe when this was swept with a frequency of 1 kHz between -150 V and $+50$ V (black stars). The latter results show systematically higher values. We consider the results from Eq. (1) to be more reliable since it is known that electron temperature measurements from Langmuir probe current-voltage characteristics in hot plasmas tend to deliver higher results [3].

The PIC simulation of the ball-pen probe

The basic idea of the direct plasma potential measurement by the ball-pen probe [1,2] is to adjust $R = |I_{sat}^- / I_{sat}^+|$ in Eq. (2) to be equal to one. If this is achieved, the floating potential of the probe V_{fl} is equal to the plasma potential Φ as follows from

$$V_{fl} = \Phi - T_e \ln(R) \quad (2)$$

Figure 3 shows the first results of the PIC simulations (XOOPIC) of the ball-pen I-V characteristics for different collector positions when it was partially exposed in plasma ($h > 0$). The probe current is normalized to the ion saturation current. It is evident that the value of the ratio R and the floating potential V_{fl} depend on the collector position. This is in a good agreement with the experiment and with theoretical calculations. The relation between R and V_{fl} can be approximately described by a linear function as seen in Fig. 4. The value of the plasma

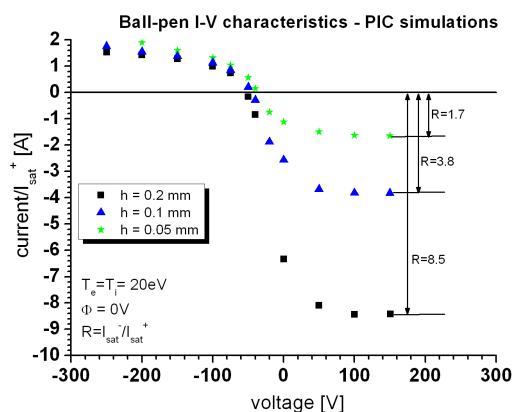


Fig. 3 I-V characteristics of the ball-pen probe for several collector positions calculated by PIC simulations ($T_e=T_i=20$ eV, $\Phi=0$).

potential is according to the basic idea (Eq. 2) estimated as $\Phi = -24\text{V}$, which is below given value of the plasma potential ($\Phi = 0\text{V}$) in the PIC simulation. The discrepancy can be explained by detailed analysis of the potential in the vicinity of the probe head. The first rough estimation is that it is fortunately less than 0V .

References

- [1] J. Adamek et al., Czech. J. Phys., **54** (2004), C95.
- [2] J. Adámek et al., Czech. J. Phys., **55** (2005), 235-242.
- [3] J.P. Gunn, Rev. Sci. Instr., **75** (2004) 4328.

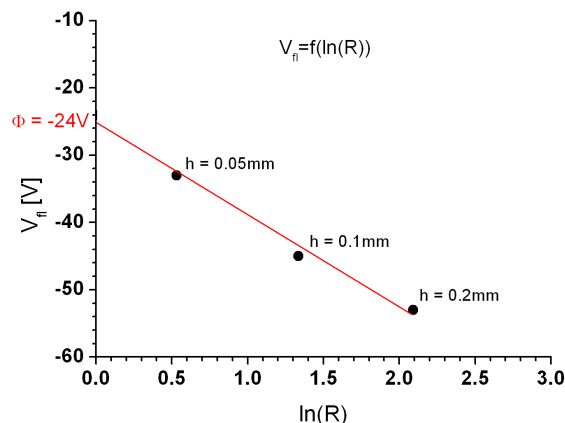


Fig. 4 The dependence of the ball-pen probe potential V_p on the logarithm of the ratio R .

VUV imaging Seya-Namioka spectrometer & 2D fast detection system

V. Piffel, Vl. Weinzettl

In collaboration with:

A. Burdakov, S. Polosatkin, Budker Institute of Nuclear Physics, Novosibirsk, Russia

Recently, a VUV Imaging Seya-Namioka Spectrometer & 2D Fast Detection System was successfully developed. The system monitors the radial profiles of the chord-integrated line emission power of the dominating low-Z plasma impurities in 50 – 200 nm wavelength range. The spatial resolution is about 3 mm. Optical enlargement of the system is 2.93, so the viewed part of the plasma is 70 mm high. The design of the spectrometer is based on the use of a spherical dispersion grating.

In Figure 1, the optical scheme of Seya-Namioka spectrometer is shown. The two-dimensional detection system consists of two channel-plates set with a working area $\phi=38$ mm in diameter. The output electrons are accelerated onto the scintillator of the fiberoptic lightguide, which is consequently used as a vacuum throughput. The image of the radial intensity distribution of the chosen lines sequence could be taken during the whole period of the plasma discharge with 1 ms exposition time. The Fast CCD camera, 320 x 156 pixels, 1 kHz frames rate is optically coupled to the lightguide output of the detection system.

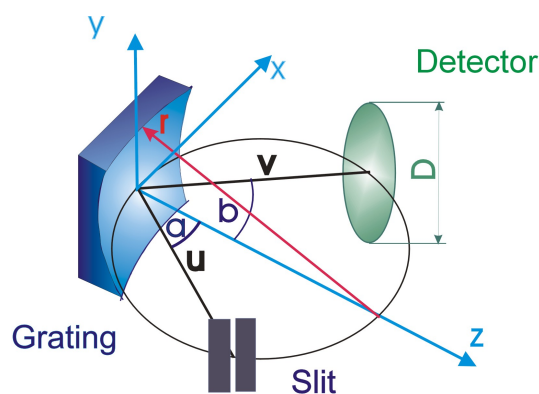


Fig. 1. Scheme of Seya-Namioka VUV spectrograph

Ion temperature measurements in the tokamak scrape-off layer

R. Pánek, J. Stöckel, M. Hron, and R. Dejarnac

In collaboration with:

M. Kočan, Department of Experimental Physics, Comenius University, Bratislava, Slovakia

J.P. Gunn, Association EURATOM-CEA/DSM/DRFC, Cadarache, France

The ion temperature, T_i , in the tokamak scrape-off layer (SOL) is notoriously difficult to measure and thus rarely available (e.g. [1]). We describe a new Langmuir probe, the segmented tunnel probe (STP), that measures ion and electron temperatures, and parallel ion current density simultaneously with high temporal and spatial resolution. Here, we focus on the measurements of ion temperature.

The STP consists of a hollow conducting tunnel a few millimeters in diameter and typically 5 mm deep, closed at one end by an electrically isolated conducting back plate. The tunnel axis is parallel to the total magnetic field. To repel electrons, the conductors are negatively biased. The ions flowing into the tunnel orifice get un-magnetized by an intense radial electric field in the magnetic pre-sheath, and redistributed between the back plate and the tunnel, Fig. 1 (left). The axial distribution of ion flux into the tunnel decays with a characteristic length scale that is determined by the ratio of the radial acceleration and the incident parallel ion velocity. The latter is a function of the ion sound speed. Therefore, if the tunnel is divided into two segments, the ion temperature can be obtained from the ratio of ion current to the first and the second segments, $R_c = I_{\text{seg1}}/I_{\text{seg2}}$. To measure the plasma flows in the SOL, two tunnels are mounted back-to-back in a Mach probe arrangement, Fig. 1 (right).

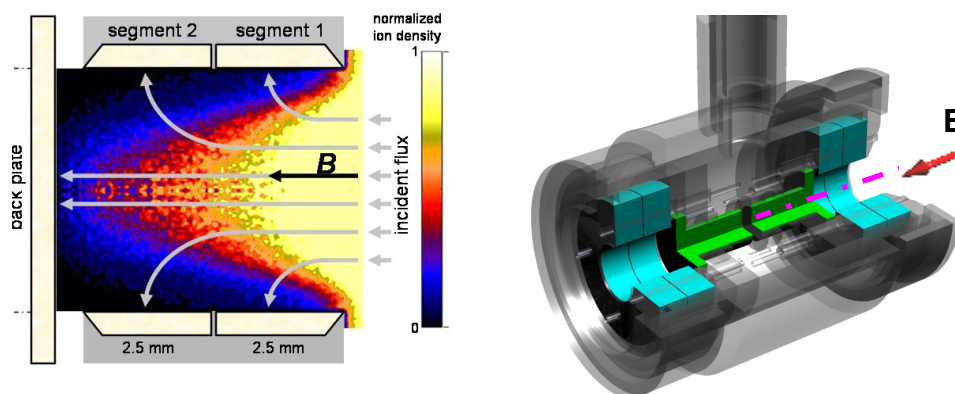


Fig. 1 *Left: Scheme of the STP tunnel. The ion trajectories are shown by black arrows. Right: Schematic drawing of the probe head. Two segmented tunnels are mounted back-to-back in a Mach probe arrangement.*

The advantage of this probe is that it operates in DC mode and thus provides fast measurements of the above mentioned quantities. Moreover, due to a clearly defined tunnel orifice, the STP is not subject to the uncertainties of collecting area from which classical convex probes suffer.

Particle-in-cell (PIC) simulations were used for the probe calibration for ion and electron temperature measurements. The two-dimensional PIC code XOOPIC [2] has been used. Due to the axial symmetry of the probe, the XOOPIC code enables a simulation of the whole region inside the tunnel. More than 100 simulations for typical values relevant to SOL

conditions have been performed. From the simulation database we derived the analytical fitting formulae for $T_i = T_i(R_c, T_e, J_{//,i})$

$$T_i = 1.488 \cdot 10^2 + 2.539 \cdot 10^{-4} T_e^2 + 72.452 J_{//,i}^{-1} - 37.51 R_c \quad \text{for } J_{//,i} = 1 - 3 \text{ kAm}^{-2} \quad (1)$$

$$T_i = 3.081 \cdot 10^2 + 0.347 T_e + 2.107 \cdot 10^2 J_{//,i}^{-1} - 91.488 R_c \quad \text{for } J_{//,i} = 3 - 6 \text{ kAm}^{-2} \quad (2)$$

A prototype of the STP has been built and tested in the CASTOR tokamak. The ion currents collected by each segment and the back plate were measured separately with 1 μ s temporal resolution. A radial scan of the plasma parameters was performed on a shot-to-shot basis in reproducible discharges.

Using Eqs. (1) and (2), the radial profile of the ion temperature in CASTOR was obtained. Fig. 2 shows a typical radial profile of ion and electron temperatures in CASTOR measured by the STP, plotted against the radial distance from the plasma centre, r . In addition, T_e from the STP [3] is compared with similar measurements obtained from the radial array of Langmuir probes (so called ‘‘rake probe’’).

In addition, an evidence of the correct measurement of the ion and electron temperature is shown by scaling T_i and T_e with n_e . In Fig. 3, the ion and electron temperatures, simultaneously measured by the STP, are plotted against the local plasma density n_e . T_i decays proportionally to $1/n_e$ approximately, while the temperature ratio T_i/T_e varies from ~ 3 at the lowest density to ~ 1 at $n_e \cong 10^{18} \text{ m}^{-3}$.

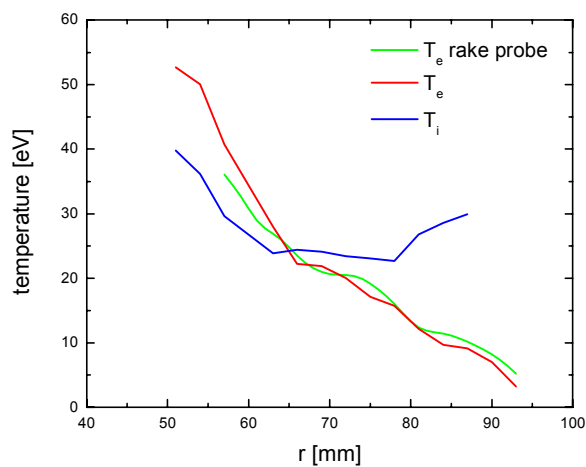


Fig. 2 Radial profiles of the ion and electron temperatures, parallel ion current density, and electron density (from top to bottom) in CASTOR measured by the STP and the rake probe.

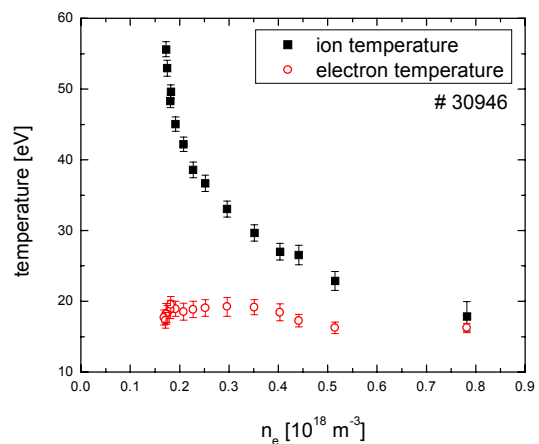


Fig. 3 Scaling of T_i and T_e measured by the STP with the plasma density n_e .

References

- [1] R.A. Pitts et al., Review of Scientific Instruments **74** (2003) 4644.
- [2] J.P. Verboncoeur, A. B. Langdon, N. T. Gladd, Comp. Phys. Comm. **87** (1995) 199.
- [3] J.P. Gunn, Physics of Plasmas **8** (2001) 1040.

Fast bolometry on the CASTOR tokamak

V. Weinzettl, E. Dufková, J. Zajac

In collaboration with:

M. Kočan, FMFI UK, Bratislava, Slovakia

D. Sarychev, RRC "Kurchatov Institute", Moscow, Russia

The two arrays of the fast AXUV-based bolometers were installed on the CASTOR tokamak in mutually perpendicular directions. The first array equipped with 16 channels is placed inside the bottom tokamak port; the second one operating with 19 channels is located at the same poloidal cut and placed inside the horizontal port at the low field side (LFS). Bolometers look at the plasma column through the aperture slit ("camera obscura"). The slits have rectangular shape with the size 4x0.2 mm and 4x0.19 mm respectively, what was optimized to reach reasonable intensity together with the requested spatial resolution of 11 mm and 9 mm. Each channel detects a plasma radiation along the appropriate chord covering the whole poloidal plasma cross-section of 17 cm in diameter, so that a spatial profile of the radiated power can be reconstructed. Output currents from the diodes are amplified and converted to voltage by the preamplifier unit constructed in KI Moscow. The unit and the data acquisition PC are located very close to the array itself (less than 2 m) so that the temporal resolution is not influenced by the connecting cables and is given only by a sampling rate of the collecting card. It is usually 20 μ s in standard measurements or 1 μ s for fast events studies.

Bolometric data are integrated over the chords. An obtained dependency of the radiated power on the distance of the chord from the plasma centre is usually peaked during a typical CASTOR discharge [1]. Fitting the data with Gaussian curve, it is possible to estimate the centre of radiation losses (roughly corresponding to the plasma column position), radiation FWHM (full width at half of maximum) and the maximum radiated intensity. In some cases, namely at the beginning of the discharge, the plasma profile is not peaked, but hollow. Then the data don't fit a Gaussian distribution; consequently more complicated approximations are used. Asymmetric Abel inversion is used for a reconstruction of the radiation profile from single array data at each time step assuming a radial symmetry in one direction (Fig. 1). The tomography based on the Cormack method, which combines data from both arrays, is under implementation at present.

Usage of fast bolometers is very suitable for analyses of the edge plasma biasing experiments [2-6]. The biasing causes a gradual increase of the total radiated power, a quick rise of FWHM and a shift of maximum radiation (Fig. 2). Very fast changes of plasma radiation can be studied thanks to the high temporal resolution of AXUV based bolometers (Fig. 3). In the biasing experiments with the electrode inserted deeply in a hot plasma region, relaxation events and a fast oscillation were induced. In this case, plasma rapidly changes its

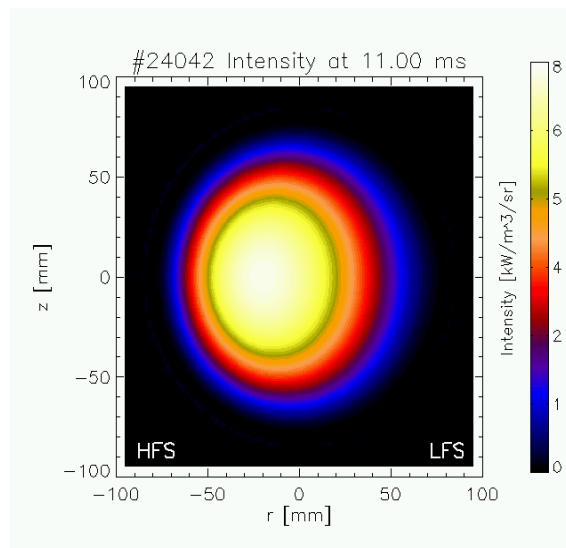


Fig. 1. Reconstruction of the radiation profile using asymmetric Abel inversion.

radiation profile from centred to hollow during 30 μ s. This is followed by an increase of total

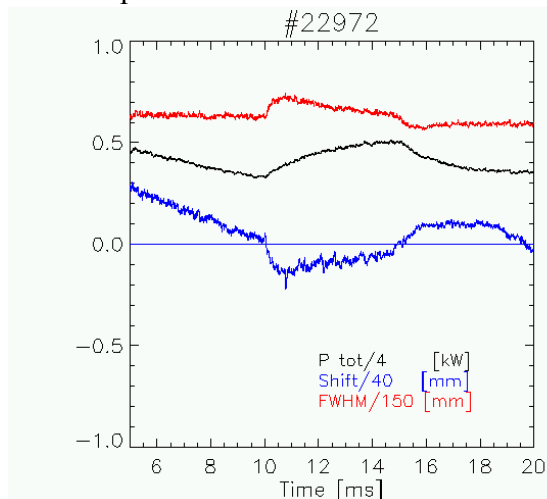


Fig. 2 Effect of biasing ($U_B=150V$, $r_B=50$ mm) on FWHM, total radiated power and plasma column shift.

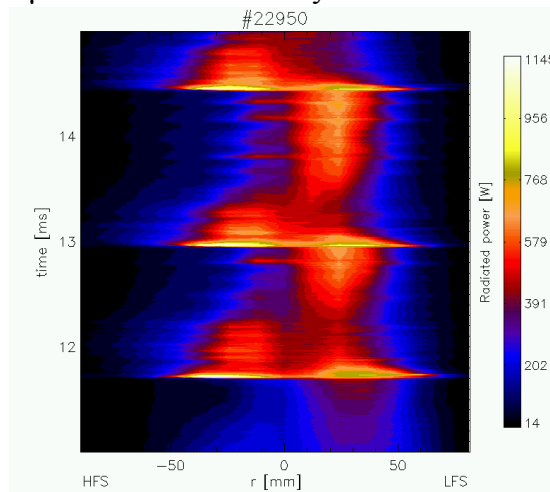


Fig. 3 Relaxations during a biasing phase of the discharge ($U_B= -300V$, $r_B=45$ mm).

radiated power and the radiation profile becomes broader. Then plasma slowly relaxes back to its original state with a characteristic time 500 μ s, sometimes with a few smaller relaxations. Very fast oscillations (10-50 kHz) were observed in the biasing experiments with a segmented probe. Meanwhile the Langmuir probes and bolometers detect 10 kHz oscillations at the plasma edge, 40-50 kHz vibrations were seen namely by central bolometric chords. Their typical duration was 0.2 ms; in exceptional case up to 1 ms. These oscillations affect the radiation width and the intensity in the opposite way so that the total radiated power remains constant.

Radiation from the edge plasma region is influenced by turbulent events. Subtracting the mean value from a bolometric signal, changes of radiation caused by turbulences can be visualized. The cross-correlation and multi-fractal analyses were used to get information on the presence, lifetime and poloidal rotation frequency of turbulent structures (Fig. 4). An implementation of the Singular Value Decomposition (SVD) method is envisaged for these purposes.

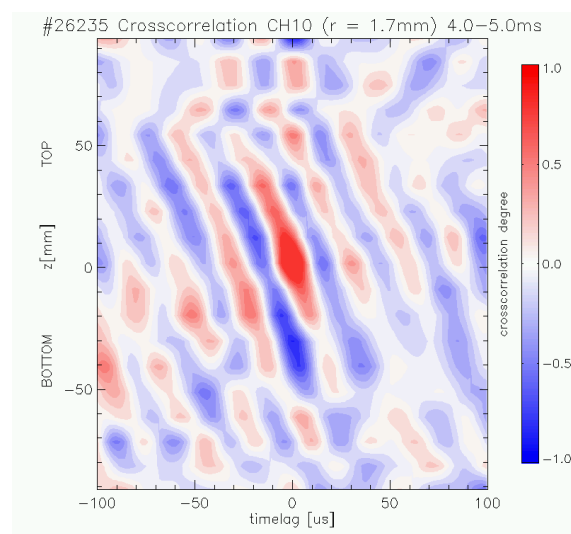


Fig. 4. Contour plot of the cross-correlation functions between reference bolometric channel No. 10 and the other channels. The presence of moving structures indicating by a high level of correlation can be seen.

References

- [1] E. Dufková, V. Weinzettl, D. Sarychev, M. Kočan: *Fast bolometry on the CASTOR tokamak*, 32nd EPS Conf. on Plasma Phys. Tarragona, 27 June - 1 July 2005, ECA Vol.29C, P-2.074 (2005).
- [2] M. Spolaore et al.: *Relaxation phenomena induced by edge plasma biasing experiments in the CASTOR tokamak*, Czech. J. Phys. 55 (2005) 1597-1608.

- [3] M. Spolaore et al.: *Relaxation phenomena during edge plasma biasing in the CASTOR tokamak*, 32nd EPS Conf. on Plasma Phys. Tarragona, 27 June - 1 July 2005, ECA Vol.29C, P-4.031 (2005)
- [4] J. Zajac, V. Weinzettl, E. Dufková, V.P. Budaev: *Multifractal analysis of tokamak plasma turbulence in biasing experiments*, 32nd EPS Conference on Plasma Phys. Tarragona, 27 June - 1 July 2005, ECA Vol.29C, P-5.019 (2005).
- [5] V. Weinzettl, V. Piffel, J. Matějčíček, E. Dufková, J. Zajac, R. Dejarnac, V. Peřina: *Biasing experiments with solid and porous electrodes*, 32nd EPS Conference on Plasma Phys. Tarragona, 27 June - 1 July 2005, ECA Vol.29C, P-4.006 (2005).
- [6] V. Weinzettl, V. Piffel, J. Matějčíček, E. Dufková, J. Zajac, R. Dejarnac: *The effect of the use of different electrode materials for edge plasma biasing on plasma density and floating potential modifications*, Czech J. Phys., Vol. 55 (2005), No.12, 6106C.

Development of an advanced probe for edge tokamak plasmas

M. Tichý, R. Hrach (FMP)

In collaboration with:

P. Kudrna, A. Marek, J. Šimek, M. Lahuta, Z. Pekárek, O. Bařina, Faculty of Mathematics and Physics, Charles University, Prague, Czech Republic

R. Schrittwieser, R. Gstrein, P.C. Balan, C. Ionita, S.B. Olenici, R.P. Apetrei, OAW, Innsbruck University, Austria

Test of practical application of the first version of 3-D particle code for probe diagnostic in CASTOR tokamak

In order to develop more precise models of diagnostic systems in CASTOR tokamak, a fully three-dimensional particle computer code is under the construction. In 2005 a first version of a three-dimensional code for the simulation of processes in high-temperature plasma in the presence of magnetic field was successfully tested and the results of this testing were presented during two international conferences – 9th European Vacuum Congress EVC-9, Paris [1] and 32nd EPS Conf. on Plasma Physics, Tarragona [2] – and published in [3] and [4].

The present version is based on the standard particle-in cell technique, but instead of the successive over-relaxation method, the more advanced Poisson solvers using the Fourier transform were introduced. However, even with these improvements the three-dimensional particle code is slow and in future its efficiency must be improved significantly. For 2006 several further solvers will be incorporated into the 3D model and both the precision and efficiency of the resulting computer codes will be analysed. The algorithms being tested are: conjugate gradients approach, multigrid technique, finite elements method and hybrid fluid-particle technique.

Optimization of the ball-pen and emissive probe design for direct measurement of plasma potential

We performed experimental research on the emissive probe in collaboration with the group of Prof. Roman Schrittwieser of the Innsbruck University. The aim of the research was (i) to experimentally estimate the precision with which the emissive probe measures the plasma potential, and (ii) to investigate the region of the electron accelerating part of the emissive probe characteristic. Results have been presented at the conferences SAPP and ISPC [5,6].

References

- [1] J. Šimek, R. Hrach, O. Bařina, V. Hrachová, *Multi-dimensional codes for particle modeling in Tokamak edge plasma*, 9th European Vacuum Congress EVC-9, Paris 5.-7.4.2005, France.
- [2] J. Šimek, R. Hrach, *Multi-dimensional particle codes in modeling in low-temperature and high-temperature plasmas in the presence of magnetic field*, 32nd EPS Conf. on Plasma Physics, Tarragona 27.6.-1.7.2005, Spain.
- [3] J. Šimek, R. Hrach, O. Bařina, V. Hrachová, *Multi-dimensional codes for particle modeling in Tokamak edge plasma*, Vacuum (in print).
- [4] J. Šimek, R. Hrach, *Multi-dimensional particle codes in modeling in low-temperature and high-temperature plasmas in the presence of magnetic field*, 32nd EPS Conf. on Plasma Physics, Tarragona 2005, Spain, Editors van Milligen B.Ph. and Hidalgo C., ECA Vol. 29C (2005), P-4.003, 4 pages.
- [5] M. Holík, O. Bilyk, A. Marek, I. Picková, P. Kudrna, M. Tichý, *Measurements with Langmuir and Emissive Probe in Magnetically Supported DC Discharge in Cylindrical Symmetry*, Proc. 15th Symposium on Applications of Plasma Processes and 3rd EU-Japan Joint Symposium on Plasma Processing, Grand Hotel Permon, Podbanske, Slovakia, January 15 – 20, 2005, Edited by K. Hensel, Š. Matejčik, J.D. Skalný and N.J. Mason, ISBN 80-223-2018-8, pp. 175-176.
- [6] A. Marek, M. Holík, O. Bilyk, I. Picková, R. P. Apetrei, R. Schrittwieser, Codrina Ionita-Schrittwieser, P. Kudrna, M. Tichý, *Magnetized Plasma in Cylindrical Coordinates – Experiment and Model*, 17th Intern. Symposium on Plasma Chemistry, (ed. by J. Mostaghimi, T.W. Coyle, V.A. Pershin, H.R. Salimi Jazi), Toronto, Canada, August 7-12, 2005, Abstracts and full-papers CD, abstract p.197-8, CD - ISPC-635.pdf (6 pages).

Improvement of the radiometer on CASTOR - design the antenna for oblique view of the plasma

J. Zajac, J. Preihaelter, J. Urban

In collaboration with:

S. Nanobashvili, Andronikasvili Institute, Tbilisi, Georgia

Antenna construction. A new antenna for microwave radiometry was constructed in 2005 to study ECE – EBW conversion. The so-called X-O-B conversion is characterized by a propagation oblique to the plasma boundary. The antenna construction (bent circular waveguide) is seen in Figs.1 and 2.

Results. The antenna was used for the 18 - 26 GHz radiometry band. A suitable toroidal field was set to have the ECE profile in the Castor radius range. The radiated temperature profile measured by a calibrated radiometer is shown in Figs. 3 and 4. The ECE and electron temperature could be evaluated from the radiated temperature if the EBW conversion efficiency is known. The EBW conversion efficiency wasn't evaluated because the measured radiated temperature profile is quite far from the expected one. The radius of the maximum of the radiated temperature does not correspond to



Fig. 1 Antenna with tokamak flange



Fig. 2 Detail of shaped antenna mouth place in the narrow tokamak port

the plasma centre. Possible reason is that a high background continuous radiation overlaps the ECE.

Conclusion. The radiometry experiments in 2005 on Castor have not been successful since the antenna for oblique reception was not selective enough to suppress the background radiation. The antenna receives radiation from a too wide space angle, probably due to the reflections on the tokamak chamber close to the antenna mouth. The narrow port does not allow for a better arrangement of the bent waveguide. For that reason, a new mirror antenna will be prepared next year.

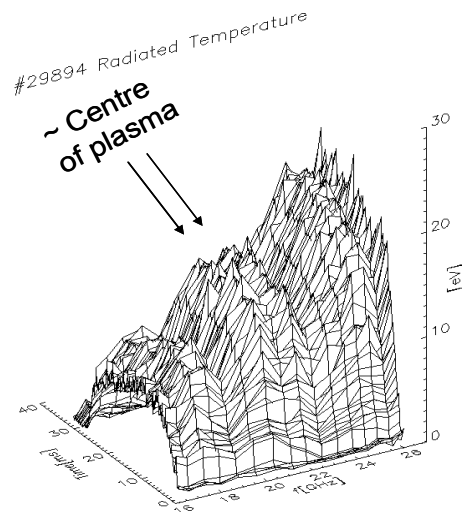


Fig. 3 Radiated temperature profile

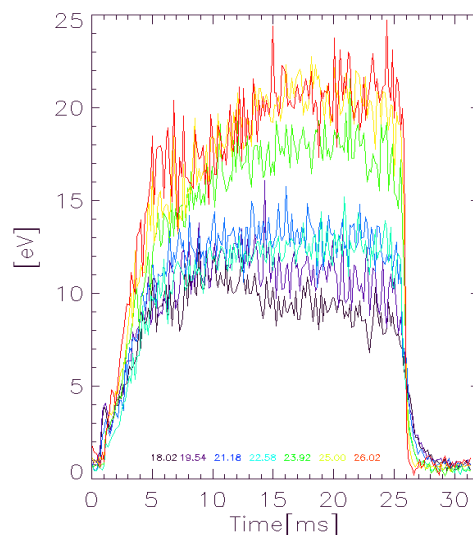


Fig. 4 Radiated temperature profile,
colours = frequency, frequency \sim ECE radius

3 Wave Interactions in Plasmas

Modeling of tokamak edge plasma flows and interpretation of probe diagnostics in the presence of suprathreshold electrons by the quasineutral particle-in-cell (QPIC) method

V. Fuchs, R. Dejarnac, V. Petržílka, L. Krlín

In collaboration with:

J. P. Gunn, L. Colas, Association EURATOM-CEA, CEA/DSM/DRFC, Centre de Cadarache, 13108 Saint Paul Lez Durance, France

In 2005, we have continued our 2004 effort to develop and apply a quasi-neutral particle-in-cell code (QPIC) for tokamak edge plasma studies. The principal purpose of this QPIC kinetic code is the modeling of plasmas, where non-Maxwellian ion and non-Maxwellian and/or supra-thermal electron populations can be expected. In such plasmas, Boltzmann electrons cannot be assumed and both particle populations have to be described explicitly. Such a situation arises, for example, along magnetic field lines, which pass near a lower hybrid (LH) grill. The high- n_{\parallel} (parallel refractive index) part of the grill electric field spectrum interacts with resonant electrons which, as a result, are accelerated and heated (typically from 25 eV to 1-2 keV). Tokamak edge components connected to such magnetic field lines can suffer damage from the LH-generated fast particles. An associated problem is the interpretation of probe diagnostics in the presence of suprathreshold particles, since standard Langmuir probe theory assumes thermal Maxwellian electrons. The QPIC code automatically accounts for the ion response to electron acceleration. Clearly, ions, which are accelerated towards a material surface through a sheath region are also non-Maxwellian.

The work described is a pioneering effort, which enables simulating large scrape-off layer regions (typically tens of meters), where the Debye length is of order 10^{-5} m, so that standard PIC simulations require an impractical computation effort. The QPIC simulation time is about 2 orders of magnitude smaller than PIC simulation time.

Our results can be summarized as four separate themes as follows.

- 1) Calibration of QPIC using known kinetic results, and extension of Mach probe theory for a double Maxwellian distribution [1].
- 2) Interpretation of Langmuir probe diagnostics in the presence of LH-generated supra-thermal electrons [2], and the study of fast electrons near ion cyclotron antennas [3].
- 3) Measurements, supported by computation, of scrape-off layer flows in the Tore Supra tokamak [4].
- 4) Development of a novel integration technique for the particle equations of motion in QPIC [5].

1 In order to demonstrate the power of the QPIC approach, we extended the Chung-Hutchinson [6] collisionless kinetic theory of a Mach probe, which assumes isothermal, Maxwellian electrons, to include an isotropic, two-temperature electron distribution function.

The kinetic equations for ion and electron motion in the probe wake are solved using the QPIC method, which compares qualitatively well with the results of a simple fluid model. We find that the measured Mach number decreases slightly with increasing hot electron concentration, but the main effect is seen on the measured electron temperature. Due to the fact that the probe is sensitive to even a tiny population of hot electrons, the resulting ion sound speed can be overestimated by up to a factor of two, leading to measurements of absolute flow speed that are too large [1]. Figures 1-4 below show some of the properties of the QPIC solutions.

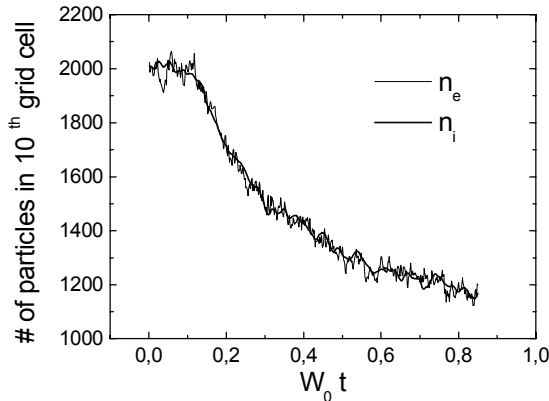


Fig. 1 Quasi-neutrality: the number of ions (thick curve) and electrons (thin curve) in the tenth grid cell during the initial phase of a typical simulation. Particles are assigned the unperturbed source distribution at $t=0$. The collection of ions by the probe leads to a rapid drop in density during the formation of the pre-sheath.

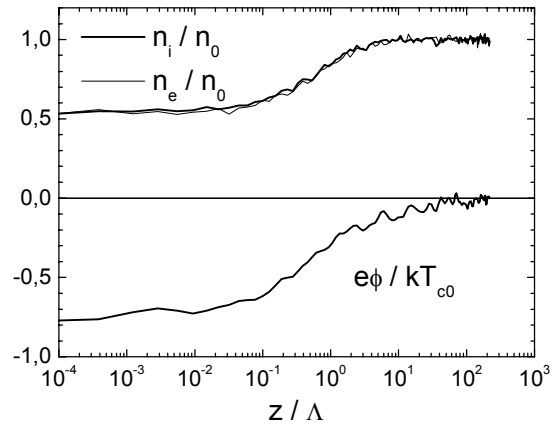


Fig. 2 Quasi-neutrality: instantaneous ion (thick curve, top panel) and electron (thin curve, top panel) densities, and electric potential (bottom panel).

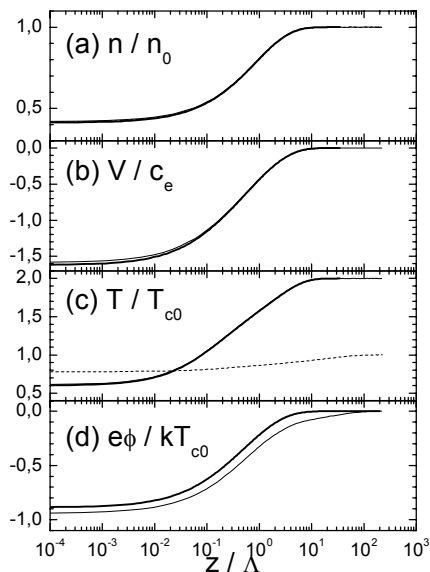


Fig. 3 Equilibrium (a) density, (b) speed, (c) temperature of ions (thin full curves) and electrons (thin dashed curves) calculated by QPIC, to be compared with the Boltzmann electron model of Chung and Hutchinson (thick curves). The potential (thin=QPIC, thick=Chung&Hutchinson) is shown in panel (d).

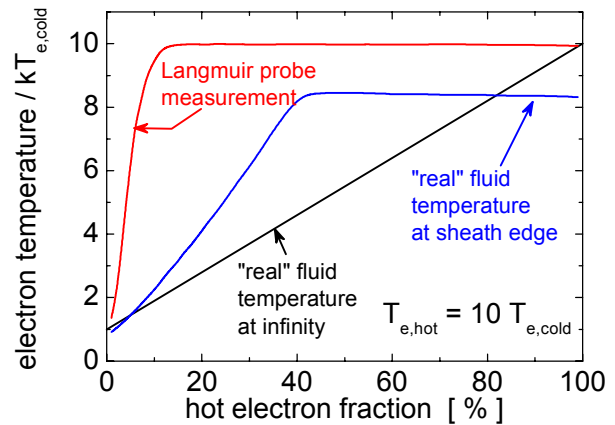


Fig. 4 Simulated electron temperature versus the hot electron fraction. The real fluid temperature at the sheath edge $z=0$ and at infinity are compared with the apparent electron temperature that a Langmuir probe would measure.

2 We developed a self-consistent description of a presheath plasma and an interpretation of Langmuir probe characteristics in the presence of non-Maxwellian supra-thermal electrons. The supra-thermal electrons are generated in the vicinity of a lower hybrid (LH) grill [6] and flow along magnetic field lines to a Langmuir probe. The presheath plasma is bounded by the sheath-presheath interface at one end and plasma at the other end. We study this plasma edge problem computationally using a QPIC code. The LH grill - edge electron interaction is treated by a Monte-Carlo method described in [7]. For conditions of the Tore Supra edge plasma and LH grill ($f_{LH}=3.7$ GHz, $E_0=3$ kV/cm, wave-guide+septum width=1.05 cm) the pre-sheath remains quasi-neutral throughout with an appreciable density depression and temperature increase in the grill region, in agreement with previous test electron simulations [7]. Near the wall, a precipitous density drop is caused by ion loss. A proportional number of most energetic electrons are allowed to reach the wall while maintaining equal particle flows. This allows the floating potential V_f to be inferred. For typical Tore Supra LH grill conditions we obtain $V_f=-17.7 T_{e0}$, compared with $V_f=-1.45 T_{e0}$ at thermal conditions (we use an ion-to-electron mass ratio $m_i/m_e=200$). We showed that most assumptions made in the standard interpretation of measured probe V-I characteristics are violated [2]. Figures 5 and 6 below show the difference between the computed and measured temperatures in the presence of suprathermal electrons.

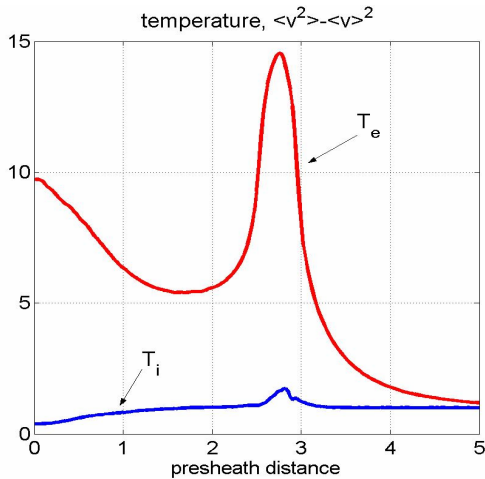


Fig. 5 Computed electron and ion temperatures [keV] from QPIC, as a function of normalized distance from the probe (0...probe, 5...thermal plasma boundary). The electron temperature is seen to strongly peak in the LH grill region and rise again towards the probe as the sheath potential screens lower-energy electrons.

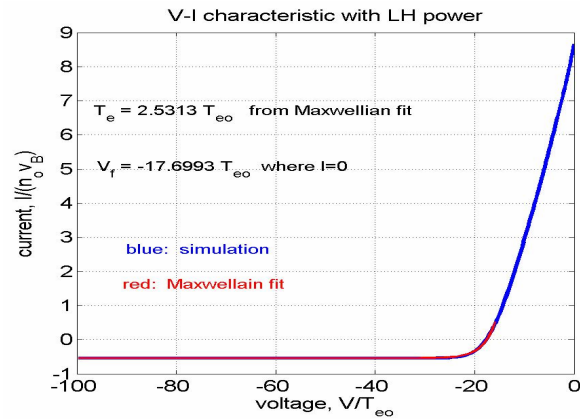


Fig. 6 Computed V-I characteristic and electron temperature determined by the standard method from a Maxwellian fit, to be compared with T_e at the probe from Fig. 5. Thermal plasma probe theory gives $V_f \approx -2T_{e0}$ for an ion-to-electron mass ratio $\mu=200$, so that a Maxwellian fit to the V-I characteristic in the LH case provides an indication of the presence of suprathermals. The fitted value of the local T_e is, however, incorrect.

3 Near-sonic parallel flows are systematically observed in the scrape-off layer (SOL) of the limiter tokamak Tore Supra, as in many X-point divertor tokamaks. The poloidal variation of the Mach number of the parallel flow has been measured by moving the contact point of a small circular plasma onto limiters at different poloidal angles. The resulting variations of flow are consistent with the existence of a poloidally nonuniform core-to-SOL outflux concentrated near the outboard midplane. Strong variations of the SOL width up to a factor of 10 suggest that this localized outflux is due to enhanced radial transport. The plasma that gets

ejected into the SOL can expand radially to the wall if magnetic field lines have long connection lengths and pass unobstructed across the outboard midplane [4].

4 We developed an area-preserving implementation of the 2nd order Runge–Kutta integration method suitable for the equations of motion in the QPIC code. For forces independent of velocity the scheme possesses the same numerical simplicity and stability as the leapfrog method, and is not implicit for forces, which do depend on velocity. It can be therefore easily applied where the leapfrog method in general cannot. We discuss the stability of the new scheme and test its performance in calculations of particle motion in three cases of interest. First, in the ubiquitous and numerically demanding example of the nonlinear interaction of particles with a propagating plane wave, second, in the case of particle motion in a static magnetic field and, third, in a nonlinear dissipative case leading to a limit cycle. Of special interest is the role of intrinsic stochasticity introduced by time-differencing, which can destroy orbits of an otherwise exactly integrable system and therefore constitutes a restriction on the applicability of an integration scheme in such a context. This leads to the nonlinear stability condition $\Delta t \omega_B \leq 1$, where Δt is the time step and ω_B the particle bounce frequency [5]. Figure 7 below gives an example of integration using the proposed new SIMP method.

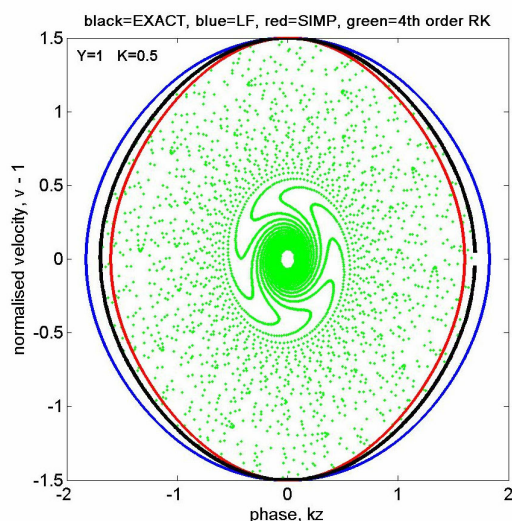


Fig. 7 Comparison of a nonlinear wave orbit computed by various integration techniques. $Y = \omega_B / \omega$, $K = (Y\Delta t)^2$, where ω_B is the electron bounce frequency and Δt is the integration time step. Nonlinearity is weak when $K \ll 1$. We denote by LF the leapfrog method, by RK the Runge-Kutta technique, and by SIMP the present semi-implicit midpoint method. We note that the standard 4th order RK method collapses because of area non-preservation.

References

- [1] J. P. Gunn and V. Fuchs, *Mach probe interpretation in the presence of suprathermal electrons*, submitted to The Physics of Plasmas.
- [2] V. Fuchs, J. P. Gunn, R. Dejarnac, *Langmuir probe characteristics in the presence of suprathermal electrons generated by a lower hybrid grill*, 32nd EPS Conference on Plasma Physics, 27 June-1 July 2005, Tarragona, Spain, P4.005.
- [3] V. Petržílka, V. Fuchs, L. Krlin, L. Colas, et al., *Electron acceleration near ICRF antennas*, ibid.
- [4] J.P. Gunn, C. Boucher, I. Āuran, V. Fuchs et al., *Plasma flows in the scrape-off layer of the Tore Supra tokamak*, The International Conf. PLASMA-2005 on Research and Application of Plasmas, Opole-Turawa, Poland, 6-9 Sept., 2005, AIP Conference Proceedings **812**.
- [5] V. Fuchs and J.P. Gunn, *On the integration of equations of motion for particle-in-cell codes*, J. Comput Phys. 214 (2006) 299, appeared online 21 Nov., 2005.
- [6] K S. Chung and I. H. Hutchinson, Phys. Rev. **A38**, 4721 (1988).
- [7] V. Fuchs, J.P. Gunn, M. Goniche, and V. Petržílka, Nucl. Fusion, **43** (2003) 341.

Positive biasing of plasma in front of LH antennas

F. Žáček, V. Petržilka

In collaboration with:

M. Goniche, P. Devynck, Association Euratom/CEA, Cadarache, France

Lower hybrid waves (LHW) are commonly used in tokamaks for non-inductive generation of electrical current. However, if LH power of order of MW is used in big machines, a detrimental effect of parasitic acceleration of edge particles in front of the RF antennas has been discovered. Namely, such particles (with energy up to several keV) hit the surface of the first wall connected directly by magnetic field lines and create “hot spots” with strongly localized wall erosion.

The small tokamak CASTOR enables direct measurements of the plasma as well as of the electric field behaviour just in front of the LH antenna (i.e. directly in the wave-plasma interaction region) using Langmuir probes. Recently, a well-expressed decrease of the insulated probe potential down to minus 200V has been observed in a narrow layer (several mm in the radial direction) in the interaction region on this machine [1]. Because the floating potential is sensitive to the presence of energetic electrons, a generation of such non-thermal accelerated electrons at LH wave application could be deduced from this fact.

As the accelerated electrons are pushed away from the grill mouth along the magnetostatic field lines, they leave the heavier ions behind and according to theory an electrostatic field and consequent plasma flows are generated [2,3]. However, the increase of the plasma potential in the interaction region could not be observed up to now. Using an emissive Langmuir probe in front of the CASTOR LH antenna, the first direct measurement of the plasma potential have been achieved [4,5]. It has been shown that positive plasma “biasing” also takes place in a very narrow layer just at the grill mouth, see Fig.1a). The effect scales linearly with the power applied, see Fig.1b).

References

- [1] F. Zacek, V. Petržilka, M. Goniche, P. Devynck, S. Nanobashvili: Radially scanned probe measurements in front of the CASTOR lower hybrid antenna, *Contrib. Plasma Phys.* **44** (2004), No 7-8, 635-642
- [2] V. Petržilka et al., LH driven plasma density variations and flows in front of LH grills and resulting reflection coefficient changes and thermal loads, 30th EPS Conf. on Contr. Fusion and Plasma Physics, St. Petersburg 2003, ECA Vol. **27A**, P-1.195
- [3] V. Fuchs et al., Quasineutral simulations of plasma response to the lower hybrid antenna electric field, 31th EPS Conf. on Contr. Fusion and Plasma Physics, London 2004, ECA Vol. **28G**, P-5.142
- [4] F. Zacek, V Petrzilka, M. Goniche: Positive biasing of plasma in front of LH antennae, *Plasma Phys. Control. Fusion* **47** (2005) L17-L24.
- [5] F. Zacek, V. Petržilka, M. Goniche: Radial and toroidal electric field measurements in front of the CASTOR tokamak LH launcher, 32nd EPS Conf. on Plasma Phys., Taragona June 27 – July 1, 2005, P4.004

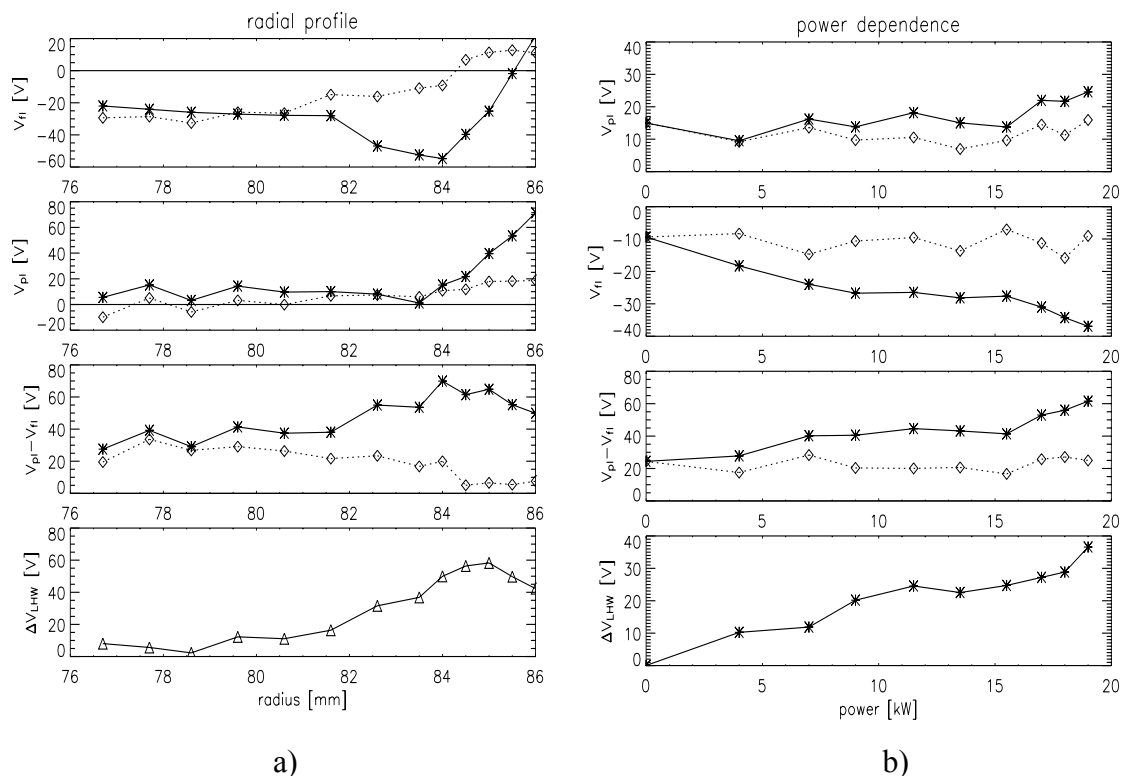


Fig. 1 a) Comparison of radial profiles of the cold (V_{fi} , floating) and emissive (V_{pl} , plasma) probe floating potentials in OH (diamonds) and LHW (asterisks) discharge phase. The difference of both potentials $V_{pl} - V_{fi}$ is shown also. The last trace denoted as V_{LH} (triangles) is a net change of $V_{pl} - V_{fi}$ due to the LHW with respect to its ohmic value. b) Power dependence of the LHW effect measured by the probe in the potential “well” of the probe floating potential at $r=85\text{mm}$ in Fig.b).

Numerical simulation of EC emission in MAST

J. Preinhaelter, J. Urban, P. Pavlo

In collaboration with:

M. Valovič, V. Shevchenko, UKAEA Culham, GB

L. Vahala, ODU, Norfolk, VA, USA

G. Vahala, W&M, Williamsburg, VA, USA

During last few years we developed a code for the simulation of EBW emission from spherical tokomaks, specially for MAST and NSTX. On MAST, we found good agreement between the simulation of EBW emission and the detected signals for L-modes and ELMy H-modes. On the other hand, the emission from ELM free H-modes in MAST suggests that the magnetic field in the transport barrier as determined by EFIT is too low. Typically, the detected signal in the 16-60 GHz band has five peaks, each corresponding to the emission from subsequent electron cyclotron harmonics (see Fig. 1).

The gaps between the peaks correspond to the frequencies at which the upper hybrid frequency coincides with some of the electron cyclotron harmonics. From the position of the gaps in the spectrum of the detected signal, we can determine the magnitude of the magnetic field.

We found that ECE spectra of ELM-free H-modes suggest that the magnetic field in the transport barrier is deformed with respect to that determined from EFIT [1,2]. At present, we

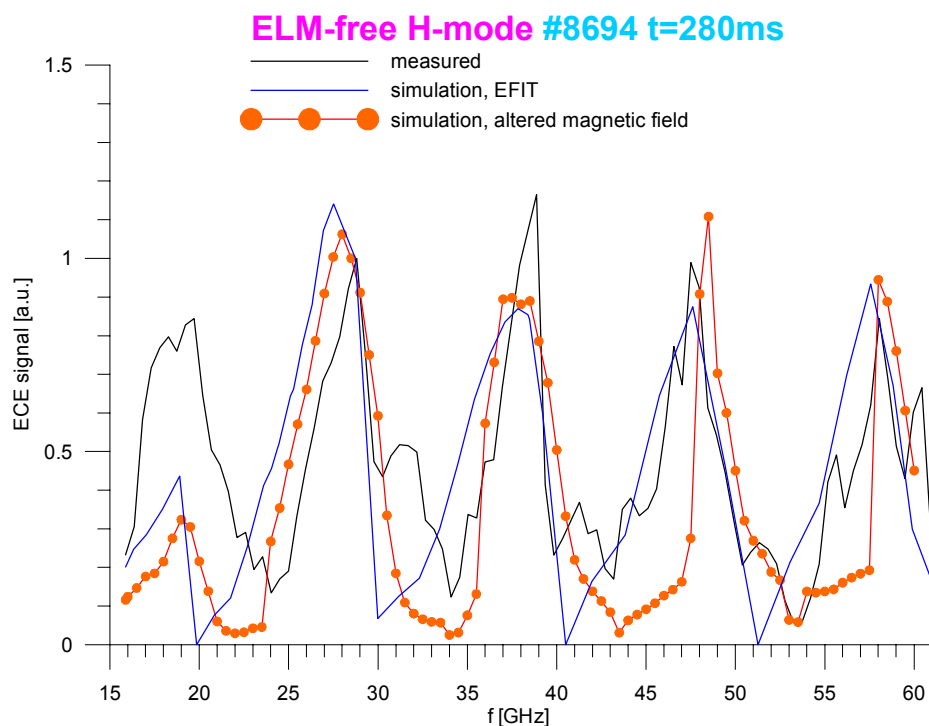


Fig. 1 Frequency spectrum of .EBE Detected signal and simulations.

have no real interpretation for the bump on the total magnetic field (see Fig. 2) and its reconstruction was not fully self-consistent.

The adaptive finite elements solver of Maxwell equations in an inhomogeneous plasma, which is used in the simulations for EBW-X-O conversion efficiency estimation, has been further improved. An initial guess for mesh density was implemented, resulting in a speed-up of the code [3]. Our code has been upgraded to full 3D geometry and used to study EBW propagation in the WEGA stellarator to interpret the EBW heating experiments.

References

- [1] J. Preinhaelter, G. Taylor, V. Shevchenko, J. Urban, M. Valovic, P. Pavlo, L. Vahala, G. Vahala: *EBW simulation for MAST and NSTX experiments*, 16th RFPP Topical Conference proceedings, Park City, Utah USA (2005). AIP Conference Proceedings 787,ed. Stephen J. Wukitch, Paul T. Bonoli,(2005), 349-352J
- [2] J. Urban, J. Preinhaelter, V. Shevchenko, G. Taylor, M. Valovic, P. Pavlo, L. Vahala, G. Vahala: *Methodology of electron Bernstein wave emission simulations*, 32nd EPS Plasma Physics Conference proceedings, Tarragona, Spain (2005).
- [3] J. Urban, J. Preinhaelter: *Adaptive finite elements for a set of 2nd order ODE's*, 19th ICNSP & APPTC proceedings, Nara, Japan (2005).

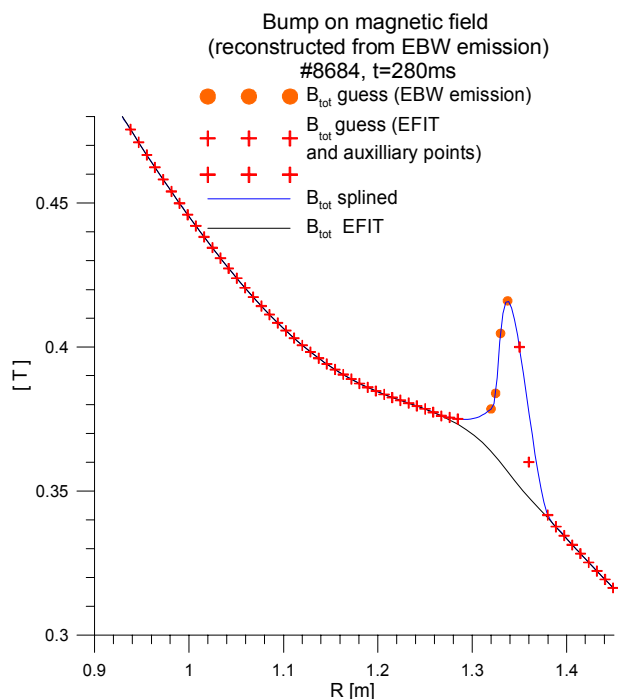


Fig. 2 Comparison of the EFIT profile of the magnetic field and the field reconstructed from the EBW signal for #8694.

Fast particle energy measurements in the scrape-off layer during lower hybrid current drive experiments on Tore Supra, and the analysis and interpretation of the measurements

V. Petržílka, F. Žáček

In collaboration with:

J. Gunn, M. Goniche, P. Devynck, A. Ekedahl, E. Gauthier, J.-Y. Pascal, F. Saint-Laurent, Association Euratom/CEA Cadarache, France

A retarding field analyzer (RFA) was used during lower hybrid (LH) current drive experiments in the Tore Supra tokamak, as in [1], to measure the flux of supra-thermal particles emanating from the near field region in front of the LH grill mouth. The RFA was reciprocated in ~ 250 ms up to 1 cm behind the last closed flux surface. The RFA entrance slit was biased to -50 V with respect to the vacuum vessel ground in order to repel thermal electrons. The ion-repelling grid was grounded such that all ions could reach the collector. The secondary electron grid was biased to -200 V.

For specific values of the safety factor and of the RFA position, a strong negative current was measured both on the entrance slit and on the collector. This occurs when at least one of the wave-guide rows is magnetically connected to the RFA, and only when the launcher is active, Fig. 1. We note that no thermal electrons pass through the RFA entrance slit in the ohmic regime. This is verified by sweeping the voltage of the entrance slit from $+10$ V down to -50 V, Fig. 2. The ion current saturates already at -10 V. The RFA collector therefore measures pure ion current.

The peaks of the negative current, seen in Fig. 1, indicate: (1) the presence of an electron flux that exceeds the ion flux, (2) the applied potentials are not negative enough to repel the electrons. The peak of the negative current is observed at the same position on the ingoing and outgoing phases of the probe reciprocation. The electron flux is localized in a layer ~ 1 cm thick. The outer edge of the fast electron layer coincides with the leading edge of the LH antennae C2 and C3 within the uncertainty of the magnetic measurements (at most ± 5 mm), Fig. 3a. The spatial resolution (~ 5 mm) allows the radial width

of the collected fast electron beam to be assessed as less than 1 cm. This result is consistent with measurements obtained by infra-red imaging of connected in-vessel components. The electron current on the entrance slit and on the collector comes in rapid bursts (typical frequency in the 10-20 kHz range), Fig. 3b. The form of the bursts is very similar on the

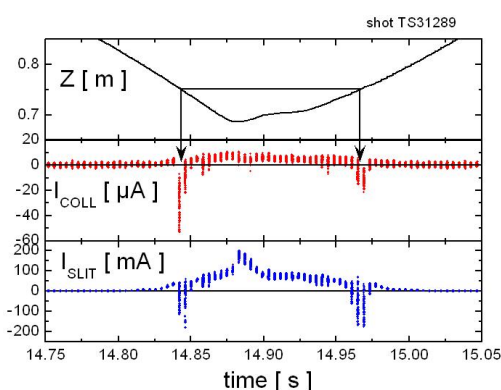


Fig. 1 Temporal evolution of ion currents during a probe reciprocation, LH power launched.

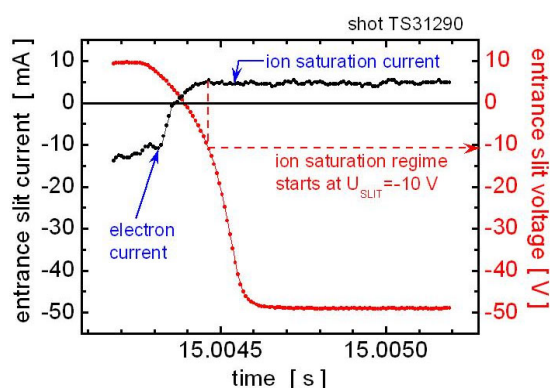


Fig. 2 RFA entrance slit current in ohmic regime, no LH power launched.

collector and on the entrance slit. In Fig. 3b, the interpolated ion saturation currents are subtracted from the signals to extract the pure electron component.

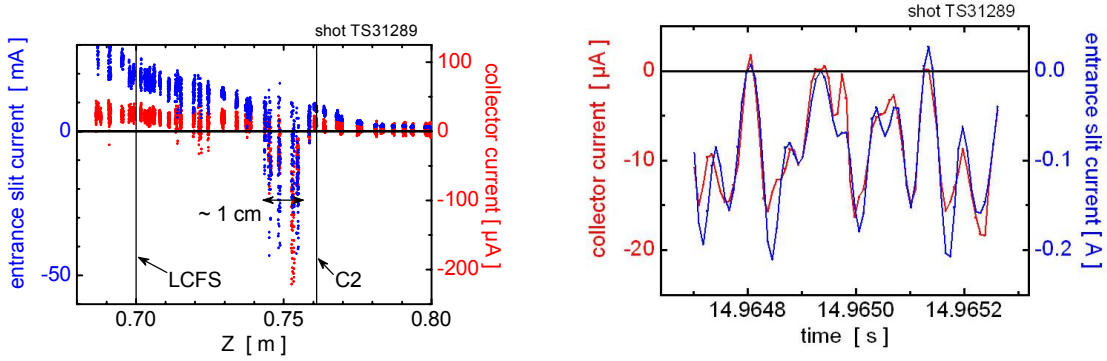


Fig. 3 *a* (left panel): A more detailed structure of the negative peak as seen in Fig.1, plotted as a function of the vertical RFA position. *b* (right panel): Detailed temporal structure of the peak of the negative current.

In order to explore the spatial energy distribution in the fast electron beam, we introduced a transmission factor, defined as the ratio of the electron current densities at the entrance slit and collector. Here we show the transmission factor of the largest bursts, Fig. 4. The transmission is higher in the center of the beam. Electrons that reach the collector have at least 150 eV of kinetic energy as they pass through the entrance slit. The variation of transmission factor could be qualitatively indicative of the width of the electron distribution function. As Fig. 3a shows, the peak of the RFA slit and collector currents, arising due to the fast electron beam, is radially shifted about 1 cm into the plasma from the magnetic surface, on which the mouth of C2 and C3 launchers is located. The radial location of the maximum of the transmission factor, Fig. 4, which apparently coincides with the radial location of the most energetic electrons in the beam, is also about 1 cm shifted radially into the plasma. Accounting for the magnetic ripple shows that, in fact, the beam is generated about 2 centimeters in front of the LH grills mouth.

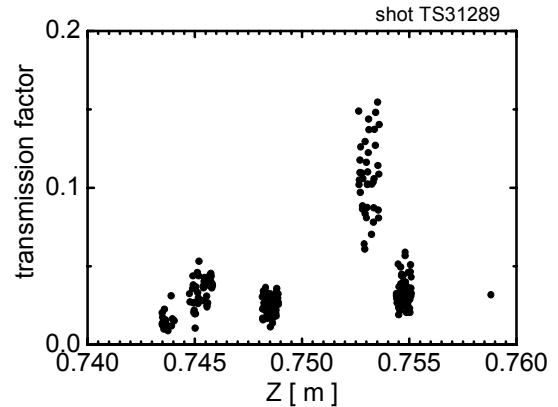


Fig. 4 Transmission factor as a function of the radial position in the electron beam.

This is in agreement with observations of the hot spots locations in Tore Supra [2] and in JET [3]. However, the original theory predicts the generation of a fast particle beam in locations radially nearer to the grill mouth flux surface, where the higher spatial harmonics of the LH wave still are not damped [4]. The presence of fast electrons in experiments observed at larger radial distances of the order of centimeters from the grill mouth could possibly be explained by the presence of spontaneously excited random fluctuating fields in front of the grill mouth. However, this does not explain why fast electrons were not found at radial distances very near to the grill mouth.

We conclude by noting again that the RFA measurements indicate that the fast electron beam is generated at a distance of 1 or 2 centimeters in front of the LH grills. And, for the first time, qualitative data about the accelerated electron distribution function were obtained.

References

- [1] M. Goniche, et al., 31st EPS Conference, London, June 2004, P-4.110.
- [2] M. Goniche, et al., Nuclear Fusion **28** (1998) 919.
- [3] M. Goniche, et al., JET report JET-R(97)14; K. Rantamaeki, et al., to appear in Plasma Phys. Controlled Fusion.
- [4] V. Fuchs, et al., Phys. Plasmas **3** (1996) 4023.
- [5] V. Petržílka et al.: invited paper, Varenna Fusion Theory Workshop 1998, p. 95.

Electron acceleration near ICRF antennas

V. Petržílka, V. Fuchs, L. Krlín

In collaboration with:

L. Colas, M. Goniche, Association Euratom/CEA Cadarache, France

S. Heuroux, LPMI, Université Nancy, France

V. Bobkov, F. Braun, R. Dux, R. Neu, J.M. Noterdaeme, Association Euratom/IPP Garching, Germany

1. Introduction

It is demonstrated that thermal electrons can be accelerated to an energy of several keV, when moving along magnetostatic field B lines near an ICRF (Ion Cyclotron Resonance Frequency) antenna. The electron can gain energy in passing the near antenna rf field inhomogeneity, because of the temporal phase changes of the field, which do not average out on the electron quiver motion time scale. This process is similar to electron acceleration in front of lower hybrid wave antennas [1], when the electron passes in front of the septum between waveguides. The electron energy rises by repeated passes through the near antenna rf field inhomogeneity, as the electrons are reflected at the sheath on ICRF antenna components, such as parts of the antenna box and antenna guard limiters, until the electron kinetic energy reaches or overcomes the sheath potential. In turn, the sheath potential corresponding to the rectified rf potential can be enhanced by those energetic electrons [2] which hit the antenna parts and the kinetic energy of which is larger than the sheath potential, if the electron flux becomes greater than the local Bohm flux. The increased sheath potential can cause stronger ion acceleration and plasma convection near the ICRF antennas [3]. This novel acceleration process can thus participate in the creation of high thermal loads (hot spots) observed on antennas. For the numerical modeling, the rf field was computed with the ICANT code [4] for 1 MW launched in monopole and dipole phasings by a Tore Supra antenna, or with the HFSS code (ANSOFT®) for 1 MW launched in dipole phasing by an ASDEX Upgrade antenna. We use test particle computations to estimate the energy gain of electrons as a function of time and as a function of the RF electric field intensity.

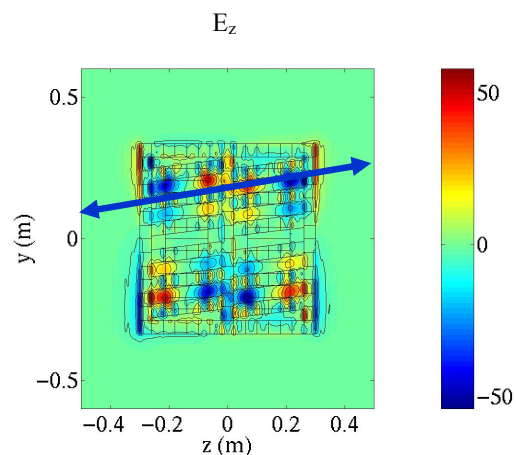


Fig. 1. E_z (kV/m) field of the Tore Supra antenna, still in vacuum and just in front of the Faraday screen, the rf frequency is 48 MHz, the boundary plasma density $8 \times 10^{18} \text{ m}^{-3}$.

2. Electron Acceleration

An ensemble of 300 test electrons with a thermal Maxwellian velocity distribution at 30 eV is injected at equal distances along the line (which is parallel to B), Fig. 1. Motion along this line illustrates the case of electrons accelerated when going through regions of maximum oscillating fields in the antenna vicinity, just in front of the Faraday screen.

At first, it is assumed that the electrons are always reflected by the sheath potential U at the end of the arrows at the blue line, at $z = -0.5$ and 0.5 , where the guard limiters are located. In other words, we at first assume that U is larger than the electron kinetic energy. The motion of the test electrons is followed in time. Fig. 2a shows the ensemble averaged total electron energy W_T . The electron energy in Fig. 2a grows, but it eventually saturates as a function of time. This growth is due to velocity space diffusion of electrons in the resonant part of the ICRF spectrum experienced by electrons bouncing between the sheaths. This is similar to the electron acceleration mechanism at a lower hybrid antenna [1].

As the energy of electrons is growing, the assumption of total reflection at the sheaths is necessarily violated. However, the electron energy and the sheath voltage grow together. This process will need to be investigated as the next step. After some time interval, the sheath voltage should reach a new equilibrium value. When the new value of the sheath voltage will be determined, its consequences for the edge plasma convection may be estimated, as was done in [3].

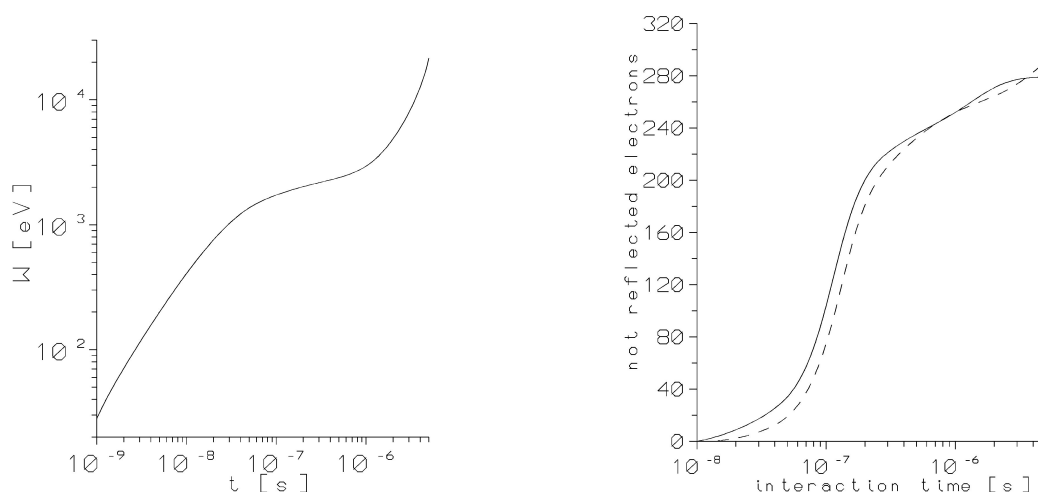


Fig. 2 a) The total energy gain W_T along the blue line as a function of time. It is assumed that electrons are reflected at the ends of the blue line. b) The number of the electrons out of the total number of 300 injected electrons, which are not reflected (because their energy is larger than U) at the ends of the blue line. Solid line: The sheath potential $U = 3Te + (U_{rf}/2)(1 + \cos(\omega t))$; dashed line: $U = 3Te + U_{rf}$; $U_{rf} = 1500$ V.

In the calculations represented in Fig. 2b, we dropped the assumption that all electrons are reflected at the sheath. Fig. 2b then gives the number of electrons, which are not reflected by a finite sheath potential U , after a certain acceleration time along the blue line. Figure 3 gives the scan along the poloidal coordinate y of the electron acceleration in front of the ICRF antenna for dipole and monopole Tore Supra antenna phasings. Here it is again assumed, as in Fig. 2a, that the electrons are always reflected by the sheet. The electron path was followed for two microseconds over 40 poloidally (coordinate y) equidistant lines along B with a tilt of 7 degrees. The radial plane, in which the fields are computed, is 1 cm in front of the box; the current straps are recessed minus 2.5 cm into the box; this means that the particle moves

3.5 cm in front of the straps; plasma is 5.5 cm in front of the straps, i.e. plasma is 2 cm in front of the plane, where the particle moves, and 3 cm from the box boundaries.

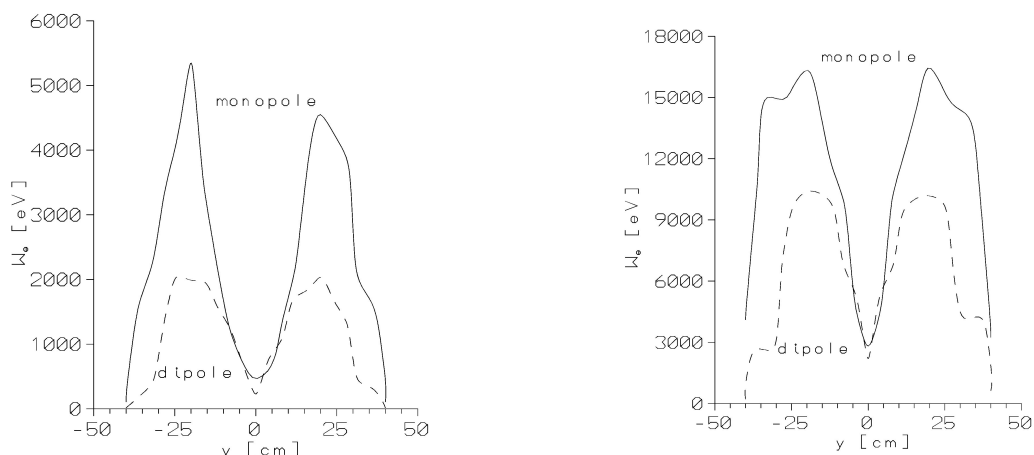


Fig. 3 Left: Ensemble averaged final energy of 300 thermal test electrons. Right: Maximum electron energy, which was acquired by the most accelerated electron. The peaks of the curves correspond to the poloidal peaks of the electric field amplitude, cf. Fig. 1. The electrons bounce between guard limiters at $z=-50$ and 50 cm.

It can be seen that the maximum electron acceleration takes place at the line passing through the poloidal maximum of the electric field amplitude. Finally, we complement the preceding modeling of electron acceleration by the Tore Supra ICRF antenna by results, shown in the table below, of calculations of electron acceleration along three magnetostatic (tilt 7 deg - the Faraday screen has a tilt of 15 deg) field lines of an ASDEX Upgrade ICRF antenna. The lines were chosen in order to intersect three locations poloidally in the center and in the upper and lower halves of the antenna, where spectroscopic observations of the antenna guard limiter are made. Traces of the energetic electron beam might possibly be observed there as bright spots:

	vacuum	water load
upper line	288 eV	1718 eV
center line	1443 eV	303 eV
lower line	282 eV	1066 eV

The fields were calculated in two cases: (i) the antenna radiates into vacuum, (ii) the antenna load is modeled by water in the field calculations. The sheath potential was chosen as $U=3Te+(U_{rf}/2)(1+\cos(\omega t))$, like in Fig. 2b. It can be seen that the load significantly changes the acceleration pattern: Without the load, the acceleration is strongest at the central line, but with the load, the opposite is true. In conclusion, a novel process of electron acceleration near the ICRF antenna, the physics of which is similar to the well-known electron acceleration process in front of the LH grills [1], was identified and explored. It was shown that the novel acceleration mechanism can produce energetic electrons near ICRF antennas, which then can produce hot spots directly, or indirectly by enhancing the sheath potential and in turn the ion acceleration in the sheath

References

- [1] V. Fuchs et al., Phys. Plasmas **3** (1996) 4023.
- [2] D. Tskhakaya, S. Kuhn, V. Petrzilka, R. Khamal, Phys. of Plasmas **9** (2002) 2486.
- [3] M. Bécoulet et al., Phys. Plasmas **9** (2002) 2619.
- [4] S. Pécoul et al., Computer Physics Communications **146** (2002) 166.

4 Atomic Physics and Data for Edge Plasma and Plasma-Wall Interactions

Energy transfer and chemical reactions in collisions of ions with surfaces

Z. Herman, J. Žabka, A. Pysanenko (J. Heyrovsky Institute of Physical Chemistry)

In collaboration with:

T. D. Märk and coll., Association EURATOM-ÖAW, Innsbruck, Austria

In a systematic study of interaction of slow molecular ion species with surfaces relevant to plasma and fusion systems, we continued scattering studies of slow (10-50 eV) hydrocarbon ions with carbon surfaces at room temperature, and heated to about 600°C. Earlier, we described results for collisions of C₁ and C₂ hydrocarbon ions. Here, we concentrate on collisions of C₃ hydrocarbon ions and a comparison of dication and cation collisions, using model C₇ hydrocarbon ions.

The experimental method [1-5] consisted in directing the projectile ion reactant beam of a well-specified incident energy under a pre-selected angle (in our case 30° with respect to the surface) towards a carbon surface, and in measuring mass spectra of product ions as well as their translational and angular distributions. The data provide information on ion survival probability of the projectile ions in ion-surface collisions, on surface-induced dissociation processes and on chemical reactions with the surface material. The data can also serve to determine the mechanism of reactions at surfaces, to elucidate energy transfer in collisions with surfaces, the extent of inelasticity of the collisions and the degree of incident-to-internal energy transfer for ions of increasing complexity. The surface used in these experiments was a sample of highly-oriented pyrolytic carbon (HOPG), shown earlier to behave very similarly to samples of tokamak carbon tiles. This surface could be studied either at room temperature, when it was covered -as shown earlier- by a layer of hydrocarbons, or at a temperature of about 600°C, when this hydrocarbon layer was effectively removed.

1. Collisions of low-energy hydrocarbon ions C₃H_n⁺ and C₃D_n⁺ (n=2-8) with room-temperature and heated carbon surfaces

Mass spectra of ion products show an increasing extent of fragmentation of the projectile ions with increasing incident energy. Though some of the investigated ions (C₃H₈⁺, C₃H₇⁺, C₃H₆⁺, C₃H₅⁺, C₃H₄⁺, C₃H₃⁺, C₃H₂⁺ and some of their D-labeled variants) and their fragmentation products may exist in isomeric forms, no specific effect on the extent of fragmentation was observed. Interactions of radical cations in this series, namely interactions of C₃H₈⁺ and C₃H₆⁺ with room temperature surfaces showed ion products formed in chemical reactions of H-atom transfer with the hydrocarbons on the surface. In this reaction the protonated projectile ion and its decomposition products are formed (as shown in collisions, e.g., of C₃D₈⁺ and formation of H-containing fragmentation products). However, unlike C₁ and C₂ hydrocarbons [3], no carbon-chain build up reaction (formation of C₄-hydrocarbon ions) was observed with the C₃-projectile ions to any measurable extent. Mass spectra of

product ions interacting with a heated carbon surface were devoid of the product of the H-atom transfer reaction and showed only direct fragmentation of the projectile ions.

Survival probability of the ions. Measurements of the absolute survival probability of the studied ions (ratio of intensity sum of all ions formed in surface interactions to the intensity of the incident projectile beam, in percent) showed that on the room-temperature surface with incident angle of 30° with respect to the surface, the survival probability was about 1-10 % for the closed-shell ions investigated ($C_3H_7^+$, $C_3H_5^+$, $C_3H_3^+$) and about 0.5-2 % for radical cations $C_3H_8^+$ and $C_3H_6^+$, i.e. somewhat larger for the closed-shell ions. For the measured non-hydrocarbon ions of fairly high recombination energy it was much smaller: for Ar^+ 0.002% and for CO_2^+ 0.0015 %.

Translational energy and angular distributions of product ions. The measurements with the C_3 -hydrocarbon projectile ions showed that the product ions were formed in strongly inelastic collisions. The peak translational energy was about 45% for the collisions with the room-temperature (hydrocarbon-covered) surface and 66% for collisions with the carbon surface heated to $600^\circ C$ (hydrocarbon-free) (an example see Fig. 1).

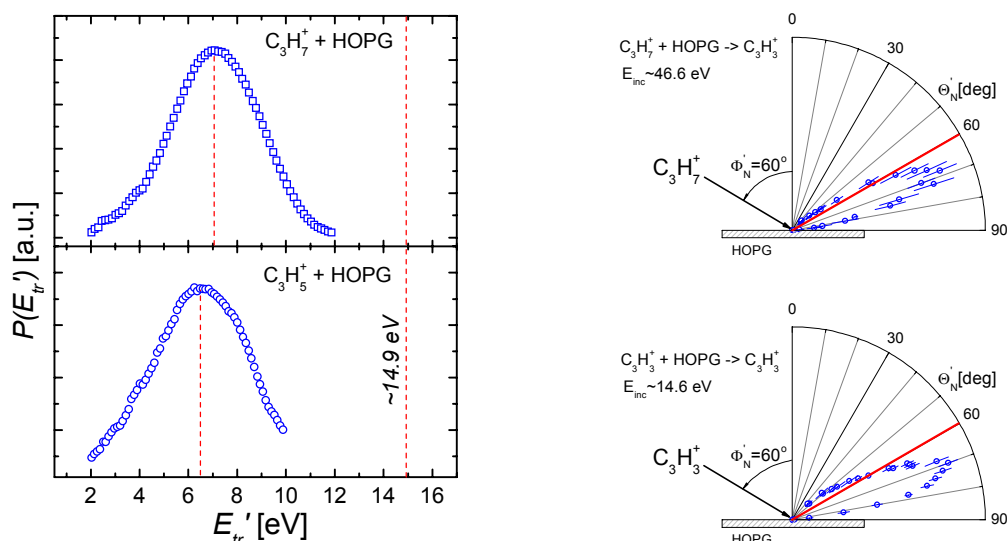


Fig. 1 Translational energy distributions of inelastically scattered undissociated product ions $C_3H_7^+$ and $C_3H_5^+$ from collisions of these projectile ions with a room-temperature HOPG surface (incident energy 14.9 eV). Right: examples of angular distributions of product ions scattered from a room-temperature HOPG surface at the indicated incident energies.

Angular distributions of the scattered product ions were very similar (Fig. 1, right): for an incident angle of 30° (with respect to the HOPG surface at room-temperature) the distributions peaked at a slightly sub-specular angle of about 20° with the angular width of about $18-19^\circ$ (full width at half maximum).

2. Surface collisions of dication and cations $C_7H_n^{2+/+}$ (n=8,7,6)

Collisions of cations and dications $C_7H_8^{+/2+}$, $C_7H_7^{+/2+}$, and $C_7H_6^{2+}$ [4,6] generated by electron ionization of toluene with a HOPG graphite surface were investigated in scattering experiments at the incident energy of 25.3 eV, incident angle of 30° (with respect to the surface) and at surface temperatures of 300 and 900 K. The survival probability of ions was rather large, about 10 % for the cations and about twice as large for the dications. Only

singly-charged ions were observed in the mass spectra of product ions for both singly charged and doubly charged incident ions. In agreement with the earlier conclusion of others, the primary process in surface collisions of the dications is a single-charge exchange between the approaching dication and the surface at larger distances; hence, the mass spectrum of product ions in fact results from surface interactions of internally excited monocations. This conclusion was supported by measured translational energy distributions and angular distributions of the major product ions which are very similar for both dication- and cation collisions. Two mechanisms of formation for the fragment ions observed were suggested: either via unimolecular decomposition of the inelastically scattered projectile ion or via decay of the protonated projectile formed by endoergic hydrogen transfer from the surface-hydrocarbons to the projectile ion. The translational energy distributions of ions originating from dissociation of the surface-excited projectile ions peaked at higher energies than those of the ions resulting from decomposition of surface-protonated precursor ions.

References

- [1] Z. Herman, T.D. Märk: “*Collisions of hydrocarbon ions of energies 10-50 eV with carbon surfaces: Ion survival, dissociation, chemical reactions, scattering.*” in: “*Data for molecular processes in edge plasmas*”, I.A.E.A. TechDoc., I.A.E.A. Vienna (in print).
- [2] Z. Herman: “*Studies of hydrocarbon ion collisions with carbon surfaces at IPP.CR.*” EFDA Newsletter, Vol 2005/3, p.7 (June 5, 2005).
- [3] J. Jašík, J. Žabka, L. Feketeová, I. Ipolyi, T.D. Märk, Z. Herman: “*Collisions of slow polyatomic ions with surfaces: Dissociation and Chemical Reactions of $C_2H_2^+$, $C_2H_3^+$, $C_2H_4^+$, $C_2H_5^+$ and their deuterated variants $C_2D_2^+$ and $C_2D_4^+$ on room-temperature and heated carbon surfaces.*” J. Phys. Chem. A **109** (2005), p.10208-10215.
- [4] J. Jašík, J. Roithová, J. Žabka, A. Pysanenko, L. Feketeová, I. Ipolyi, T.D. Märk, Z. Herman: “*Surface-induced dissociation of dications and cations: Collisions of dications $C_7H_8^{2+}$, $C_7H_7^{2+}$ and $C_7H_6^{2+}$ and a comparison with the respective cations $C_7H_8^+$ and $C_7H_7^+$.*” Int. J. Mass Spectrom. **249-250** (2005), p.162-170.
- [5] Z. Herman, P. Španěl, M. Polášek, J. Roithová: “*Ion chemistry in the gaseous phase and in collisions with surfaces*” (in Czech). Czech J. Phys. **55** (2005) p. 591.
- [6] L. Feketeová, T. Tepnual, V. Grill, P. Scheier, J. Roithová, Z. Herman, T.D. Märk: “*Surface-induced dissociation and reactions of cations and dications $C_7H_8^{+/2+}$, $C_7H_7^{+/2+}$, and $C_7H_6^{2+}$: Dependence of mass spectra of product ions on incident energy of the projectiles.*” J. Phys. Chem. A (in print).

5 JET Collaboration

In 2005, our Association continued to support the EFDA JET Public Information activities in the form of a full time secondment to the CSU (J. Mlynář). This work significantly contributed, among others, to the following outputs: four issues of the EFDA JET Bulletin, three articles on JET in the EFDA Newsletters, the 2006 EFDA JET calendar, new “Fusion Basics”, three new “Focus On” articles and monthly “World Year of Physics” articles for the JET public webpage, regular JET news on public and users webpages, and a talk on Public Information at the 2005 ICENES Conference in Brussels [1].

Task force D (Diagnostics)

The continuous work in data analysis using inverse reconstruction methods resulted in co-authorship in SXR [2] and neutron data tomography [3 - 5].

Task force E (Exhaust)

Within TF-E, IPP.CR continued its involvement in the edge plasma studies using probes. The data analysis of earlier experiments, made from the home laboratory, was a main part of the involvement.

Processing of the turbulent transport probe data suggests an energy transfer between flows and turbulence, described in the publications [6,7]. The results obtained using the retarding field analyzer characterized the edge plasma in forward and reversed field configurations in [8].

Task force H (Heating)

Within TF-H, IPP.CR concentrated on modeling ITER-relevant shots with a large distance between the Lower Hybrid (LH) grill and the separatrix. We explored also a special feature of some of these shots, when the magnetic field surfaces from in front of the LH grill mouth at the outer mid-plane are crossing the wall somewhere near the top of the machine or at the inner wall.

For the modeling, we used the fluid EDGE-2D code. The crossing of the wall by magnetic surfaces is modeled by introducing a sink into the code, which is dependent on both radial and poloidal coordinates. The width of the computational grid was enlarged, and its poloidal resolution was significantly amended. It was assumed that the ionization by the LH wave is produced due to the local SOL (Scrape-off-Layer) electron heating by the wave in a radially narrow belt (layer) in the SOL, with the poloidal width corresponding to the LH grill poloidal height.

In the computations, the important output is the plasma SOL radial density profile: Having a not too low SOL density in front of the LH grill mouth is important for LH wave coupling. For example, the slope and magnitude of the measured plasma density radial profile for a shot with the distance between the separatrix and the LH launcher 8cm, exhibiting hot spots on the inner divertor apron attributed to LH parasitic fast electrons, are reproduced by

the modeling, with a far SOL temperature locally elevated by the LH power up to about 10 eV [9].

As mentioned above, we studied the influence of the crossing of the wall by the magnetic surfaces on the SOL density profile, under varying LH heating and gas puffing rates. The influence of the radial width of the local SOL LH heating layer was investigated, too. In addition to the SOL density and temperature profiles, the radial profile of the ionization source was computed. Let us note that the ionization source was and can be measured in the Tore Supra (TS) tokamak, and we believe that a comparison of these TS results with our computations can bring some interesting insight into the SOL LH heating and ionization physics, even if our modeling is now done for the JET magnetic field configuration.

References

- [1] J. Mlynar, R. Kamendje, D. Borba, R. Antidormi, M.T. Orlando, C. Carpenter and F. Casci: Public Information in European Fusion Energy Research: Methods and Challenges, in: B. Verboomen, H. Ait Abderrahim, P. D'hondt (Eds.), ICENES 2005-Proceedings of the 12th International Conference on Emerging Nuclear Energy Systems, Brussels, 21-26 August 2005, ISBN-907-69711-02 (2005); JET Preprint EFDA-JET-PR(05)27.
- [2] V.V. Plyusnin, V. Riccardo, R. Jaspers, B. Alper, V.G. Kiptily, J. Mlynar, S. Popovichev, E. de La Luna, F. Andersson and JET EFDA contributors Study of runaway electron generation during major disruptions in JET, *submitted to Nucl. Fus.*
- [3] G. Bonheure, J Mlynar et al.: 2-D spatial distribution of D-D and D-T neutron emission in JET ELMy H-mode plasmas with Tritium puff, Proc. 32nd EPS Plasma Physics Conference, 27 June-1 July, Tarragona, Spain.
- [4] A. Murari, L. Bertalot, G. Bonheure, S. Conroy, G. Ericsson, V. Kiptily, K. Lawson, S. Popovichev, M. Tardocchi, V. Afanasyiev, M. Angelone, A. Fasoli, J. Källne, M. Mironov, J. Mlynar, D. Testa, K.D. Zastrow and JET EFDA contributors: "Burning Plasma" Diagnostics for the Physics of JET and ITER, Plasma Phys. Control. Fusion 47 (2005) B249-B262.
- [5] G. Bonheure, S. Popovichev, L. Bertalot, A. Murari, S. Conroy, J. Mlynar, I. Voitsekhovitch and JET EFDA contributors: Neutron Profiles and Fuel Ratio nT/nD Measurements in JET ELMy H-mode Plasmas with Tritium Puff, EFDA-JET-PR(05)06, *submitted to Nuclear Fusion*.
- [6] E. Sánchez, C. Hidalgo, B. Gonçalves, C. Silva, M.A. Pedrosa, M. Hron, and K. Erents: *On the energy transfer between flows and turbulence in the plasma boundary of fusion devices*, Journal of Nuclear Materials **337-339** (2005) pp. 296-300.
- [7] B. Gonçalves, C. Hidalgo, C. Silva, M.A. Pedrosa, M. Hron: Turbulence experiments in reversed and standard-B field configurations in the JET tokamak, Proc. of 32nd EPS Plasma Physics Conference, 27 June – 1 July 2005, Tarragona, Spain
- [8] R.A. Pitts, P. Andrew, X. Bonnin, A.V. Chankin, Y. Corre, G. Corrigan, D. Coster, I. Duran, T. Eich, S.K. Erents, W. Fundamenski, A. Huber, S. Jachmich, G. Kirnev, M. Lehnen, P.J. Lomas, A. Loarte, G.F. Matthews, J. Rapp, C. Silva, M.F. Stamp, J.D. Strachan, E. Tsitrone and contributors to the EFDA-JET Workprogramme: *Edge and divertor physics with reversed toroidal field in JET*, Journal of Nuclear Materials **337-339** (2005) pp. 146-153.
- [9] V. Petrzilka, et al., to be presented at the 33rd EPS CFPP Conference, Rome 2006.

III TECHNOLOGY

1 Technology Tasks

OVERVIEW OF TECHNOLOGY TASKS

Most of the technology tasks within Association EURATOM/IPP.CR deal with the properties of various diagnostic and structural elements and materials of future thermonuclear reactors, before and under neutron irradiation. For the latter purpose, two irradiation sites are utilized: light water experimental fission reactor LVR-15 (operated by NRI plc), and the isochronous cyclotron U-120M with the maximum proton energy of 37 MeV (operated by NPI ASCR). Both devices are located in Řež about 20 km from Prague and they are integrated within the Association EURATOM/IPP.CR.

In 2005, technology research of the Association EURATOM/IPP.CR covered the following areas:

- **Tritium Breeding and Materials**
 - ❖ **Breeding Blanket** (1 task, 5.1a)
 - ❖ **Materials Development** (4 tasks, 5.1a)
- **Physics Integration**
 - ❖ **TPDC Diagnostics - Ceramics** (1 task, 5.1a)
- **Vessel/In Vessel**
 - ❖ **Blanket** (3 tasks, 5.1a + 2 tasks, 5.1b)

The tasks are listed below; further on, some of these tasks are described in more detail.

Article 5.1a

Tritium Breeding and Materials - Breeding Blanket

TW5-TTBC-005 *Helium Cooled Lithium Lead: Process and Auxiliary Components*,
Deliverable 2: Development and testing of components for the liquid metal loop (cold traps, high temperature flanges and circulation pump) (coordinated by NRI Řež; staff V. Masařík, K. Šplíchal, P. Hájek, J. Berka, M. Zmítko)
Status: in progress, see page 51 for more details.

Tritium Breeding and Materials - Materials Development

TW2-TTMS-001b *RAFM Steels: Irradiation Performance*,
Deliverable 3: Static and dynamic toughness testing at the transition temperature. Neutron irradiation of plates and weldments after up to 2.5 dpa at 200-250°C and post irradiation examination (coordinated by NRI Řež; staff: K. Šplíchal, P. Novosad, W. Soukupová, M. Kytka)
Status: in progress, see page 52 for more details.

TW2-TTMS-003b *RAFM Steels: Compatibility with Hydrogen and Liquids*

Deliverable 4: In-pile PbLi corrosion testing of TBM's weldments (stiffeners and bottom plate relevant) (coordinated by NRI Řež; staff V. Masařík, K. Šplíchal, J. Berka, P. Hájek, J. Zmítková, M. Zmítko)

Status: in progress, see page 53 for more details.

TW3-TTMS-003 *RAFM Steels: Compatibility with Hydrogen and Liquids*

Deliverable 1: Crack growth kinetic and fracture toughness on EUROFER 97 in presence of hydrogen (up to 10 wppm) at RT, 250° C (coordinated by NRI Řež; staff: M. Zmítko, K. Šplíchal, V. Masařík, P. Hájek, J. Berka, J. Zmítková)

Status: in progress

TW5-TTMN-002 *Measurement of activation cross sections at neutron energies below 35 MeV*

Deliverable 5: Activation experiment on tantalum in the NPI p-D₂O neutron field (coordinated by NPI Řež, P. Bém)

Status: delivered, see page 54 for more details.

Physics Integration - TPDC Diagnostics

TW4-TPDC-IRR CER

Deliverable 12: Report on in-situ radiation effects on pre-selected candidate Hall probes (coordinated by IPP, I. Ďuran)

Status: delivered

Vessel/In Vessel – Blanket

TW3-TVB-INPILE *In-pile experiment on PFW Mock-ups*

Deliverable 3: Perform in-pile testing of Be protected PFW mock-ups under heat flux (coordinated by NRI Řež; staff: M. Zmítko, J. Bohatá, T. Klabík, P. Hájek)

Status: in progress

TW4-TVB-TFTEST2 *Thermal fatigue tests of Be coated Primary First Wall Mock-ups*

(coordinated by NRI Řež; staff T. Klabík, V. Masařík, P. Hájek, M. Zmítko)

Deliverable 3: Construction of the facility for thermal fatigue tests of Be coated primary first wall mock-ups

Status: in progress

TW5-TVM-PSW **Manufacture and characterization of Tungsten Plasma Spray Coatings for large area protection** (coordinated by IPP, J. Matějčíček)

Status: in progress

Article 5.1b

Vessel/In Vessel – Blanket

TW3-TVB-FWPAMT **Mechanical testing of a panel to shield block attachment system**

(coordinated by FNSPE Prague, V. Oliva)

Status: in progress

TW3-TVV-SEGDIS **Analysis of welding distortions obtained in manufacturing of VV segment** (coordinated by IAM Brno, L. Junek)

Status: delivered, see page 55 for more details.

Development and testing of components for the liquid metal loop (cold traps, high temperature flanges and circulation pump)

Task: TW5-TTBC-005 *Helium Cooled Lithium Lead: Process and Auxiliary Components, Deliverable 2*

Field/Area: Tritium Breeding and Materials / Breeding Blanket

Coordinated by NRI Řež; staff V. Masařík, K. Šplíchal, P. Hájek, J. Berka, M. Zmítka

Achievements:

This task is focused on the development and testing of key components for the Pb-Li liquid metal facility of the new reference design of the Helium Cooled Lithium Lead (HCLL) Test Blanket Module (TBM). Based on previous design studies of Pb-Li auxiliary system for the HCLL TBM the following components shall be developed: cold traps, high temperature flanges and circulation pump. Development of these components shall be supported by their testing in Pb-Li liquid metal conditions (260-500°C, 5-30 mm/s). The aim is to demonstrate their feasibility and operation performance regarding cold traps purification efficiency, flanges reliability and manipulations.

The manufacturing of the Liquid Metal Loop (LML) (Fig.1) has been finished except the circulation pump and cold traps. The loop consists of the expansion tank with main heater, cold trap, heat exchanger, drain tank, piping and sampling devices. The main part of the loop is mounted, except the circulation pump and the cold trap, which will be finished after the delivery of sheet steel with a sufficient corrosion resistance to the eutectic melts. A loop controlling system, parameter monitoring system and data acquisition were developed and manufactured. The operation performances of these systems were verified. Their assembly will be performed after finalization of the loop component.

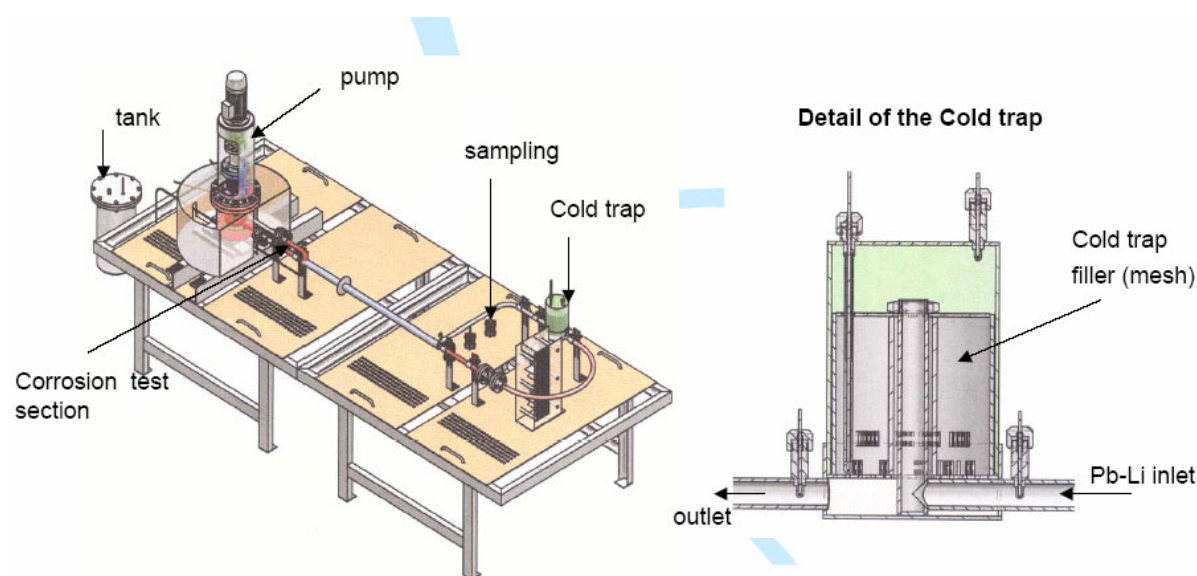


Fig. 1 Schematic layout of the Liquid Metal Loop (LML) for TBM components testing and materials compatibility / corrosion tests.

In-pile PbLi corrosion testing of TBM's weldments (stiffeners and bottom plate relevant)

Task: TW2-TTMS-003b *RAFM Steels: Compatibility with Hydrogen and Liquids*,
Deliverable 4

Field/Area: Tritium Breeding and Materials / Materials Development

Coordinated by NRI Řež; staff V. Masařík, K. Šplíchal, J. Berka, P. Hájek, J. Zmítková,
 M. Zmítko

The main objective of this task is to study corrosion behaviour of EUROFER material including weldments in liquid metal Pb-Li under neutron irradiation. The eutectic liquid metal alloy Pb-15.7Li will be used in the European Helium Cooled Lithium Lead (HCLL) Test Blanket Module (TBM) concept and its compatibility with EUROFER structure material is an issue. The target neutron flux representing material damage up to 1-1.5 dpa should be achieved by neutron irradiation.

Neutron irradiation is being performed in the research reactor LVR-15, using a dedicated Pb-Li in-pile rig (Fig. 3). The in pile rig contains four corrosion plain specimens (38 x 8 x 1.5 mm) and three tensile test specimens (Ø 2mm) of weld metal of EUROFER joint. The temperature of the rig hot leg is held at $500^{\circ}\text{C} \pm 10^{\circ}\text{C}$ and that of the cold leg at $320\text{-}340^{\circ}\text{C}$, cf. Fig. 4. The pressure of the inert part is kept at 120 kPa, the outer part at 240 kPa. The irradiation campaign started on February 2005 and to achieve the desired material damage, it is expected to continue till mid 2006.

For the foreseen post-irradiation examination (PIE), dedicated equipments have been designed, prepared and verified, e.g. a furnace for Pb-Li melting and the EUROFER specimens' recovery from the irradiation rig, an apparatus for cleaning the EUROFER specimens from Pb-Li residue by washing them in liquid sodium at higher temperatures.

After the irradiation campaign the Pb-Li in-pile rig will be transported into the hot cells for dismantling and subsequent PIE.

Reports:

K. Šplíchal, J. Berka, M. Zmítko: Compatibility of EUROFER martensitic steel with Pb-17Li at 550°C , Proceeding of Conf.: Corrosion and its influence on strength and lifetime of steel structure, Brno, 2005

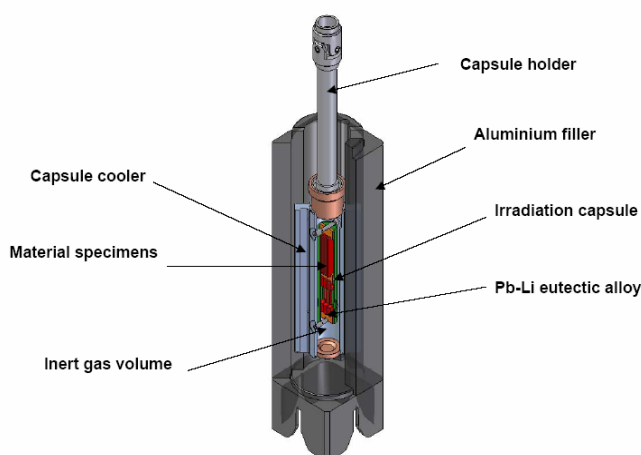


Fig. 3 Pb-Li in-pile rig with EUROFER specimens

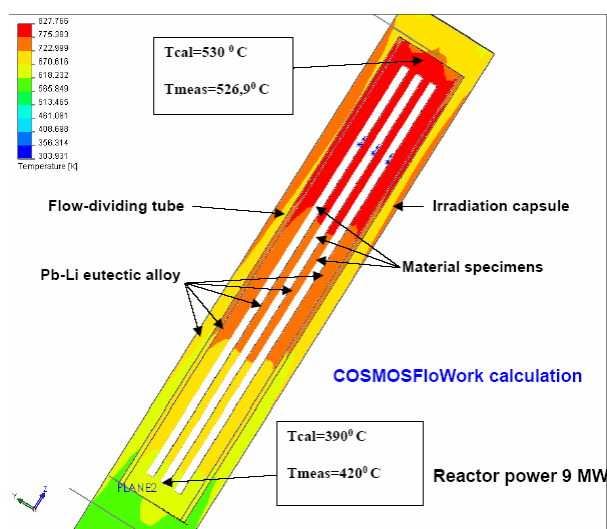


Fig. 4 Temperature distribution in the Pb-Li in-pile rig.

J. Zmítková: Simulating and evaluation of thermodynamics condition and operational parameters of Pb-Li irradiation rig, NRI Report 12 161, Řež, 2005

K. Šplíchal, V. Masařík, L. Zmítková: In pile Pb-Li testing of TBM weldments under LVR-15 reactor condition, EFDA meeting, Garching, 2005

Activation experiment on tantalum in the NPI p-D₂O neutron field

Task: **TW5-TTMN-002 Measurement of activation cross sections at neutron energies below 35 MeV, Deliverable 5**

Field/Area: Tritium Breeding and Materials / Materials Development

Coordinated by NPI Řež; P.Bém

Neutronics evaluation of the International Fusion Materials Irradiation Facility (IFMIF) with a d-Li white neutron source extending up to 55 MeV needs validation of activation and transmutation cross sections above 20 MeV for the set of materials/elements. As a part of experimental benchmarking of the IFMIF neutron calculations, an activation experiment has been carried on tantalum as it is a considerable source of gamma-emitting radio-nuclide constituent of the Eurofer-97 steel.

The tantalum samples were activated in an IFMIF-like white neutron field produced by the p(37 MeV)+D₂O reaction up to 1.5×10^{11} n/s/cm². All investigated Ta samples were stacked in packets containing the monitoring foils (Al and Au). An additional test of space- and energy integration effects on the spectral flux was performed setting the stacks of foils at different distances from the target. The internal consistency of the resulting activities was checked. In the present report, the results of the activation benchmark test are given for the Ta sample irradiated at shortest distance from the target.

Up to 15 μ A of proton beam current was delivered on the target. The neutron source strength during the irradiation is proportional to the proton beam current, recorded by a calibrated current-to-frequency converter and a scaler on a PC. Spectral neutron flux (see Fig. 5 and Ref. [1]) was determined utilizing the dosimetry-foil method [1].

The activities of induced radio-nuclides of samples were investigated by gamma-spectrometers (two calibrated HPGe detectors of 23 and 50% efficiency, FWHM 1.8 keV at 1.3 MeV) after different cooling time intervals up to 150 days. Evaluation of the spectra was performed utilizing the NPI code DEIMOS. By analyzing the spectra, the resulting specific

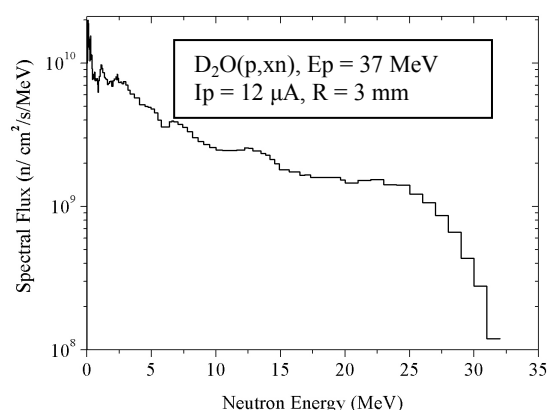


Fig. 5 Spectral neutron flux.

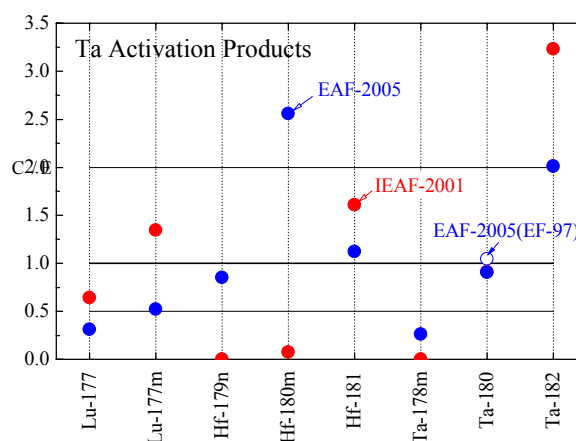


Fig. 6 Calculation-to-Experiment ratios.

activities A_{sp} in Becquerels per kilogram to the end of irradiation were obtained. They were analyzed by the FISPACT inventory code with the EAF 2005 library. In Fig. 6, the

Calculation-to-Experiment ratios C/E with ALARA/EAF-2001 (red solid circles) and FISPACT/EAF-2005 (blue solid circles); (open blue circle) are given.

In summary, beyond the $^{181}\text{Ta}(n,\gamma)^{182}\text{Ta}$ one, the activation products of the following reactions were investigated:

- $(n,p)^{181}\text{Hf}$, $(n,2n)^{180}\text{Ta}$, (n,d) , $^{180\text{m}}\text{Hf}$ - (to be compared to benchmark experiments carried out with the 14 MeV neutron source),
- $(n,n\alpha)^{177}\text{Lu}$, $^{177\text{m}}\text{Lu}$, $(n,t)^{179\text{n}}\text{Hf}$ - (first benchmark experiment on these reactions), and
- $(n,4n)^{178\text{m}}\text{Ta}$ - (no experimental data of cross sections are available up to now).

The following conclusions have been drawn:

- a) C/E ratios exceed 2 for half of the inventories,
- b) the analysis points out the necessity of updating the specific cross sections in the EAF-2005 library above 15 MeV. A detailed analysis and discussion of results are given in Refs. [2], [3].

Present and previous results of activation benchmark tests in the IFMIF-like spectrum on the NPI neutron source are presented also in the Ref. [4].

The work was performed in a close collaboration with the IFMIF specialists of FZ Karlsruhe.

References

- [1] P. Bém et al, Experimental determination of the NPI p-D₂O neutron source spectrum for activation benchmark tests, EFF-DOC-944, EFF/EAF Monitoring Meeting, NEA Data Bank, Paris, 29-30 November 2005.
- [2] M.Honusek, et al., Validation experiments on Tantalum activation in the NPI p-D₂O neutron of IFMIF-like spectrum, EFF-DOC-945, *ibid*
- [3] S.P.Simakov et al., Analysis of the NPI Řež validation experiment for Ta activation cross-sections in an IFMIF-like neutron spectrum, EFF-DOC-951, *ibid*
- [4] R. A.Forrest, J.Kopecky, M.Pillon, K.Seidel, S.P.Simakov, P.Bém, M.Honusek and E.Šimečková, Validation of EASY-2005 using integral measurements, UKAEA Report, UKAEA FUS 526, 2005

Analysis of welding distortions obtained in manufacturing of VV segment

Task: TW3-TVV-SEGDIS (5.1b)

Field/Area: Vessel/In Vessel / Blanket

Coordinated by IAM Brno, L. Junek

To meet the objectives of this task, the following two lines have been followed:

1. Validation steps. The method of solution is still under development. We have addressed the case in which the construction is fixed during the welding operation by stiff supports. The supports are removed after welding, and the construction is released and distorted. Three experiments have been done, and also numerically simulated. 2D and 3D models have been prepared. A comparison between the calculated and the measured distortion, shrinkage and residual stresses has been performed. The aim of these numerical analyses and experiments is to determine the appropriate solution method for an accurate prediction of the distortion after unclamping the construction.

2. Numerical simulation as a support during a real industrial mock-up experiment. Before

manufacturing of the vacuum vessel poloidal segment mock up (VVPSM), validation mock-up (VMO) and local modelling validation mock-up (LMVMO) have been prepared by the ANSALDO and SIMIC Companies. Both mock-ups have already been finished. Numerical prediction of the residual stresses and of the distortion for both mock-ups has been obtained as well. Here, a new local/global approach for distortion prediction has been applied. Five local models and three global models have been prepared. The input parameters needed (mainly the size and shape of the deposits, the welding power and velocity) have been taken from experiments.

A CAD model of the vacuum vessel poloidal segment VVPSM has been constructed, and a global VVPSM model is under preparation.

2 Underlying Technology Tasks

Four tasks have been solved as underlying technology tasks to complement the EFDA Work Programme in 2005.

Measurement of activation cross sections at neutron energies below 35 MeV: activation experiment on tantalum in the NPI p-⁷Li neutron field

Task: IPP.CR UT2005 npi

Field: Tritium Breeding and Materials: Materials Development

Principal investigator : *Pavel Bém, NPI Řež*

A number of elements, relevant to the International Fusion Materials Irradiation Facility (IFMIF), were identified for which neutron activation data were found inadequate or missing. The task is devoted to the measurement of activation cross sections at neutron energies in the 25-35 MeV range employing a quasi-monoenergetic neutron field generated in the p-Li reaction by protons from the variable-energy cyclotron U-120M. For the investigation, the Tantalum nuclide (constituent of EUROFER steel) was selected in accordance with requests, formulated by the "Requirements for FP6 Work Programme on Nuclear Data" for IFMIF. The present report deals with the cross-section measurement on Ta in close connection with the integral validation experiment carried out in parallel utilizing the IFMIF-like white spectrum of the NPI p+D₂O neutron source.

The present task was aimed to develop a quasi-monoenergetic neutron field for energies between 10 to 35 MeV that will extend presently available white neutron fields of the NPI neutron facility. The ⁷Li(p,n) reaction on a thin lithium target, induced by the variable-energy proton beam of the NPI cyclotron is used for the production of a quasi-monoenergetic neutron field. A carbon backing for the thin Li target is utilized. The Li-foil-target technique was investigated employing a proton beam of the cyclotron. A versatile chamber-holder for Li-foils and a multipurpose target chamber with cooling system were developed with this aim. Several foil/backing configurations and cooling methods were investigated at different proton currents to determine the optimum arrangement with respect to the working lifetime of the Li target. At present, a stable operation of the source was achieved under cooling of the foil and the carbon backing separately. For the 24 MeV proton beam of 2 μA current, the system permits a neutron fluence of about 1.5 x 10⁸ n/sr/s

The tantalum samples of 15 mm in diameter and of 0.75 mm thickness and chemical purity of 99.9% (Goodfellow CL product) were activated in a quasi-monoenergetic neutron field based on the ⁷Li(p,n) source reaction. All investigated Ta samples were stacked in packets containing the "reference" dosimetry foils of gold. The neutron flux was monitored by integration of the proton beam current and by the activity induced by protons in the ⁷Li target as well. To test the space- and energy integration effects on the spectral flux from the p+Li source, the stacks of foils were set at different distances from the Li target.

The activities of induced radio-nuclides of samples were investigated after different cooling time intervals by gamma-spectrometers (two calibrated HPGe detectors of 23 and 50% efficiency). The internal consistency of the resulting activities was checked. In summary, 9 reactions were investigated at three neutron energies between 22 and 35 MeV:

(a) The products of $^{181}\text{Ta}(n,n\alpha)^{177}\text{Lu}$, $(n,4n)^{178}\text{Ta}$, $^{178\text{m}}\text{Ta}$ and $(n,5n)^{177}\text{Ta}$ reactions were investigated for the first time (no cross-section data are available at present).

(b) New data were obtained for reactions $(n,\gamma)^{182}\text{Ta}$, $(n,p)^{181}\text{Hf}$, $(n,d)^{180\text{m}}\text{Hf}$, $(n,t)^{179}\text{Hf}$ and $(n,2n)^{180}\text{Ta}$ (no cross-section data are available above energy of 20 MeV).

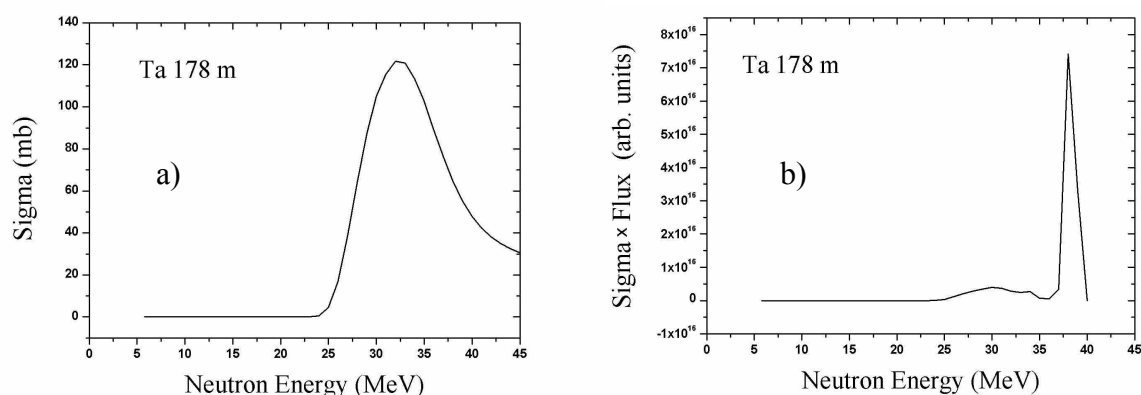


Fig. 1 a) Cross-section and b) its product with the neutron spectrum for the $^{181}\text{Ta}(n,4n)^{178}\text{Ta}$ reaction

The analysis of the resulting specific activities and reaction rates is carried out in terms of C/E ratio (E – measured reaction rate, C - the predicted value of this observable calculated for the same neutron energy and spectrum). The neutron flux and spectra across the Ta samples are calculated using the double-differential cross section data of the $^7\text{Li}(p,n)$ reaction measured by other authors. Activation cross-sections data for selected reactions of neutrons on ^{181}Ta nuclide were taken from the EAF-2005 library. In Fig. 1, the cross section for the $^{181}\text{Ta}(n,4n)^{178}\text{Ta}$ reaction (a) and the product of primary neutron spectra (for 40 MeV neutron energy) and this cross sections (b) are illustrated. The strong underestimation of the measured cross section (by a factor of 4) is indicated compared to the value calculated by the latest version of the EAF-2005 library [1]. A similar conclusion stems also from the results of a recent integral validation experiment on Ta employing the NPI white-spectrum neutron source [2,3].

The work was performed under a close collaboration with IFMIF specialists of FZ Karlsruhe.

References

- [1] S.P. Simakov, et al.: Analysis of the NPI Řež validation experiment for Ta activation cross-sections in an IFMIF-like neutron spectrum, EFF-DOC-951, EFF/EAF Monitoring Meeting, NEA Data Bank, Paris, 29-30 November 2005.
- [2] M. Honusek et al.: Validation experiments on Tantalum activation in the NPI p-D2O neutron field of IFMIF-like spectrum, EFF-DOC-951 ibid.
- [3] R. A. Forrest, J. Kopecky, M. Pillon, K. Seidel, S.P. Simakov, P. Bém, M. Honusek and E. Šimečková: Validation of EASY-2005 using integral measurements. Report UKAEA FUS 526, 2005.

Validation of new methodology of recovery strain hardening. Simulation of SS during multipass welding

Task: IPP.CR UT2005 iam

Field: Vessel/In Vessel

Principal investigator : *Luboš Junek, IAM Brno*

Numerical simulation including a viscoplastic material model has been applied to the multipass welding process. In the previous year, several welding experiments were performed and also numerically simulated using a combined material model. This year, new numerical

simulations of the experiments using viscoplastic model have been done, and a comparison of various material models has been performed. Based on the numerical calculation and the experience with viscoplastic material behaviour, the new tool has been adopted during non-linear plastic simulation to realistically simulate the viscoplastic behaviour for high temperatures.

Development of methods of fracture toughness and notch toughness measurement with irradiated sub-size specimens

Task: IPP.CR UT2005 1 nri

Field: Tritium Breeding and Materials: Materials Development

Principal investigator : Karel Šplíchal, NRI Řež plc

(Coordinated by NRI Řež; staff K. Šplíchal, P. Novosad, W. Soukupová, M. Kytka)

Objectives:

The main objective is to develop methods of static fracture toughness and notch toughness measurement with irradiated sub-size specimens and to compare the data obtained with the ones measured with standard testing specimens. This task is related to the EFDA Work Programme task TW2-TTMS-001b-D3, which does not include measurement of notch toughness. The comparison of the notch toughness data measured with sub-size and standard specimens enables the verification of the obtained results and will be used for the design purposes of the ITER blanket components.

Achievements:

The activities related to this deliverable have been focused on the following: (i) an adaptation of devices for three-point bend testing and fatigue pre-cracking, (ii) verification of the adapted devices, and (iii) comparison of the notch toughness data measured with sub-size and standard specimens.

Two equipments have been adapted for fracture toughness testing on the INSTRON machine 1342 in the hot cell. The equipment for three-point bend testing has been modified for irradiated sub-size specimens, i.e. the supporting and loading parts have been replaced so that they enable testing of the KLST specimen with size 3 x 4 x 27 mm³. The rate of specimens loading and test temperature measurement have been verified. The remote control device in the hot cell has been adapted for the insertion of specimens in testing equipment. The other equipment has been adapted for pre-crack preparation of the KLST specimens. Parameters of the cycling loading device have been modified to achieve pre-crack in a length up to 2 mm. Verification and comparison of both specimens (sub-size and standard specimens) have been performed.

Development of methods for post-irradiation examination of in-pile compatibility of EUROFER with Pb-17%Li

Task: IPP.CR UT2005 2 nri

Field: Tritium Breeding and Materials: Materials Development

Principal investigator : Vladimír Masařík, NRI Řež plc

(Coordinated by NRI Řež; staff V. Masařík, K. Šplíchal, J. Berka, P. Hájek, E. Vlasák)

Objectives:

The main objective is to develop and verify some suitable methods to assess surface interaction and corrosion properties of EUROFER specimens exposed to Pb-17Li under irradiation conditions. The methods will be used for the post-irradiation examinations (PIE)

of specimens exposed in the frame of the task TW2-TTMS-003b-D4: In-pile Pb-Li corrosion testing of TBM's weldments up to 2 dpa. This task does not include all required methods of PIE and further works are therefore needed.

Achievements:

The methods for extraction of corrosion and tensile specimens from Pb-17Li after irradiation exposition in the dedicated in-pile rig were designed and developed. The developed methods are able to ensure the following remote control procedures in the hot cell:

- to keep the inner volume of the irradiation rig under inert Ar atmosphere after dismantling of the irradiation capsule,
- to place the rig in a heating device where melting of the Pb-17Li eutectic mixture will take place and the removal of Pb-Li from the rig will be performed under Ar atmosphere,
- to isolate the corrosion and tensile specimens after cutting of the irradiation rig,
- to take a sample of the Pb-17Li eutectic mixture for further chemical and radiochemical analysis under inert Ar atmosphere and preparation of suitable samples for ICP-MS and gamma-spectroscopy,
- to remove Pb-17Li eutectic from EUROFER corrosion and tensile specimens by washing them in a sodium melt.

In the frame of this task all the necessary tools (e.g. for irradiation rig and irradiation capsule cutting) and equipments (e.g. heating device) have been designed and fabricated in the workshop and after that their performances have been tested in the hot cell conditions. Based on the experience obtained the working procedure has been précised and a Working Manual has been issued.

Report:

Working Manual for Dismantling and PIE of Pb-Li Irradiation Rig, NRI Internal Report DRS 1104 (in Czech), December 2005

IV

Keep-in-Touch Activities on Inertial Confinement Fusion

Activities of the Prague Asterix Laser System (PALS) in the field of inertial confinement fusion have been carried out in close collaboration with Institute of Plasma Physics and Laser Micro-fusion, Warsaw, Poland, with participation of scientists from Russia, France and Australia. The experimental work was focused on investigation of various types of laser targets relevant for inertial fusion.

1. Investigation of ablation pressure dynamics in structured laser targets

Person in Charge: J. Ullschmied, IPP

Participants in the project: K. Jungwirth, B. Kralikova, E. Krousky, K. Masek, M. Pfeifer, K. Rohlena, J. Skala (PALS laboratory, CR)

Collaborators from other laboratories:

T. Pisarczyk (principal investigator), A. Kasperczuk, S. Borodziuk, P. Pisarczyk (Poland)

N. N. Demchenko, S.Yu. Gu'skov, V.N. Kondrashov, V.B. Rozanov (Russia)

Ph. Nicolai, V.T. Tikhonchuk (France)

H. Hora (Australia)

J. Limpouch, M. Kalal (FNSPE, Czech Technical University in Prague, CR)

Introduction

Shock wave generation, energy transfer, and crater creation by a powerful laser pulse in multi-layer media were studied in the framework of cooperation of the Czech and Polish EURATOM Associations. As a main diagnostic tool the three-frame laser interferometric system developed for PALS at IPPLM was employed. Parameters of the craters produced by laser beam in the targets were reconstructed by means of the crater replica technology. An original two-dimensional analytical theory and computer simulations were applied for interpretation of the measured data. The experimental and theoretical results of these studies concern the efficiency of the laser energy absorption and of the ablation loading in various single- and double-target configurations, as well as the parameters of a two-dimensional shock wave generated at the direct laser action and at the laser-driven macroparticle impact.

Shock wave generation and crater creation in laser targets

Shock wave generation, energy transfer, and crater creation in multi-layer solid target media on interaction with a powerful laser pulse were studied systematically at the PALS laser facility in co-operation with scientists from the Association EURATOM/IPPLM-PL. Motivation of these experiments is to find optimum conditions for energy transfer from a laser beam to various structured targets of interest in inertial fusion research, including double targets with solid flyers, multilayer targets made of different materials, and targets with ablative foam layers. Basic data on the target plasma dynamics, such as the time development of the plasma density spatial profile and velocities of the solid target parts, were obtained by means of multiframe laser shadowgraphy and interferometry. The crater parameters were measured by an optical microscopy technique applied to wax replicas of the craters.

A huge amount of experimental material has already been collected, and it is now being analyzed and interpreted by using current advanced theoretical models of laser ablation and

shock wave generation. The obtained data have also been exploited at numerical simulations of the laser ablation and crater creation processes, which are under progress in several cooperating laboratories.

Laser beam interaction with solid structured targets

Shadowgraphic and interferometric measurements of plasma ablation and macroparticle acceleration were performed by means of the three-frame laser interferometric system developed for PALS at IPPLM. Each of its interferometric channels is an independent interferometer of the folding wave type, the imaging part of which is equipped with a CCD camera Pulnix TM-1300 (1300×1030 pxl). An optical delay line makes it possible to obtain three delayed and spatially resolved interferograms (frames) during a single laser shot. The plasma density profiles calculated on the base of the interferograms are presented in the form of isodensitograms, an example of which is shown in Fig. 1. A plasma stream boundary is represented here by the electron density contour $n_e = 10^{18} \text{ cm}^{-3}$. The subsequent equidensity lines are separated by $\Delta n_e = 2 \cdot 10^{18} \text{ cm}^{-3}$.

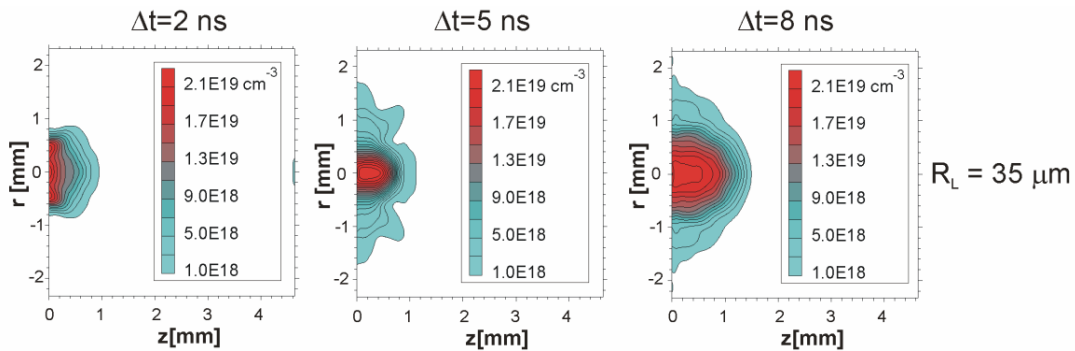


Fig. 1 Sample sequence of three electron isodensitograms of Al plasma obtained during a single laser shot.

The plasma velocities and electron density profiles were measured for a large set of different solid targets at various target irradiation conditions (at different laser intensities and laser beam colors). During the last IPPLM mission at PALS the crater creation efficiency on solid planar Al targets was studied on irradiation of the targets by the first harmonic of the iodine laser beam ($\lambda = 1.315 \mu\text{m}$, laser energy 360 J, pulse duration ~ 400 ps), at laser focal spot radii R_L varying from $35 \mu\text{m}$ to $500 \mu\text{m}$. Interferograms taken at 2 ns, 5 ns, and 8 ns after the laser pulse covered the early phase of plasma stream evolution. The sets of plasma isodensitograms obtained for six different R_L showed a gradual evolution of the plasma configuration with the growing focal spot radius. At smaller R_L (at higher laser intensities), the total plasma electron number is minimum (Fig. 2), while the crater volume reaches its maximum, after a local minimum at $R_L = 300 \mu\text{m}$ (Fig. 3). The shape of expanding plasma plume also changes, from multidirectional expansion at smaller R_L to a predominantly axial one in the opposite case.

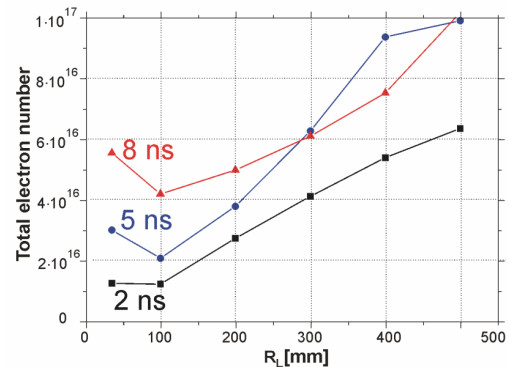


Fig. 2 Total electron number versus focal spot radius for three instants of plasma expansion.

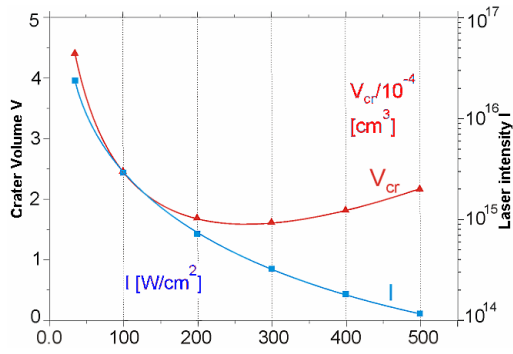


Fig. 3 Craters volume and intensity of target irradiation versus the focal spot radius.

All the observed dependencies can be explained by the transition from one-dimensional axial plasma expansion at larger focal spot radii to two-dimensional expansion at higher focal intensities.

In 2005, shock wave generation in planar multilayer and cascade targets was also studied. The targets made of combinations of different materials, such as polyethylene, Al, Cu and Pb, were irradiated by the third harmonic PALS laser beam ($\lambda_3 = 0.438 \mu\text{m}$). Processing of the collected experimental data is still in progress.

Laser beam interaction with flyer targets

In these experiments the impact of Al flyers with a solid planar target was investigated. The flyer disks, 300 μm in diameter and 6 μm thick, were ablatively accelerated to high velocities by the PALS iodine laser beam. The beam energy range was varied in the range 30 - 390 J, while the laser spot size was maintained at 250 μm . The plasma expansion and the disk motion were observed by means of a multiframe imaging laser interferometer. The measuring period was rather long (2 ns – 23 ns after the laser pulse), covering both the pre-impact and post impact phases. The obtained sequences of interferograms show both the primary plasma, which ablatively accelerates the disk, and the evolution of the plasma produced by the disk

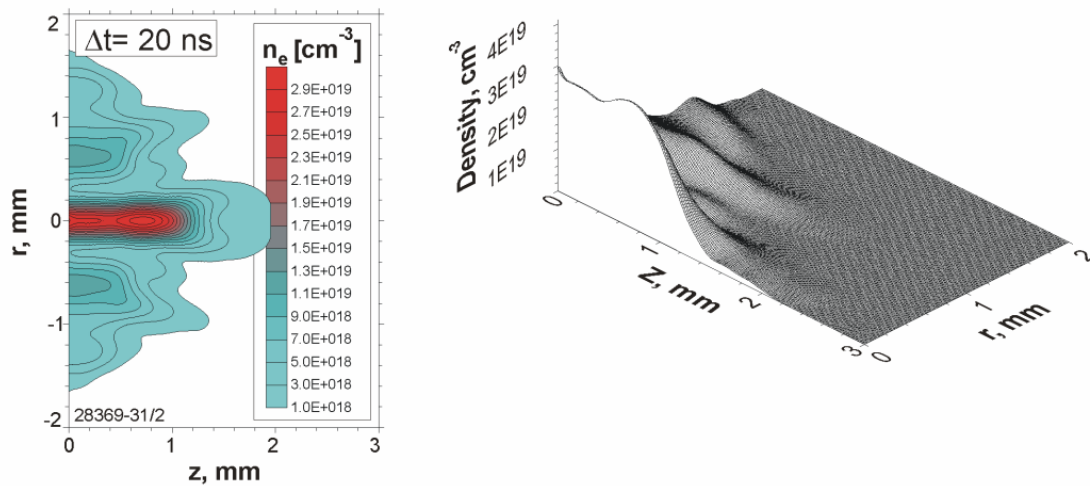


Fig. 4 Electron isodensitogram and electron density distribution of plasma in the post-impact phase.

impact (see the illustrative example in Fig. 4).

The results of the flyer impact investigations are described in more detail in the 2005 Report of the Association EURATOM/IPPLM (PL). In recent experiments on interaction of a slightly defocused laser beam with planar metallic targets, remarkably stable dense plasma jets have been observed. Their interpretation was worked out in collaboration with V.T. Tikhonchuk and Ph. Nicolai from the French CELIA laboratory (to be published).

Publications

- [1] S. Borodziuk, N.N. Demchenko, S.Yu. Gus'kov, K. Jungwirth, M. Kalal, A. Kasperczuk, V.N. Kondrashov, E. Krousky, J. Limpouch, K. Masek, P. Pisarczyk, T. Pisarczyk, M. Pfeifer, K. Rohlena, V.B. Rozanov, J. Skala, J. Ullschmied: High power laser interaction with single and double layer targets. *Optica Applicata*, Vol. 35, (2005), No. 2, p. 242-262.
- [2] S.Yu. Gus'kov, S. Borodziuk, M. Kalal, A. Kasperczuk, V.N. Kondrashov, J. Limpouch, P. Pisarczyk, T. Pisarczyk, K. Rohlena, J. Skala, . Ullschmied: Investigation of shock wave loading and crater creation by means of single and double targets in the PALS-laser experiment. *Journal of Russian Laser Research*, Vol. 26 (2005), No. 3, p. 228-244.
- [3] T. Pisarczyk, S. Borodziuk, N.N. Demchenko, S.Yu. Gus'kov, K. Jungwirth, M. Kalal, A. Kasperczuk, V.N. Kondrashov, B. Kralikova, E. Krousky, J. Limpouch, K. Masek, M. Pfeifer, P. Pisarczyk, K. Rohlena, V.B. Rozanov, J. Skala, J. Ullschmied: Optical investigation of flyer disk acceleration and collision with massive target on the PALS laser facility, 32 EPS Conf. on Plasma Phys. & 8 Intl. Workshop on Fast Ignition of Fusion Targets, Tarragona, 2005, ECA Vol.29C http://eps2005.ciemat.es/papers/pdf/P1_141.pdf.
- [4] S. Borodziuk, N.N. Demchenko, S.Yu. Gus'kov, K. Jungwirth, M. Kalal, A. Kasperczuk, B. Kralikova, E. Krousky, V.N. Kondrashov, J. Limpouch, K. Masek, M. Pfeifer, P. Pisarczyk, T. Pisarczyk, K. Rohlena, V.B. Rozanov, J. Skala, J. Ullschmied: Numerical modelling of strong shock waves and craters for the experiments using single and double solid targets irradiated by high power iodine laser PALS, 32nd EPS Conf. on Plasma Phys. and 8th International Workshop on Fast Ignition of Fusion Targets, Tarragona, 2005, http://eps2005.ciemat.es/papers/pdf/P1_142.pdf, P1-142, ECA Vol.29C
- [5] T. Pisarczyk, S. Borodziuk, N.N. Demchenko, S.Yu. Gus'kov, K. Jungwirth, M. Kalal, A. Kasperczuk, B. Kralikova, E. Krousky, J. Limpouch, K. Masek, P. Pisarczyk, M. Pfeifer, K. Rohlena, V.B. Rozanov, J. Skala, J. Ullschmied: Optical investigation of powerful laser actions on massive and flyer targets. *International Conference Plasma 2005 & 3 rd GPPD & 5th FPSTP*, Opole-Turawa, 2005, I-11.
- [6] A. Kasperczuk, S. Borodziuk, N.N. Demchenko, S.Yu. Gus'kov, K. Jungwirth, M. Kalal, B. Kralikova, E. Krousky, J. Limpouch, K. Masek, P. Pisarczyk, T. Pisarczyk, M. Pfeifer, K. Rohlena, V.B. Rozanov, J. Skala, J. Ullschmied: Plasma and shock generation by indirect laser pulse action. *International Conference Plasma 2005 & 3rd GPPD & 5th FPSTP*, Opole-Turawa, 2005, P4-01.
- [7] S. Borodziuk, N.N. Demchenko, S.Yu. Gus'kov, K. Jungwirth, M. Kalal, A. Kasperczuk, B. Kralikova, E. Krousky, J. Limpouch, K. Masek, P. Pisarczyk, T. Pisarczyk, M. Pfeifer, K. Rohlena, V.B. Rozanov, J. Skala, J. Ullschmied: Flyer target acceleration and energy transfer at its collision with massive targets. *International Conference Plasma 2005 & 3rd GPPD & 5th FPSTP*, Opole-Turawa, 2005, P4-08.

2. Laser imprint smoothing by low-density foam layers

Person in Charge: J. Ullschmied, IPP

Participants in the project: E. Krousky, K. Masek, M. Pfeifer, O. Renner, J. Skala (PALS laboratory, CR)

Collaborators from other laboratories:

J. Limpouch (principal investigator), M. Kalal, J. Kuba, M. Sinor (FNSPE CTU Prague, CR)

I.V. Akimova, N.G. Borisenko, N.N. Demchenko, S.Yu. Gus'kov, A.I. Gromov,

A.M. Khalenkov, V.N. Kondrashov, S.F. Medovshikov, Y.A. Merkuliev, W. Nazarov,

V.G. Pimenov, V.B. Rozanov (Russia)

A. Kasperczuk, T. Pisarczyk, P. Pisarczyk (IPPLM Poland)

Interaction of high-power laser beam with foam layers

Low-density foams covering the laser target may smooth the laser imprint and thus improve the spherical symmetry of target irradiation in direct-drive inertial fusion schemes. Transparent underdense foam layers may be exploited as dynamic phase plates, which can randomize and partly wash out inhomogeneity patterns inside laser beams. Foams are also used in equation of state (EOS) studies to increase achievable shock wave pressure. This was the motivation for the experimental and theoretical studies of interaction of high-intensity laser beams with foam layers performed at the PALS facility since the year 2004, in collaboration with physicists from the Faculty of Physical Science and Nuclear Engineering, CTU in Prague, from the Polish Association EURATOM/IPPLM-PL, Warsaw, and from Russia; the P.N. Lebedev Physical Institute RAS, Moscow, and TRINITI, Troitsk.

The targets, supplied by Russian Institutes, were made of different materials of densities 4 – 20 mg/cm³, which included agar (C₁₂H₁₈O₉) foams with large semiclosed pores of diameter 30-100 μm, fine structured TAC (cellulose triacetate - C₁₂H₁₆O₈) foams with pores in the range 0.5-3 μm, and fine structured (TMPTA – trimethylol propane triacrylate) foams with submicron pore diameter. The above foams with high Z additions (Cl, Sn, SnO₂) were also used. In all the cases an aluminium foil, 2, 5 or 10 μm thick, was attached to the rear side of the foam layer.

The targets were irradiated with the first and third harmonic PALS beam of energy in the range of 100 J - 200 J. For evaluation of the speed of energy transfer through the porous foam material an X-ray streak camera Kentech was used, while the shock-wave arrival on the rear side of the target was monitored by an optical streak camera Hamamatsu. The velocity of the accelerated foil was measured by the three-frame optical interferometer/shadowgraph developed for PALS at IPPLM Warsaw.

Experimental results

The interferometric measurements of foil acceleration showed that the foil shape remains smooth without any signature of small-scale structures present in the incident laser beam. The measured foil velocity reached values of up to 10⁷ cm/s, the conversion efficiency of the laser energy into the kinetic energy of Al foil was estimated as up to 14%. The experimental results compare well with two-dimensional hydrodynamics simulations performed by means of 2D Lagrangian code ATLANT-HE, and with an approximate analytical model [8-11].

The lateral streaked slit X-ray images of the foam plasma made it possible to measure the speed and shape of the penetrating shock wave. In particular, two stages of homogenisation of porous matter, important for comprehension of the anomalously high absorption of laser radiation in supercritical foams, have been identified: the first, considerably fast stage of partial homogenisation is followed by a much slower second stage, leading to a uniform medium. In the laser shot shown in Fig. 5 the thermal wave propagates into the foam layer 400 μm thick with an average speed of 3.4×10⁷ cm/s. It reaches the foil rear side at 1.1 ns after the X-ray emission onset, when also the Al foil at the target rear starts to radiate. A weak fast pre-heating of the foil, as well as plasma expanding from the front target surface are also seen. Optical streaks of the thermal plasma radiation at the rear side of the target reflect the transverse dimension and structure of the shock wave. The streak in Fig. 6, taken in the same laser shot as Fig. 5, shows the main optical emission appearing at 2.1 ns, preceded again by a faster and narrower preheat. A small spot at the top left is a fiducial mark showing the laser beam position in time.

The experiment proved that the shock transition time increases with the pore size, foam density, and also with the contents of high-Z additions in plastic foams. The penetration of

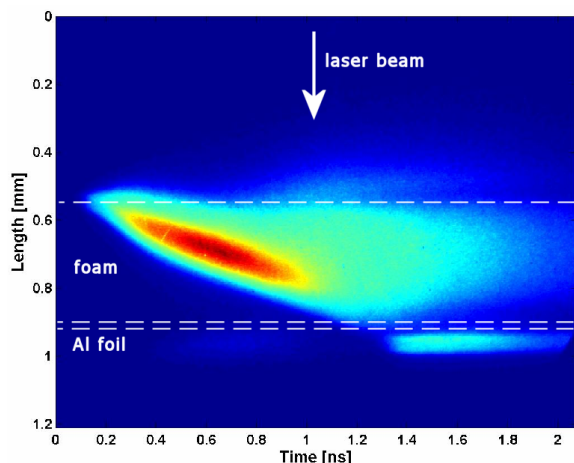


Fig. 5 Axial X-ray streak of the foam target with Al foil

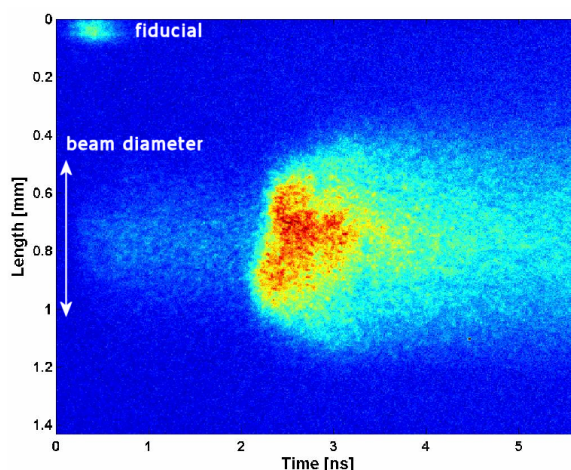


Fig. 6 Transversal optical streak of plasma at the rear-side of the target

radiation into foam with large cells is limited to about $100\ \mu\text{m}$ (1-3 cell diameters) during the whole laser pulse. From the point of view of energy transport, the 3-dimensional networks of TAC foams are no worse than those of TMPTA and are much better than agar foams. Radiation transport during laser pulse in TAC doped with Cu-clusters was faster than in TAC with no dopant, whereas plasma from TAC doped with Cu-clusters cooled down quicker than with no clusters. Thus, high-Z cluster dopant appears to be an effective tool for controlling energy transport in plasma.

For interpretation of the collected experimental data we used a new 2D Arbitrary Lagrangian Eulerian (ALE) hydrodynamic code, developed at FNSPE CTU in Prague. The code overcomes a collapse of Lagrangian codes at modeling the experiments with foams and double targets. A detailed comparison of experimental results with numerical simulations and with an analytical model is in progress.

References

- [8] J. Limpouch, N.N. Demchenko, S.Yu. Gus'kov, A.I. Gromov, M. Kalal, A. Kasperczuk, V.N. Kondrashov, E. Krousky, K. Masek, M. Pfeifer, P. Pisarczyk, T. Pisarczyk, K. Rohlena, V.B. Rozanov, M. Sinor, J. Ullschmied: Laser interactions with low-density plastic foams, *Laser and Particle Beams*, 23 (2005), p. 321-325.
- [9] I.V. Akimova, N.G. Borisenko, A.I. Gromov, A.M. Khalenkov, V.G. Pimenov, V.N. Kondrashov, S.F. Medovshikov, J. Limpouch, E. Krousky, K. Masek, J. Kuba, M. Pfeifer; Intensive (up to $10^{15}\ \text{W}/\text{cm}^2$) laser light absorption and energy transfer in subcritical media with or without high-Z dopants, *Proceedings of VIII Zababakhin Scientific Talks, Snezhinsk, Russia, 2005*, (in press).
- [10] J. Limpouch, N.G. Borisenko, N.N. Demchenko, S.Yu. Gus'kov, A. Kasperczuk, A.M. Khalenkov, V.N. Kondrashov, E. Krousky, J. Kuba, K. Masek, W. Nazarov, P. Pisarczyk, T. Pisarczyk, M. Pfeifer, V.B. Rozanov, J. Ullschmied: Laser Interactions with Foam-Foil Layered Targets, 32nd EPS Conf. on Plasma Phys., Tarragona 2005, ECA Vol.29C, http://eps2005.ciemat.es/papers/pdf/O2_022.pdf.
- [11] J. Limpouch, N.G. Borisenko, N.N. Demchenko, S.Yu. Gus'kov, A. Kasperczuk, A.M. Khalenkov, V.N. Kondrashov, E. Krousky, J. Kuba, K. Masek, Yu.A. Merkul'ev, W. Nazarov, P. Pisarczyk, T. Pisarczyk, M. Pfeifer, O. Renner, V.B. Rozanov: Laser Absorption and Energy Transfer in Foams of Various Pore Structures and Chemical Compositions, *Proc. IFSA2005 WPo15.7, Biarritz, 2005* (in press).

V Training, Education, Outreach and Public Information Activities

1. Training and Education

Joint experiments on small tokamaks

G. Van Oost¹⁾, M. Berta²⁾, J. Brotánková³⁾, R. Dejarnac³⁾, E. Del Bosco⁴⁾, E. Dufková³⁾, I. Ďuran³⁾, M.P. Gryaznevich⁵⁾, M. Hron³⁾, A. Malaquias⁶⁾, G. Mank⁶⁾, P. Peleman¹⁾, J. Sentkerestiová³⁾, J. Stöckel³⁾, V. Weinzettl³⁾, S. Zoletnik²⁾, J. Ferrera⁴⁾, A. Fonseca⁷⁾, H. Hegazy⁸⁾, Y. Kuznetsov⁷⁾, A. Ossyannikov⁹⁾, A. Sing¹⁰⁾, M. Sokholov¹¹⁾, A. Talebitaher¹²⁾

- 1) Department of Applied Physics, Ghent University, Ghent, Belgium
- 2) KFKI-RMKI, Association EURATOM, Budapest, Hungary
- 3) Institute of Plasma Physics, Association EURATOM/IPP.CR
- 4) INPE, São José dos Campos, Brazil
- 5) EURATOM/UKAEA Fusion Association, Culham Science Centre, Abingdon, UK
- 6) IAEA, NAPC Physics Section, Vienna, Austria
- 7) Institute of Physics, University of São Paulo, Brazil
- 8) EAEA, Cairo, Egypt
- 9) Saint Petersburg State University, Russia
- 10) Plasma Physics Laboratory, University of Saskatchewan, Canada
- 11) RRC “Kurchatov Institute”, Moscow, Russia
- 12) Plasma Physics Research Center, Teheran, Iran

The first Joint (Host Laboratory) Experiment on “Joint Research Using Small Tokamaks” (JRUST) involving twenty scientists from seven countries has been carried out from 28 August to 9 September, 2005 on the CASTOR tokamak at the Institute of Plasma Physics of the Academy of Sciences of the Czech Republic (IPP Prague). This activity was jointly organized by IPP Prague and KFKI (Central Research Institute for Physics of the Hungarian Academy of Sciences) Budapest, under the auspices of the International Atomic Energy Agency (IAEA). Within the framework of the Coordinated Research Project JRUST, it has been supported by the IAEA and the ICTP Trieste (International Centre for Theoretical Physics). The objective of the joint experiment was to perform studies on the topics of plasma edge turbulence and plasma confinement based on broad international participation to benefit from the added value of international expertise exchange. The edge plasma studies have a long tradition on the CASTOR tokamak (appropriate equipment, large amount of expertise, etc.). Another goal of this joint experiment was the development of tools for remote participation and data exchange. These two aims are expected to be of relevance for ITER. The Joint Experiment has been performed under an intensive international cooperation and with an important component of remote operation and data exchange. This initiative highlighted the role of small tokamaks in the exchange of expertise and their potential to contribute significantly to the development of remote operation.

This 1st Joint (Host Laboratory) Experiment on “Joint Research Using Small Tokamaks” has clearly demonstrated that small tokamaks are suitable and important for broad international cooperation, providing the necessary environment and manpower to conduct dedicated joint research programmes. The contribution of small tokamaks to the mainstream fusion research such as edge turbulence, improved confinement, and diagnostics development in the present case can be enhanced through coordinated planning. The activities under this IAEA Coordinated Research Project are already paying visible dividends.

The development of remote participation tools is of wide interest, and a close collaboration with other tokamaks will help to develop standard platforms for the exchange of data from several machines, and to allow for the remote operation of diagnostics. The goal is to connect small tokamaks through a network where it would be possible to plan, implement and run experiments to address particular topics, taking profit of the potential of running similar or complementary experiments simultaneously on several machines.



The outputs of the Joint Experiment triggered a high interest from the participants to further develop and refine the collaborative research in several of the topics studied. The overview of the Joint Experiment will be presented at an IAEA conference [1], and two detailed reports on the results of the JE are expected to be submitted for publication in peer reviewed journals.

- [1] G. Van Oost et al.: "**Joint Experiments on Small Tokamaks**", accepted as a presentation No. EX/P4-34 on 21st IAEA Fusion Energy Conference, 16-21 October 2006, Chengdu, China.

2. Outreach and Public Information

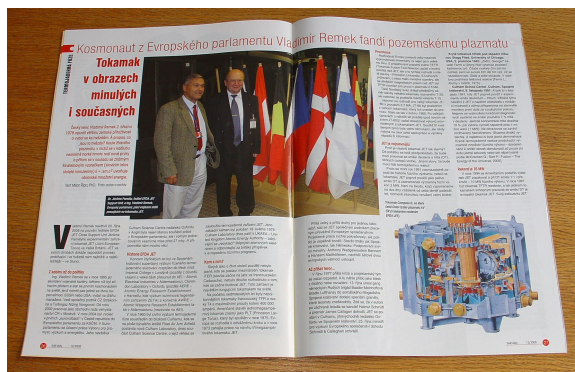
M. Řípa, V. Weinzettl, P. Chráska, J. Stöckel, E. Dufková, IPP

In 2005, the main point of our Association's PI activities was to advertise and to inform the public on the intended transfer of the **COMPASS-D tokamak from Culham, UKAEA, and its reinstallation in IPP Prague**. To ensure a good public acceptance and to get the support of the national government, a strong effort was devoted to the dissemination of the basics of the thermonuclear fusion and its potential benefits for mankind. The level of involvement of IPP

staff in these PI activities can be demonstrated by a large number of printed articles, given lectures, TV and broadcast interviews. We also sought support at top political level, and were happy to get positive response from the national government, and also from several Czech members of the European Parliament, especially from Vladimír Remek. The decision on ITER in June 2005 provided a solid ground for our intention to put the Czech participation in the European fusion programme at a higher level by replacing the existing experimental tokamak CASTOR by a more modern device with ITER-like plasma shape, namely, COMPASS-D. In November, the Czech Government allocated special funds for the transfer and reinstallation of COMPASS-D.



In the middle of the year, an important project called **Otevřená věda (Open Science)**, financed by the European Social Funds and focused on secondary school students and teachers, was started. Under the management of Vladimír Weinzettl, six secondary school students began their long-term traineeships with their tutors at IPP, two of them in the Tokamak department. Also, in the frame of this project, the first summer school for secondary school physics teachers was organized in Nové Hradky.



In response to the unsatisfied demand of the general public for the book "**Řízená termojaderná syntéza pro každého**" (Controlled thermonuclear fusion for everyone) the first edition of which was sold out in no time, the authors prepared the second edition of 2000 impressions, in cooperation with the ČEZ a.s. company, the biggest electricity producer in the Czech Republic. As the first result of all above-mentioned activities, extremely high number of students and enthusiasts visited our Institute's laboratories, also - but not exclusively - during the Open Door Days.



LIST OF ACTIVITIES

The following list summarizes the public outreach activities of our Association.

Books

Řípa M., Weinzettl V., Mlynář J., Žáček F.: **Řízená termojaderná syntéza pro každého. (Controlled thermonuclear fusion for everyone)** 2nd release. ISBN: 80-902724-7-9, ČEZ & IPP, 2005, 2000 impressions

Papers

- Milan Řípa: **Poblouznění termojadernou fúzí (Infatuation by thermonuclear fusion)**, Česká hlava a svět vědy, 3 (2005), No. 2, p. 22
- Milan Řípa: **Odpověď na otázku (FAQ)**, 21.století, No. 5, 2005, p. 42-43
- Milan Řípa: **Hlad po energii uspokojí jaderná fúze (Fusion will meet an energy hunger)**, MF Dnes, 16 (2005), No. 107, 7/5/2005, p. C/9
- Milan Řípa: **Termojaderná fúze (Thermonuclear fusion)**, part I, EKO, XVI (2005), No. 5, p. 25–28
- Milan Řípa: **Termojaderná fúze (Thermonuclear fusion)**, part II, EKO, XVI (2005), No. 6, p. 13–15
- Milan Řípa: **ITER je cesta (ITER is the way)**, Elektroinstalatér, XI (2005), No. 4, p. 50 – 55
- Milan Řípa: **ITER**, 3. pól, 5 (2005), No. 4, p. 4–5
- Vladimír Weinzettl: **O historii a perspektivách termojaderného výzkumu v tokamacích (On history and perspectives of thermonuclear research in tokamaks)**, Československý časopis pro fyziku, 55 (2005), No. 5, p. 490–496
- Milan Řípa: **Tokamak v obrazech minulých i současných (Tokamak in historical and present views)**, Svět vědy, III (2005), No. 12, p. 26–28
- Milan Řípa: **Čeští vědci o krok dál ve výzkumu fúze (Czech scientists do next step in fusion research)**, Mladá Fronta Dnes, 16 (2005), No.288, 10/12/2005, attachment Věda C/8
- Milan Řípa: **ITER – možnosti pro evropský průmysl (ITER – a chance for European industry)**, Technický týdeník, 20/12/2005, p. 1

TV & Radio broadcast

- Milan Řípa (A. Olivová): **ITER**, Ranní mozaika, rozhlas Vltava, 8/3/2005
- Jan Stöckel: **Zásoby ropy se tenčí (Oil reserves run short)**, Zprávy, Radiožurnál, ČRo 1, 17/7/2005
- Pavel Chráska, ČRo 1, 20/5/2005
- Pavel Chráska: **Termojaderná fúze (Thermonuclear fusion)**, Střepiny, Nova, 3/7/2005
- Pavel Chráska, Vojtěch Svoboda, Dana Drábová: **Češi prosazují energetickou revoluci (Czechs promote energetic revolution)**, Události, ČT 1, 24/10/2005 + Události - komentáře, ČT 1, + Zprávy, ČT 1, 25/10/2005 + Zprávy – Ostrava, ČT 1, 25/10/2005
- Pavel Chráska: **Výzkum nových zdrojů energie na základě jaderné fúze (Research of new energy sources on a nuclear fusion basis)**, Radiožurnál, Týden v tahu, ČRo 1, 5/11/2005

PALS team: **Nejjasnější rtg laser (The clearest X-Ray laser)**, České hlavy, ČT,
25/11/2005

Lectures

Milan Řípa: **Association EURATOM-IPP. CR, 5th EFDA Meeting on Public Information**, CEA Cadarache, 2nd–3rd March 2005

Vladimír Weinzettl, Milan Řípa: **Moderní trendy v jaderné fúzi (Modern trends in nuclear fusion)**, FJFI ČVUT, Praha, 10/3/2005

Jan Stöckel: **Edge plasma diagnostics in tokamaks**, MFF UK, Praha, 21/3/2005

Edita Dufková: **Energetika (Energetics)**, basic school Liberec, 8/4/2005

Pavel Šunka: **Kam až sahá čtvrté skupenství hmoty (Where does the fourth matter state reach to?)**, Nebojte se vědy, TiO AV ČR Praha, 13/4/2005

Jan Stöckel: **Fyzika a technika termojaderné fúze (Physics and technics of thermonuclear fusion)**, FJFI ČVUT, Praha, 14/4/2005

Milan Řípa, **ITER je cesta (ITER is the way)**, Gymnasium Joachima Barranda, Beroun, 14/4/2005

Milan Řípa, **ITER je cesta (ITER is the way)**, Gymnasium J.S. Machara, Brandýs nad Labem, 20/4/2005

Jan Stöckel: **Fyzika plazmatu a termojaderné slučování (Plasma physics and thermonuclear synthesis)**, Západočeská Univerzita Plzeň, 25/4/2005

Edita Dufková: **Energetika (Energetics)**, basic school, Mnichovo Hradiště, 20/5/2005

Edita Dufková: **Energetika (Energetics)**, basic school, Kolín, 3/6/2005

Jan Stöckel : **Overview of Fusion Relevant Research in the Czech Republic in the frame of the EURATOM**, 50th jubilee of the ÚJV a.s. foundation, Palác kultury Praha, 8th-9th June 2005

Vladimír Weinzettl: **Plazma a plazmová koule (Plasma and plasma sphere)**, Letní škola pro středoškolské pedagogy, Nové Hrady, 16/8/2005, contribution to the proceedings "Fyzika"

Edita Dufková: **Energetika (Energetics)**, basic school, Most, 4/10/2005

IPP and AS CR: **Energie pro 21. století (Energy for 21st century)**, AS CR, Prague, 24/10/2005

Jan Stöckel: **Co děláme v České republice ve výzkumu fyziky horkého plazmatu a vývoje fúzních technologií (What we do in Czech Republic in a research of hot plasma physics and development of fusion technologies)**, Ústav jaderného výzkumu Řež, a. s., Řež, 7/11/2005

Jan Stöckel: **Termojaderná fúze – zdroj energie pro třetí tisíciletí (Thermonuclear fusion – energy source for third millennium)**, Dny vědy a techniky, Národní technické museum Praha, 10/11/2005

Jan Stöckel: **Udržení plazmatu v magnetických nádobách typu tokamak a současný stav výzkumu termojaderné fúze (Plasma confinement in magnetic vessels of the tokamak type and a present status of the thermonuclear fusion research)**, MFF UK Praha, 23/11/2005

Jan Stöckel: **ČS podíl na výzkumu fyziky horkého plazmatu a vývoje fúzních technologií v rámci EURATOM (Czech contribution to the hot plasma physics research and**

development of fusion technologies in the frame of EURATOM), Energie pro 21. století, Akademie věd České republiky Praha, 24/11/2005

Radomír Pánek: **Nové možnosti – tokamak Compass-D v České republice (New possibilities – the COMPASS-D tokamak in Prague)**, Energie pro 21. století, Akademie věd České republiky Praha, 24/11/2005

Edita Dufková: **Energetika (Energetics)**, basic school, Krupka, 28/11/2005

Vladimír Kopecký: **Zapálíme Slunce na Zemi (We ignite the Sun on the Earth)**, Česká astronomická společnost, Štefánikova hvězdárna Praha, 30/11/2005

Edita Dufková: **Energetika (Energetics)**, basic school, Ústí nad Labem, 2/12/2005

Edita Dufková: **Energetika (Energetics)**, basic school, Hejnice, 12/12/2005

Jiří Ullschmied: **Výkonové lasery – PALS (Powerful lasers – PALS)**, Astronomická společnost, 2005

Other

□ consultation for the articles:

- Gabriela Štefaniková (Jan Mlynář, interview): **Energie pro 21. století (Energy for 21st century)**, Akademický bulletin, No. 12, 2005, p. 5-7
- Milan Koukal (Milan Řípa): **Termojaderná fúze jako nový zdroj energie (Thermonuclear fusion as a new energy source)**, 21. století, No. 2, 2005, p. 24–27
- Josef Tuček (Milan Řípa) : **Slunce ve velké pneumatice (Sun in a big tyre)**, Hospodářské noviny, 7/7/2005
- Irena Webrová (Milan Řípa, interview): **Fúze na papíře (Fusion on a paper)**, Akademický bulletin, No. 4, 2005, p.32

□ excursions:

- **Open Door Days 2005**, more than 400 visitors, 10-12/11/2005
 - to **PALS**, 250 visitors (exclusive of ODD)
 - to **Tokamak**, 314 visitors including few tens from Belgium and U.S.A. (exclusive of ODD)
- Vladimír Weinzettl – IPP participates on the project **Otevřená věda (Open Science)** financed from European Social Funds
- 6 tutors for 6 secondary school students (long-term trainee-ships)
- Milan Řípa: **Institute of Plasma Physics AS CR**, poster & presentation for "ITER Opportunities for European Industry", Barcelona, Spain, 13rd-14th December 2005
- **Tour de Plasma**, bicycling race, 13rd–16th September 2005